Exploring Mechanisms of Regulatory T cell-mediated Immune Suppression and Development of Anti-PD-L1 CAR T cells

by

Kirsten M. Pfeffer

A Dissertation Presented in Partial Fulfillment
of the Requirements for the Degree
Doctor of Philosophy

Approved October 2023 by the
Graduate Supervisory Committee:

Douglas F. Lake, Chair
Thai H. Ho
Karen E. Hedin
Masmudur M. Rahman

ARIZONA STATE UNIVERSITY

December 2023

ABSTRACT

Regulatory T cells (Tregs) suppress adaptive immunity and inflammation. In cancer, Tregs hinder therapeutic responses due to suppression of anti-tumor activity in the tumor microenvironment. Although these cells play a role in suppressing anti-tumor responses, development of therapeutics that target Tregs is limited by their low abundance, heterogeneity, and lack of specific cell surface markers. To study Treg mechanisms of suppression, a human T cell line, MoT, was identified and characterized as a model of human $Foxp3^+$ Tregs. MoT cells express surface markers consistent with PBMC-derived Tregs and inhibit proliferation of $CD4^+$ responder PBMCs in a ratio-dependent manner. Transwell membrane separation prevented suppression of stimulated $CD4^+$ PBMC proliferation by MoT cells, suggesting cell-cell contact is required for suppressive activity. Suppression was found to be independent of soluble cytokines and known immune checkpoint pathways, providing evidence that a $Foxp3^+$ Treg population suppresses immune responses by an unknown cell contact-dependent mechanism. To investigate potential cell surface molecules that mediate suppression, monoclonal antibodies (mAbs) were generated to a known immunosuppressive protein, Galectin-1, and to MoT cell surface proteins. MAbs were identified that bind and functionally block suppressive activity. Another mechanism of immune suppression involves the PD-1/PD-L1 pathway, which is exploited by tumor cells to resist T cell killing and escape immune clearance. Since PD-L1 has emerged as an effective therapeutic target, anti-PD-L1 CAR T cells were generated and demonstrated to kill PD-L1-positive tumor cells. These results expand upon the current knowledge of Treg function and CAR T cell therapy and may lead to enhanced anti-tumor immunity to improve patient responses.

DEDICATION

To my aunt Margo,

who battled renal cell carcinoma as I was beginning my research.

I continue my pursuit to improve cancer therapies.

We miss you deeply.

ACKNOWLEDGMENTS

I would first like to thank my PhD advisor and mentor, Dr. Douglas Lake. I am grateful I was able to join your lab as an undergraduate and continue in the lab through my graduate career. Your knowledge and enthusiasm fueled my passion for research in cancer immunology. You always encouraged me to be hardworking and challenged, which enabled me to achieve numerous academic and professional goals.

Next, I would like to thank my second mentor, Dr. Thai Ho. Your encouragement to publish and try new investigations pushed me to become a better scientist and researcher. As incredibly busy as you are, you always made time to brainstorm ideas and provide other viewpoints. I immensely appreciate your time and significant financial support that made this research possible.

Thank you to all of my committee members. Dr. Grant McFadden, thank you for serving as my comps chair, providing your expertise in oncolytic virotherapy and insightful suggestions. Dr. Karen Hedin, thank you for providing valuable feedback and expertise and for always having encouraging words. Thank you Dr. Masmudur Rahman for joining my committee at the end, providing great ideas and recommendations to expand my research.

Yvette Ruiz, thank you for your expertise, assistance and patience for me and all of Doug's graduate students. You trained me on all things lab related and my research would not have been possible without you. I greatly appreciate everything you do.

To my current lab mates, Alexa Roeder, Francisca Grill, Calvin Koelbel (my TA partner in crime), Megan Koehler, and Austin Blackmon and to past lab mates, Amber

Fifield and Natalie Mitchell, thank you for your friendship, feedback and so many laughs along the way. Alexa, it is such a small world how our paths crossed again, thank you for providing me the support I needed to try new protocols and help build my confidence as a scientist. Francisca, thank you for your help with experimental design and encouragement to try again when experiments failed (many times).

A huge thank you to my incredible family and friends for their tremendous support through the many ups and downs. A special thank you to my grandpa, Dr. Robert Pfeffer, who is my inspiration to pursue research and my doctorate.

Lastly, thank you to Ms. Catherine Ivy of the Ben and Catherine Ivy Foundation, the Achievement Rewards for College Scientists (ARCS) foundation, ASU Graduate College, ASU School of Life Sciences (SOLS), and ASU Graduate Professional Student Association (GPSA) for much appreciated financial support.

TABLE OF CONTENTS

APPENDIX Page

LIST OF FIGURES

Figure Page

Figure Page

CHAPTER 1

INTRODUCTION

T cell Immunology

The immune system functions as the primary defense against infection. Cells of the immune system have high diversity to be able to respond to foreign agents, yet each response is highly specific for a single antigen[1]. The immune system has evolved to defend against pathogens while maintaining self-tolerance and homeostasis[2]. It consists of innate and adaptive cells that are responsible for discriminating between "self" and "non-self," thereby protecting the body from attacking host cells[1]. Innate cells, such as neutrophils, dendritic cells and macrophages, are the first to respond to infection, producing antimicrobial compounds while informing the adaptive system to respond to the infection[3]. Adaptive cells consist of T and B cells and become activated in response to cytokines produced by innate immune cells[4]. The goal of the adaptive immune system is to fully eliminate infection and provide control of future infections from the same pathogen[4]. This is known as immune memory.

Lymphocytes, B and T cells, provide adaptive immunity and are derived from common lymphoid progenitor cells in the bone marrow. B cells mature in the bone marrow and recognize antigens in their native forms as conformational epitopes[5]. Naïve T cells originate in the thymus, a primary lymphoid organ where central and peripheral tolerance mechanisms are established. The thymus is critical for T cell development and maturation and its absence or malfunction can lead to increased risk of infection, autoimmunity or immune system dysfunction[6,7]. It has been shown that thymectomy of mice at day three post birth results in the development of organ-specific autoimmune

disease[8]. While certain T cells are important in defending the host from pathogens, other T cells play a regulatory role and are critical in protecting the host from autoimmune disease.

T cell development

Common lymphoid progenitor cells that commit to the T cell lineage become T cell precursors and migrate from the bone marrow to the thymus. The thymus is the main site of T cell maturation. T cell precursors that have newly migrated to the thymus do not express a T cell receptor (TCR), CD8 or CD4 molecules, and are classified as double negative (DN) thymocytes[9–11]. Immature thymocytes undergo TCR gene rearrangement to rearrange TCR αβ or γδ genes. Like immunoglobulin heavy chain variable regions, TCR β chain variable regions rearrange before α chain variable regions[12]. T cells express either αβ or γδ TCRs. The strength of TCR signals during selection commits to either αβ or γδ T cell lineage[11]. Strong TCR γδ signals a small number of these types of T cells to exit the thymus without classical positive and negative selection, while functional TCR αβ cells continue to become double positive (DP) $CD4^+CD8^+$ cells[13,14]. TCR αβ DP T cells undergo positive selection to select for cells that recognize self-major histocompatibility complex (MHC) by interacting with MHC class I and II molecules with self-peptides[10]. Weak or no signaling results in cell death while cells that recognize self MHC survive[15]. DP cells then test for MHC class I or II recognition by downregulating each co-receptor and testing for signal[16]. Strong MHC II signals select for $CD4^+$ while weak MHC II and strong MHC I commits to $CD8^+$ lineage[10,15,16].

After positive selection, single positive (SP) T cells move to the next step in development. The goal of negative selection is to eliminate autoreactive T cells[9,17]. Self-peptides are presented to SP T cells and the strength of recognition determines their fate. Self-reactive T cells with moderate recognition of MHC:peptide undergo apoptosis[17]. Strong recognition of self-peptide-MHC complexes result in natural regulatory T cell (nTreg) development[18,19]. nTregs are critical for maintaining self-tolerance and reestablishing homeostasis post infection[20]. T cells that survive negative selection exit the thymus as mature $CD4^+$ or $CD8^+$ T cells. The outcome of T cell development and maturation leads to self-tolerant T cells that are restricted by recognition of self-MHC.

Effector T cells

Mature, naïve T cells exit the thymus to circulate from blood to lymph nodes in search of their cognate antigen. In secondary lymphoid organs (lymph nodes, spleen, mucosal lymphoid tissues), T cell activation occurs when a naïve T cell encounters its specific antigen displayed by antigen-presenting cells (APCs). Effector T cells are functionally activated cells that execute immune function and induce systemic immune responses[20]. Effector T cells are classified as either $CD8^+$ cytotoxic cells that can perform direct cell killing of infected cells, or $CD4^+$ helper cells that activate other immune cells.

Differences in cytokine profiles further classifies the types of $CD4^+$ T cells. In response to antigen stimulation, production of different cytokines skews T cell differentiation into distinct Th lineages[20]. Th1 cells produce pro-inflammatory cytokines (IFN-γ, TNF-α, IL-2, IL-12) and are important for protection against intracellular pathogens and tumor formation[20,21]. IL-12 is secreted by APCs which induces IFN-γ

production by NK cells and naive T cells, enhancing Th1 differentiation[22]. Th2 cells respond to extracellular pathogens by production of IL-4, -5, -10, -13 cytokines, induction of IgG1 and IgE class-switching, and recruitment eosinophils[20]. Th2 cells play a crucial role in an allergic response[21]. Th17 cells are a distinct lineage but share common functions of both Th1 inflammatory and Th2 inhibitory responses and are important in anti-parasitic and anti-fungal immunity. The distinct function of $CD4^+$ Th cell subsets is dictated by their cytokine secretion.

T cell activation requires two signals: antigen-specific and costimulatory[23]. Activation is first induced by TCR/CD3 binding to target peptide:MHC complexes. Proteins must first be processed into peptides before being presented to T cells by APCs. In addition to TCR-peptide-MHC interactions, co-stimulation is crucial for effective T cell activation[24]. Co-receptors CD28 and LFA-1 are cross-linked at the site of cell-cell contact, known as the immunological synapse, which amplifies TCR signals[24,25]. Once activated $CD8^+$ T cells find and kill a target cell after which they can disengage and move on to attack additional targets bearing the same peptide antigen[25]. Upon activation, naïve $CD4^+$ T cells differentiate into distinct effector subtypes based on specific cytokine signaling[22].

$CD4^+$ effector cells activate microbicidal macrophages and induce B cell antibody secretion[26]. $CD4^+$ cells activate infected macrophages by production of IFN-γ and through membrane-bound proteins; this induces potent antimicrobial activity to kill intracellular pathogens and ingested bacteria[27]. Macrophage activation is tightly regulated by $CD4^+$ T cells to reduce localized tissue damage[27]. In secondary lymphoid organs, $CD4^+$ helper cells provide signals to promote B cell differentiation into plasma cells (Ab-secreting) or

memory B cells, and facilitate antibody isotype class switching[23,28,29]. $CD4^+$ T cells play a major role in autoimmunity, both as effector and suppressor cells, compared to $CD8^+$ T cells and B cells[8], thus are a significant cell type in adaptive immunity.

Immuno-oncology

Cancer is a disease in which the accumulation of genetic alterations leads to mutated cells dividing uncontrollably and spreading into tissues of different origin. Mutations can accumulate due to defects in DNA repair mechanisms, silencing of tumor-suppressor genes, and activation of oncogenes leading to genomic instability[30]. In the U.S., cancer is currently the second leading cause of death after heart disease and is rapidly increasing in incidence[31]. The majority of adult cancers are incurable unless diagnosed early[30]. Most remain terminal diseases, even with the emergence of new therapeutics that increase overall prognosis.

Tumorigenesis and hallmarks

The hallmarks of cancer, described by Hanahan and Weinberg, constitute a framework to understand the development of neoplastic disease and the complexity of cancer[32]. Tumorigenesis or oncogenesis is the process in which normal cells develop changes at the cellular, genetic, and epigenetic levels which leads to abnormal cell division to become cancer cells. The hallmarks provide conceptual organization of how this occurs to help understand cancer biology, although the process is much more complex. There are eight hallmarks of cancer: sustained proliferative signaling, evasion of growth suppressors, resistance of cell death, enabling replicative immortality,

induction of angiogenesis, activation of invasion and metastasis, reprogramming energy metabolism, and avoiding immune destruction[32]. The first six were originally proposed in 2000, and the last two emerged in 2011[32]. In addition, two enabling characteristics facilitate the development of these hallmarks: genomic instability and tumor-promoting inflammation[32].

As one of the most fundamental characteristics of cancer, tumors sustain proliferation while normal tissues control cell growth to ensure homeostasis. Cancer cells enable proliferative signals by overexpression of growth factors and associated cell surface receptors that lead to activation of growth stimulatory pathways[32]. Overexpressed receptors include epidermal growth factor receptor (EGF-R), platelet-derived growth factor receptor (PDGF-R), vascular endothelial growth factor receptor (VEGF-R) and receptor tyrosine kinases (RTK)[32,33]. Tumors also circumvent negative signals that limit cell proliferation, which depend on the inactivation or loss of tumor suppressor genes[32].

Cancer cells evolve strategies to resist cell death mechanisms, including apoptotic programmed cell death[30]. Apoptosis is initiated in response to cellular stress signals. Normal cells can sense abnormal conditions in the environment that influence the cell to die[34]. Tumors have a reduced ability to sense damage through loss-of-function mutations, such as those identified in the tumor suppressor p53 and Rb (retinoblastoma protein)[35,36]. Tumors also increase in anti-apoptotic regulators to avoid cell death (Bcl-2 proteins)[32,34,37]. In addition, cancer cells enable replicative immortality by overcoming barriers to unlimited proliferation such as senescence and apoptosis. One example is by overexpression of telomerases that extend telomeric DNA[32] avoiding telomere shortening which triggers senescence and cell death[38].

Tumor cells, like normal tissue, require vascularization to gain nutrients and oxygen and remove metabolic waste. Tumors generate neo-vasculature through angiogenesis, or the formation of blood vessels. The increase in pro-angiogenic factors, called the angiogenic switch, is regulated by expression of cell surface receptors that induce angiogenesis, including VEGF-R and RTKs[32,39]. Newly formed tumor vessels are highly disorganized and functionally abnormal[40]. Tumor neo-vasculature has distinctive capillary sprouting, excessive and enlarged vessel branching, increased blood flow and leakiness[32,40].

The majority of cancers move out of the primary tissue to adjacent tissues (invasion) and travel to distant sites (metastasis) where malignant cells continue to grow. The ability to invade and metastasize is a complex process that is incompletely understood[41]. Carcinomas derived from epithelial tissues alter their shape and cell-cell and cell-ECM adhesion molecules to aid in migration[32]. The sequential steps of this process are described as the invasion-metastasis cascade. First, continued growth of the primary tumor depends on increased vascularization within the surrounding host tissue, where cells locally invade[42]. Some cells begin to detach and enter nearby blood vessels or lymphatic channels where they enter circulation. Cells that survive circulation adhere to capillary cells of distant tissues, move out of the vessel by extravasation, and form small nodules where they continue to grow into larger tumors and develop a vascular network (colonization)[32,43]. Circulating tumor cells and tumor DNA isolated from liquid biopsies provide new clinical methods of early detection and diagnosis, identification of predictive biomarkers, and aid in monitoring treatment response[44,45]. Metastatic tumors are

classified as advanced stage and are highly heterogeneous. Over 90% of patient deaths from solid tumors are due to metastases that are refractory to conventional therapuetics[43].

Research within the last decade suggests two emerging hallmarks contribute to oncogenesis: reprogramming energy metabolism and evading immune destruction. The ability to reprogram cellular metabolism is crucial to fuel continued cell growth[46]. Tumor cells limit energy metabolism predominately to glycolysis and upregulate glucose transporters (GLUT1) to increase glucose uptake[32,46]. Reliance on glycolysis has been linked to activation of oncogenes and mutation of tumor suppressors, and is heightened under hypoxic conditions found within the tumor microenvironment[46]. Hypoxia, or reduced oxygen availability, stimulates a metabolic switch to promote increased glucose consumption and energy production[46]. Hypoxia and oncoproteins can increase glycolysis through upregulating HIF-1 transcription factors[32,37].

Tumors can also evade immunosurveillance by disabling mechanisms of the antitumor immune response. Cancer cells can recruit suppressor immune cells such as regulatory T cells (Tregs) and myeloid-derived suppressor cells (MDSCs) where they suppress antitumor cells including B and T cells, NK cells and macrophages[32,47]. Tumor-mediated immunosuppression is discussed further in the following sections.

Antitumor T cell immunity

T cells play a significant role in the antitumor immune response. T cells are first activated in tumor-draining lymph nodes by recognition of tumor-derived neoantigens presented by dendritic cells (DCs) on MHC molecules[48]. This results in priming and activation of tumor-specific cytotoxic T cells (CTLs). CTLs then traffic through blood

vessels to the tumor microenvironment where they recognize cancer cells that express neoantigens through TCR-MHC interactions. These tumor-infiltrating lymphocytes (TILs) can then perform direct killing of cancer cells which subsequently exposes more tumor-associated antigens that can be recognized by the immune system[48] (Figure 1).

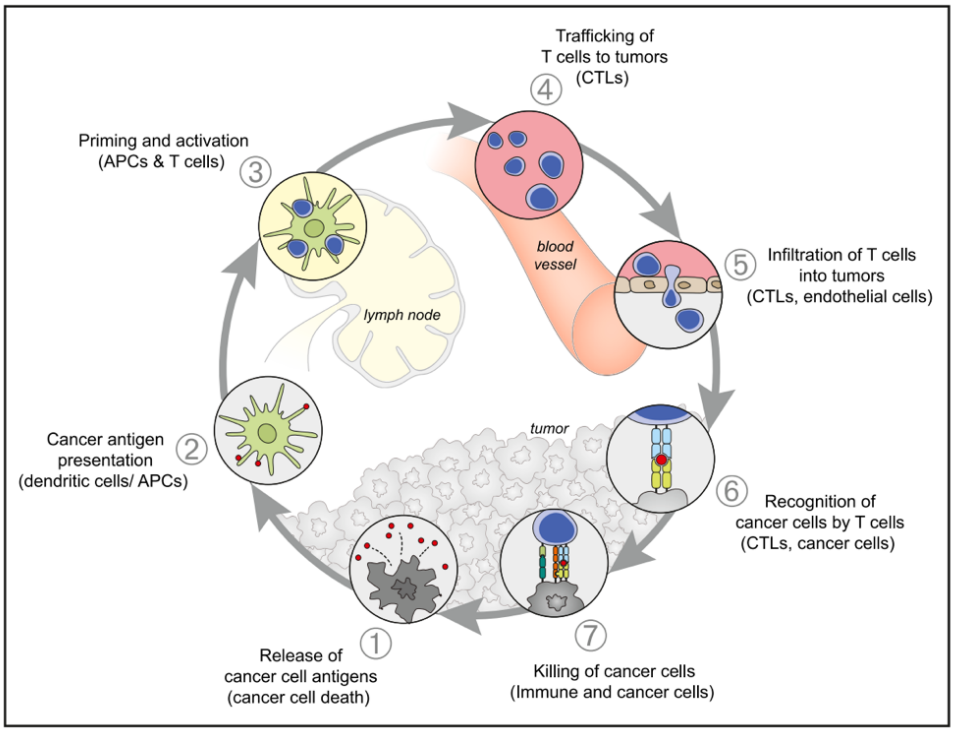

Figure 1. The cycle of generating antitumor immunity. The goal of generating an effective antitumor immune response is to activate, redirect, and amplify T cell responses. The cycle can be represented in seven steps, beginning with the release of tumor cell antigens and ending in tumor cell killing. Each of the steps are described above. Reprinted from *Immunity*, 39, Chen DS, Mellman I. Oncology meets immunology: The cancer-immunity cycle, 1-10, 2013, with permission from Elsevier.

The immune system is the initial mechanism of defense against cancer. Tumor immune surveillance is the ability of the immune system to recognize tumor-specific antigens (TSA) or tumor-associated antigens (TAA) to induce an antitumor response. Tumor antigens may arise from oncogenic viruses, aberrant epigenetic regulation of gene expression, cellular differentiation antigens, or neoantigens that arise from mutations[49]. The immune system can recognize these changes as "foreign" instead of "self," despite the fact that these tumors arose from self-tissues.

The balance between tumor growth and the ability of the immune system to recognize cancer cells has been described by the cancer immunoediting hypothesis[50]. This hypothesis first describes an elimination phase, where cancer cells are eliminated by the immune system. This is followed by an equilibrium phase where the immune system exerts selective pressure on the tumor cells giving rise to mutated cells that leads to the escape phase, resulting in uncontrolled cell growth[50,51]. As a result, tumors become non-immunogenic and can avoid immune recognition and clearance.

There are challenges to eliciting an effective, robust antitumor immune response. Since cancer arises from one's own cells, tumor antigens may be seen as self-antigens rather than foreign[52]. One example is overexpression of a growth factor receptor on tumor cells. While there may not be any mutations in the growth factor receptor resulting in neoantigens, peptides from the growth factor receptor may be presented by MHC molecules to T cells, surpassing a tolerance threshold that could result in a T cell response. Thus, tumor antigens that are recognized as self will initiate increased Treg responses instead of effector antitumor responses and inhibit infiltrating T cells from migrating the tumor site[48].

Even when antitumor T cells successfully traffic to the tumor microenvironment, they encounter additional obstacles that can diminish antitumor activity. Once T cells traffic to the tumor, the vascular endothelium creates an active barrier[53]. Tumor-reactive T cells must transmigrate through the barrier to elicit antitumor responses. Establishment of this barrier that augments tumor immune privilege may be mediated by angiogenic molecules (FGF or VEGF) that inhibit TNF-α induced T cell adhesion[54]. Endothelins expressed by the tumor endothelium also block T cell adhesion[55]. In addition to hindering adhesion, tumor endothelial cells can also express a number of immunosuppressive molecules to prevent T cell infiltration. These include Fas ligand, TNF-related apoptosis-inducing ligand (TRAIL), PD-L1, TIM-3, IL-10 and TGF-β [56–59]. When T cells make it through this barrier, they encounter suppressive mechanisms elicited by the tumor, described in the next section.

Tumors are robust, complex systems that can adapt to the surrounding environment. Cancer cells continuously interact with surrounding nonmalignant cells and adapt to changes within the tumor microenvironment[30]. Examples of this are selective pressures such as hypoxia and low vascularization that drive phenotypic heterogeneity so the tumor can adapt and persist.

Tumor-mediated suppression of the immune system

Tumors can be successfully eliminated by the host when recognized. However, tumor progression is not always prevented due to mechanisms of immunosuppression elicited by tumors, leading to immune evasion and limited therapeutic response. Tumor cells employ a number of cellular immunosuppressive strategies to evade host clearance

including reduced immunogenicity through antigen loss, downregulation of MHC, expression of immune checkpoints and induction of antitumor T cell anergy and exhaustion[42,52].

As previously discussed, the immunoediting hypothesis describes immune evasion by loss of antigens, giving rise to variants that are more aggressive and poorly differentiated. Examples are "cold tumors" that are non-inflammatory, can downregulate MHC, alter peptide processing, and decrease mutational load. All of these characteristics lead to immune escape and induction of an immunosuppressive microenvironment.

Initially, tumors may have immunogenic properties that elicit an antitumor response, but due to immune editing they ultimately inhibit or tolerize these effector cells in the tumor microenvironment[42]. T cells require co-stimulation for activation, so abnormal activation (i.e. without co-stimulation) of tumor-reactive T cells can lead to anergy and exhaustion. Tumor cells can express self-MHC but may not express the necessary costimulatory signals, and accessory cells that express costimulatory molecules may not be present. When TCR ligation occurs without co-stimulation, this can induce unresponsive, anergic T cells[42,60]. Immature APCs can also cross-present tumor antigens without co-stimulation, resulting in T cell tolerance and anergy. Anergic T cells become nonresponsive, losing the ability to proliferate or produce IL-2[42].

T cell exhaustion can also be induced by overexpression of inhibitory ligands on tumor cells such as programmed cell death ligand-1 (PD-L1). Immune checkpoints are inhibitory receptors that are upregulated on immune cells to prevent overactivation[61]. When activated, these checkpoint pathways induce inhibitory signals, resulting in T cell

exhaustion. While critical to prevent autoimmunity, tumors exploit these pathways by overexpression of immune checkpoints to reduce T cell function and avoid clearance[61].

Cancer Immunotherapies

Cancer therapies include surgical resection of the tumor, chemotherapy, radiation therapy and immunotherapies. Chemotherapy is a current form of cancer treatment that is still widely used. Classical chemotherapy poisons DNA replication mechanisms. Since tumor cells grow faster than normal cells, chemotherapy kills cells that divide rapidly. However, non-malignant cells such as neutrophils, hair follicles and cells lining the gut are also adversely affected.

Resistance to chemotherapy poses a significant obstacle for long-term survival. Therapeutic failure can be intrinsic due to genetic mutations that exist before treatment or acquired through alterations induced by drug treatment[62]. Cellular resistance emerges to traditional chemotherapy and targeted therapeutics, including kinase inhibitors and hormone therapies[63]. Resistance to traditional chemotherapy can be attributed to physiological factors, including tumor inaccessibility, drug metabolism, and inadequate delivery[63,64].

Cell or tissue-specific factors can also contribute to resistance. Common mechanisms include changes in drug export, altered DNA damage responses, and dysregulation of cell death pathways. One mechanism is the overexpression of ABC transporters that act as drug efflux pumps to lower intracellular drug concentration[62]. The majority of chemotherapies act by inducing DNA damage to trigger apoptosis. Since DNA damage signaling in cancer is impaired, cell arrest and apoptosis may not be

induced, favoring tumor growth and resistance[62]. Activation of oncogenes and inactivation of tumor suppressor genes contributes to drug resistance. For example, gain-of-function mutations in phosphatidylinositol 3-kinase (PI3K) leads to activation of Akt and mTOR signaling, which increases anti-apoptotic proteins[62]. Loss-of-function in tumor suppressor PTEN, a negative regulator of Akt, also increases Akt signaling[63]. Anti-neoplastic drugs such as Temsirolimus, an mTOR inhibitor used for targeted treatment of renal cell carcinoma (RCC), improves recurrence rates but is not curative[65].

Resistance can arise to targeted chemotherapies. Receptor tyrosine kinases (RTKs) are an important therapeutic target as they regulate intracellular signaling and contribute to the development and dysregulation of proliferation in cancer[66–68]. Tyrosine kinase inhibitors (TKIs) target pathways by blocking the receptor or its activating ligand (growth factors)[62]. Tumors that are resistant to cytotoxic chemotherapies, most notably metastatic RCC, may respond to TKIs[68]. An FDA-approved TKI, sunitinib, specifically inhibits VEGFR and PDGFR, and has been shown to reduce tumor growth and angiogenesis in metastatic RCC[69]. However, resistance arises to these targeted inhibitors. This may be mediated by mutations in the receptor or downregulation of the receptor which can lead to loss of growth factor dependence[62,70]. Mutations in downstream signaling molecules of RTKs, including Ras/Raf, also contribute to TKI resistance as the cell becomes insensitive to receptor inhibition[71].

In contrast to chemotherapy, cancer immunotherapies work to activate the patient's own immune system by targeting tumor-specific or tumor-associated antigens. Immunotherapies circumvent the issue of off-target effects by utilizing a specific target expressed by the patient's tumor. The goal of immunotherapies is to re-activate the host's

immune system to recognize and respond to cancer. In the following section, several examples of newer cancer immunotherapies are highlighted.

Immune checkpoint inhibitors

Immune checkpoint pathways are negative regulators of the immune system. Development of immunomodulators that block these pathways, such as monoclonal antibodies (mAbs), promotes therapeutic antitumor immunity. The goal of immune checkpoint therapies (ICT) are to prevent the induction of inhibitory signals that negatively regulate T cell activation[72]. The result of blocking immune checkpoints is that T cells which recognize a tumor cell would remain active and not only recognize, but also kill the cell. Many of these therapies are FDA-approved for the treatment of numerous tumor types including lung, kidney, bladder, prostate, melanoma, and lymphoma[49]. ICT has shown dramatic, durable clinical benefits in patients, transforming the field of cancer immunotherapy and replacing traditional toxic chemotherapies as frontline treatment options.

An immune checkpoint, CTLA-4, is a negative regulator of T cell proliferation and activation. CTLA-4 expression on T cells is correlated with immune suppression and prevention of autoimmunity. The mechanism of CTLA-4 mediated suppression of T cells is as follows. CD28 on T cells normally provides a co-stimulatory signal, along with TCR/CD3 primary signaling for effector T cells. Since CLTA-4 has a greater binding affinity for CD80/86 than CD28, binding of CTLA-4 to CD80/86 acts as a negative regulator of T cell activation[73]. Thus, it was hypothesized that blocking CTLA-4 ligation to CD80/86 may allow T cells to remain activated because they would not receive a

negative signal. This would have the effect of enhancing T cell antitumor activity and inducing tumor regression[73,74]. Ipilimumab is an FDA-approved recombinant human mAb that blocks CTLA-4 binding to CD80/86 and has shown to enhance T cell activation, reduce tumor growth, and increase overall survival[73].

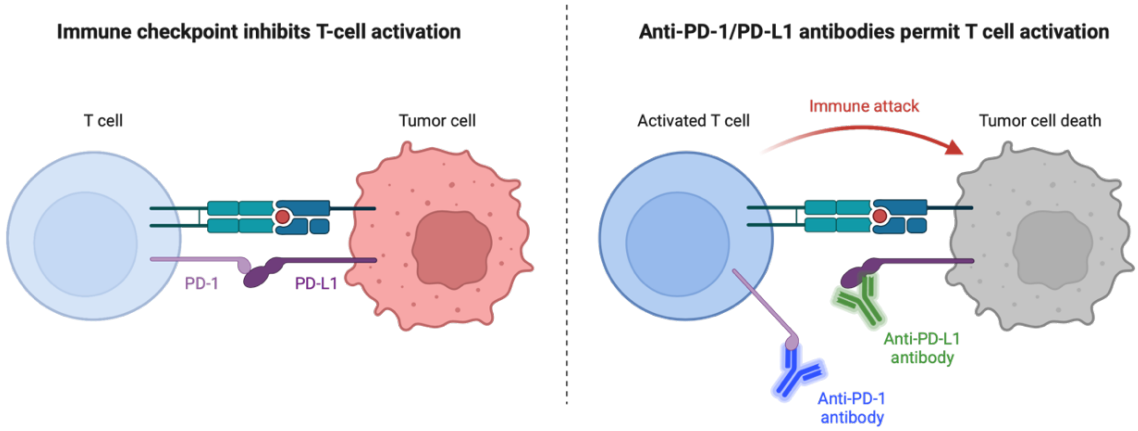

Figure 2. PD-1/PD-L1 immune checkpoint blockade therapy. Engagement of PD-1 on T cells with its ligand PD-L1 inhibits T cell activation and proliferation, leading to apoptosis. PD-1/PD-L1 blockade therapy using monoclonal antibodies to inhibit the interaction promotes T cell activation, thereby restoring antitumor activity. (Created using Biorender.com)

The PD-1/PD-L1 axis is also a validated target for immune checkpoint therapy (Figure 2). The role of programmed death-receptor 1 (PD-1) is to limit the inflammatory activity in peripheral tissue that is elicited by effector T cells, to therefore limit autoimmunity[74]. When PD-1 is expressed on activated T cells and binds to its ligand, PD-L1 on APCs, it induces a negative signal that shuts off T cell activation and proliferation[75,76]. Tumors exploit this pathway as a mechanism of resistance to T cell killing by overexpressing PD-L1[77]. Activation of this pathway in the tumor

microenvironment inhibits infiltrating antitumor T cell responses, and provided the rationale for development of PD-1/PD-L1 blockade therapies[74,78]. Two antibodies against PD-1 (nivolumab, pembrolizumab) and three against PD-L1 (atezolizumab, avelumab, durvalumab) have been developed and approved by the FDA for clinical use[77].

Another potential immune checkpoint therapy is blocking LAG-3 on T cells. Like CTLA-4 and PD-1/PD-L1, LAG-3 inhibitory receptor is being investigated as an ICT, with several antagonists being evaluated[79]. Targeting LAG-3 expressed on TILs and Tregs is also being explored as a checkpoint inhibitor therapy. LAG-3 has been associated with T cell inhibition and anergy[74]. Blockade of LAG-3 has been shown to restore cytotoxic activity of TILs and reduce inhibitory effects of Tregs[80,81]. As of 2022, there are 16 LAG-3 targeting therapies being tested in 97 clinical trials, many being tested phase I/II clinical trials to treat solid and hematologic malignancies[79]. Anti-LAG-3 monoclonal antibodies (relatlimab, fianlimab, ieramilimab, favezelimab, etc.) are being tested in combination with anti-PD-1/PD-L1 inhibitors in patients with refractory, advanced malignancies (NCT03470922, NCT01042379, NCT02460224, NCT05064059)[79]. In March 2022, the FDA approved nivolumab and relatlimab, a combination of anti-PD-1 and anti-LAG-3 monoclonal antibodies for the treatment of unresectable or metastatic melanoma.

Another immunotherapy target, CCR4, is expressed on Tregs, tumor cells and on non-Treg $CD4^+$ T cells with Th2 phenotype, but to a lesser extent[82]. Expression of CCR4 is correlated with decreased survival compared to patients that are CCR4-negative[83]. Anti-CCR4 (mogamulizumab) is a humanized monoclonal antibody that elicits enhanced antibody-dependent cellular cytotoxic (ADCC) activity on CCR4-positive tumors and

tumor-infiltrating Tregs[82,83]. More potent ADCC is attributed to the removal of fucose from the Fc region[84]. Phase II clinical trials (NCT01192984; NCT0088892) have shown that anti-CCR4 significantly reduces Tregs and exhibits promising response rates and antitumor effects[83,84].

Cellular-based immunotherapies

Adoptive T cell therapies (ACTs) are an emerging field of cancer immunotherapy that involve genetic modification of patient-derived autologous T cells that can be reinfused for therapeutic effect[48]. Chimeric antigen receptor T cells (CAR T cells) are one of the most developed and successful cellular immunotherapies, showing promising clinical outcomes in treating hematologic malignancies. Generation of CAR T cells involves *ex vivo* engineering of a patient's T cells with a lentiviral construct that encodes a single chain variable fragment (scFv) of an antibody that is specific for a tumor cell surface antigen[48]. By targeting antigens expressed on the cell surface, T cell specificity is redirected to recognize and perform direct cell killing of cancer cells in an MHC-independent manner. Since CAR T cells can recognize intact cell surface antigens, these cells are not restricted by MHC or peptide processing, therefore bypassing central tolerance. The first FDA-approved CAR T cell therapy targets CD19 on B cell malignancies and was first approved for the treatment of acute lymphoblastic leukemia (ALL). There are currently six FDA-approved CAR T cells targeting either CD19 or BCMA, and additional targets are currently being investigated in clinical studies[85].

T cells can also be redirected by transfer of antigen-specific T cell receptors. Like CAR T cells, T cells can be engineered to express TCRs that recognize tumor-specific

peptides. Tumor-specific TCRs can be isolated from T cells in cancer patients or from *in vitro* stimulation of T cells with tumor peptides[86]. A phase I/II clinical trial is investigating autologous T cells engineered to express neoantigen-reactive TCRs for the treatment of relapsed/refractory solid tumors (NCT05194735). The main disadvantage of this approach is that recognition is MHC-restricted. Thus, tumor escape mechanisms, including downregulation of MHC and altered peptide processing, pose major obstacles[86].

Another ACT involves the identification of neoantigens that are cancer-specific. Neoantigen-reactive T cell (NRT) immunotherapy targets these neoantigens, resulting in fewer off-target effects, as these cells are highly tumor-specific[87]. NRT therapy involves isolating tumor cells and CD8+ T cells from patients and identifying neoantigens by sequencing. Neoantigen-reactive T cells are generated by co-culturing CD8+ T cells with APC-expressing neoantigens; these antitumor CTLs are then expanded and re-infused into the patient[87]. A phase I/II trial combines NRTs with a PD-1 inhibitor for the treatment of advanced solid tumors that are refractory to available treatments (NCT03171220). NRTs are being tested in clinical trials but currently lack large-scale evidence of safety and efficacy.

Overall, ACTs are initially effective but many patients eventually relapse due to antigen escape variants and potentially poor persistence of the therapeutic T cells *in vivo*[88]. This may be due to culturing conditions, reduced transgene expression, T cell exhaustion, poor effector function or induction of humoral immune response[86]. Another challenge of ACTs is the overproduction of proinflammatory cytokines resulting in cytokine release syndrome (CRS), resulting in high-grade fevers and hypotension[89,90].

These side effects are usually manageable by suppressing certain cytokines such as IL-6[86]. Although adverse effects have been associated with ACTs, these therapies have shown remarkable therapeutic success for advanced tumors that are refractory to first-line therapy.

Regulatory T cells

Regulatory T cells (Tregs) are a subpopulation of $CD4^+$ T cells that suppress inflammatory immune responses and maintain homeostasis. Human Tregs are described as $CD4^+CD25^{high}$ $CD127^{low}Foxp3^+$ cells. Foxp3 is known as the master regulator of Treg transcription as it controls gene expression required for Treg development and function[18]. Tregs are defined as expressing high levels of CD25, the high-affinity IL-2 receptor α-chain, and low levels or absence of CD127, the IL-7α receptor[91]. CD127 is inversely correlated with Foxp3 and suppressive function[92]. Tregs are phenotypically and functionally diverse cells that constitute a low percentage (<1-5%) of $CD4^+$ T cells. Within this small population, high heterogeneity exists as there is not a single Treg-specific marker to differentiate them from other $CD4^+$ T cells[93].

Tregs can originate in the thymus (thymic-derived or natural Tregs, nTregs) or can be induced in the periphery after leaving the thymus (peripherally-induced, iTreg). Both subsets are able to suppress inflammatory effector T cells. nTregs recognize tissue-specific antigens; thus, depletion results in organ-specific autoimmunity[94]. Tregs can be generated *in vivo* and *in vitro* from naïve conventional $CD4^+$Foxp3- T cells[95]. *In vitro*, TCR-activated Tregs exhibit non-antigen specific suppressive function[95]. This has been demonstrated for polyclonal and antigen-specific Tregs[95,96]. In the periphery, polyclonal

Treg proliferation depends on MHC class II signals and co-stimulation but does not require recognition of cognate antigens for development, function or persistence of this population[94,97].

Immunological self-tolerance is a crucial mechanism by the immune system to avoid unwanted responses against itself. Lymphocytes that recognize self-antigens are called self-reactive T and B cells. Central tolerance is the process in which immature cells are eliminated during development in the bone marrow (B cells) or in the thymus (T cells), before reaching maturation[98]. However, self-reactive T and B cells can escape this selection process and be present in the periphery[99]. Mature lymphocytes that do not respond to self-antigens and the elimination of self-reactive cells in other lymphoid organs and tissues is called peripheral tolerance[99].

Tregs play a critical role in self-tolerance mechanisms. Tregs recognize autoreactive immune cells and help to eliminate them and/or induce anergy to sustain self-tolerance, thereby preventing autoimmunity. During an infection, Treg suppressive activity may be neutralized to promote clearance.[50] Conversely, Tregs are needed to suppress persistent inflammation after an infection is cleared. Dysregulation of Treg function plays a critical role in cancer, graft rejection and autoimmune diseases[99]. Therefore, Tregs are an important but under-studied therapeutic target.

Treg-associated markers

A major obstacle in the study of Tregs is their lack of a defined cell surface marker that can definitively distinguish them from other T cells. Tregs express high levels of CD25, and this marker is used to identify human Tregs in peripheral blood with

high suppressive function[91]. However, in humans, CD25 is also expressed heterogeneously on other activated, non-suppressive T cells[91,100]. This further supports the need for identification of Treg-specific markers.

Foxp3 is an intranuclear protein expressed in Tregs. It is critical for immune self-tolerance since dysfunction of Foxp3, such as a mutation in *FOXP3*, leads to fatal autoimmunity[18]. It is a known marker for Tregs, which allows for better phenotypic identification than measuring CD25 alone. In mice, Foxp3 and CD25 markers are constitutively expressed in murine Tregs. A Treg-deficient mouse model, scurfy mice, lack functional Foxp3[101,102]. Expression of Foxp3 makes it a potential therapeutic target, but since Foxp3 is an intranuclear protein, it has been difficult to target.

In contrast to murine Tregs, expression of Foxp3 in human Tregs is not as clear-cut. Foxp3 is important for Treg development and function, but is not exclusive to Tregs and can also be expressed in other human T cell subsets that do not exhibit suppression function[98]. Moreover, peripherally-induced Tregs may not express Foxp3[47]. Another drawback is that Foxp3 is exclusively located in the nucleus, which requires permeabilization of the cells in order to measure its expression[92]. Permeabilized cells die due to disruption of membrane integrity and therefore cannot be used in downstream functional applications[92]. Thus, Foxp3 is not an adequate marker for discriminating human Tregs from other non-suppressive T cells.

Helios, a transcription factor in the Ikaros family, is preferentially expressed by Tregs. Ikaros family transcription factors are important in hematopoietic cell development. Helios was found to be restricted to the T cell lineage and more specifically in $Foxp3^+$ Tregs[103]. Since Helios plays a role in lineage commitment and development, it

is exclusively expressed in natural, thymic-derived Tregs and not in peripherally-induced Tregs[47,103]. Therefore, Helios expression can be measured to distinguish nTregs from iTregs. Some populations of tumor-associated Tregs express Helios. The majority of Tregs isolated from blood of patients with RCC and ovarian cancers expressed Helios, suggesting thymic origin[47].

Co-inhibitory receptors

Cytotoxic T lymphocyte associated-antigen 4 (CTLA-4) is constitutively expressed on Tregs[95] and contributes to suppressive function and effector T cell anergy. The function of CTLA-4 is not to deliver an inhibitory signal to Tregs themselves, but to competitively bind to CD80/86 co-stimulatory molecules on antigen presenting cells which has the effect of sequestering CD80/86 ligands from the cell surface of APCs[104]. In this manner, Tregs utilize CTLA-4 as a mechanism of suppression by inhibiting DC activation of effector T cells at the immunological synapse[91]. CTLA-4 can also disrupt CD28 localization and inhibit TCR signaling[104]. A study by Wing et. al, found CTLA-4-deficient Tregs have impaired suppressive function, promoting tumor immunity and development of autoimmune disease[105].

Glucocorticoid-induced TNF receptor (GITR or TNFRSF18) is highly expressed on Treg cell surface but is also upregulated on effector T cells upon activation[106]. Ligation of GITR-L with TCR stimulation induces Treg proliferation[107]. Studies have shown that cross-linking GITR with a mAb agonist, as opposed to blocking, can attenuate Treg-mediated suppression and co-stimulate effector T cells, resulting in an increase in antitumor immunity[107]. However, another study using soluble GITR-L did not abrogate

suppressive activity of Tregs[106]. Therefore, the GITR-GITR-L pathway is still under investigation and regulatory function may not be dependent on GITR.

Lymphocyte activation gene-3 (LAG-3) is expressed on both nTregs and iTregs and contributes to regulatory function, playing a critical role in T cell homeostasis. Although it is upregulated on activated $CD4^+$ T cells, it is expressed at higher levels on Tregs compared to effector T cells[108]. LAG-3 is structurally similar to CD4 and binds to MHC class II with higher affinity[108]. LAG-3^+ Tregs produce high levels of IL-10 and TGF-β, exhibiting an activated phenotype. Camisaschi et al., found LAG-3^+ Tregs were selectively expanded at tumor sites, produced suppressive cytokines, and inhibited autologous responder T cells by direct cell-contact[109].

C-C chemokine receptor type 4 (CCR4) is a chemokine receptor expressed on Tregs that aids in peripheral migration. CCR4-deficient Tregs cannot migrate to certain sites of inflammation, specifically non-lymphoid tissues[110]. $CCR4^+$ Tregs exert suppressive function, produce immunomodulatory cytokines, and exhibit an effector-memory phenotype[111]. Tumor-infiltrating Tregs predominately express CCR4, providing a potential target for antitumor therapy.[47]

Overall, these markers are expressed on Tregs but do not accurately distinguish the Treg population from other lymphocyte subsets and have other functional activities. Subpopulations of Tregs have been identified due to expression of markers that are associated with antigen specific suppression, migration, homing, and activation, thereby supporting high heterogeneity of Tregs[91] and the need for the identification of Treg-specific markers.

Mechanisms of Treg-mediated Immune Suppression

Tregs suppress the activation, proliferation, cytokine production and overall effector function of T cells and other immune cells. Treg heterogeneity contributes to the many ways these cells exert suppressive activity. Tregs use different mechanisms to mediate suppression depending on the inflammatory environment. Mechanisms include turning off effector T cells by direct cell-contact, indirectly through APCs as described above, through metabolic disruption and through release of anti-inflammatory cytokines[91] (Figure 3). Suppression results in altered gene expression, inhibited growth and reduced proliferation of the target cells[112].

Indirect via CTLA-4

One of the most well-understood Treg-suppressive mechanisms involves indirect suppression of effector T cells via APCs. Tregs can downregulate or prevent expression of CD80/CD86, which is mediated by CTLA-4[95]. Thus, CTLA-4 impairs APC maturation by binding to CD80/86, which are major co-stimulatory molecules required for activation of T cells. T cells express co-stimulatory molecule CD28 that binds to CD80/86 expressed on APCs to provide co-stimulation for activation. Since CTLA-4 has a higher affinity for these molecules than CD28, this competitive binding results in impaired activation. Tregs can also physically remove CD80/86 from the cell surface of APCs by trogocytosis[113].

IL-2 deprivation

Tregs constitutively express CD25, the high affinity IL-2 receptor α chain. Since Tregs express higher levels of IL-2R and generally do not produce IL-2, these cells are highly dependent on exogenous IL-2 for growth and proliferation. By expressing high

levels of the high affinity IL-2 receptor, Tregs are able to consume this cytokine required for T cell activation and proliferation. The depletion of IL-2 so that it cannot stimulate effector T cells can result in apoptosis due to cytokine deprivation, occurring both *in vivo* and *in vitro*[112]. Tregs act as an "IL-2 sink" at the site of inflammation, resulting in T cell exhaustion, upregulation of PD-1, and susceptibility to PD-1/PD-L1 cell death[114].

Production of anti-inflammatory cytokines

Production of anti-inflammatory cytokines have been implicated in Treg suppressive function. Immunomodulatory cytokines such as IL-10, TGF-β, and IL-35 are secreted by Tregs to influence target cell function. These cytokines can directly inhibit synthesis of pro-inflammatory Th1 cytokines and elicit negative feedback in both APCs and effector T cells. Secretion of suppressor cytokines has been found to important for *in vivo* suppressive function but the role *in vitro* is more controversial and not well defined[115].

Granzyme/perforin killing

Tregs can perform direct killing of responder T cells by utilizing the cell contact-dependent perforin/granzyme pathway. Tregs produce cytotoxic granules which induce cytolysis of target cells through a perforin-dependent manner[115]. Perforin is used to traffic granzymes intracellularly, where they cleave substrates to induce cell death[116]. $CD8^+$ T cells and NK cells also use the granzyme/perforin pathway to kill target cells. Granzymes play a role in Treg antitumor immunity. Cao et al., found that tumors increased granzyme expression in Tregs, which induced NK cell and $CD8^+$ T cell death, and resulted in reduced tumor clearance and suppressed antitumor immunity[116].

Conversion of ATP to adenosine

Surface co-expression of CD39 and CD73 provides another suppressive mechanism utilized by Tregs. CD39 is an enzyme that catalytically inactivates ATP by conversion to AMP[74]. Tregs use CD39 to inactivate extracellular ATP, which is critical as extracellular ATP is important for rapidly proliferating T cells in proinflammatory immune processes[117]. CD39 removes extracellular ATP, converting to AMP, and CD73 subsequently degrades nucleosides, which consequently generates the immunosuppressive metabolite, adenosine[115,117]. Adenosine generated by CD73 nucleotidase can directly inhibit DC function and activated T cells, downmodulating immune function[117]. Binding of adenosine results in increased intracellular cAMP and leads to suppressed cytokine production and cell proliferation[112]. Studies have shown that loss of CD39 or addition of adenosine receptor antagonist can effect Treg suppression[112]. However, it has not been determined how an increase in cAMP results in downstream inhibition.

Transforming growth factor-β (TGF-β) may also play a role in Treg-mediated T cell suppression, but this mechanism remains controversial. Tregs secrete TGF-β but suppress responder T cell proliferation independent of IL-10 and TGF-β *in vitro*. Others have proposed a role for cell surface-bound TGF-β, as *in vitro* suppression requires cell-cell contact[118]. *In vivo* studies have shown suppression of T cells requires expression of TGF-β receptor on responder cells. Tregs bearing cell-surface TGF-β can interact directly with its receptor on effector T cells, resulting in inhibition of activation[118]. Although it is unclear if TGF-β production is required by Tregs, it is known that TGF-β production favors immunosuppression.

Tregs secrete or consume cytokines to downregulate effector function of cells in close proximity. Overall, suppression can be elicited in three categories: direct cell-to-cell contact, production of soluble inhibitory cytokines, and competition for cytokines required for cell growth[112] (Figure 3). It is known that these mechanisms are not mutually exclusive. Multiple suppressive pathways may be elicited simultaneously depending on the site of inflammation. There are still many unknowns in Treg-mediated suppression. Mechanisms that have been characterized *in vivo* fail to be confirmed *in vitro*, and vice versa.

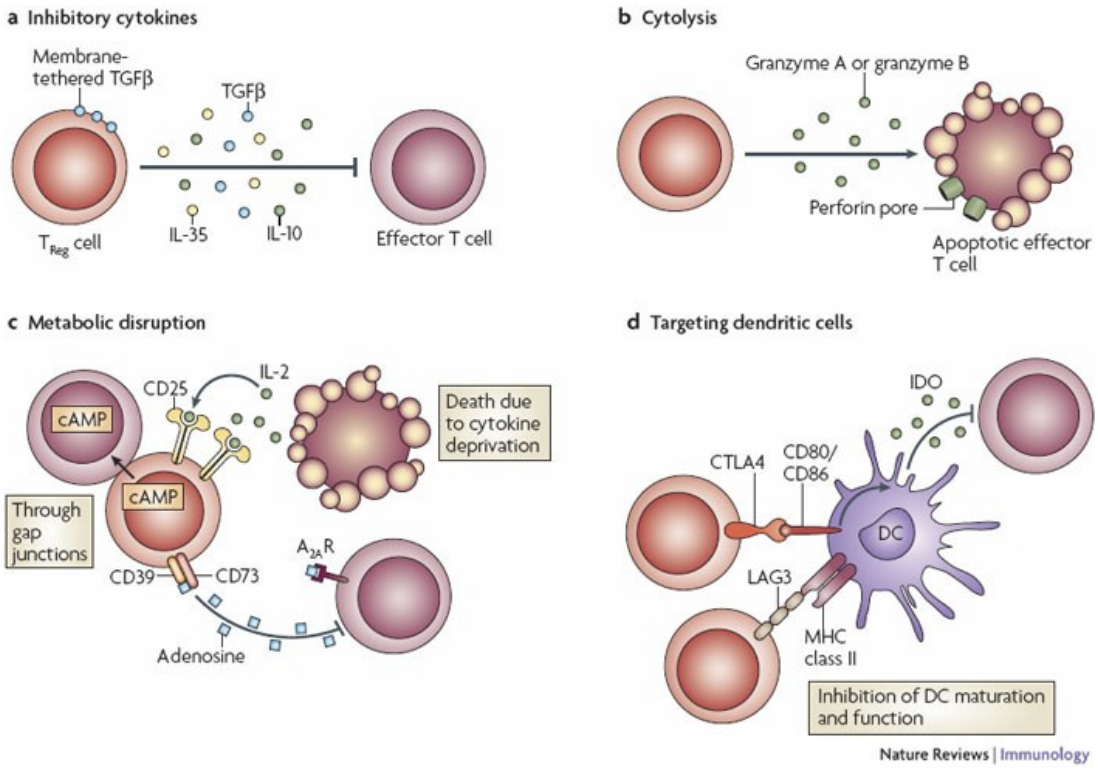

Figure 3. Mechanisms of Treg immune suppression. Four characterized mechanisms of Treg-mediated suppression include: A) production of inhibitory cytokines, B) cytolysis via granzyme/perforin pathways, C) metabolic disruption via IL-2 deprivation and generation of immunosuppressive metabolites, and D) targeting dendritic cells through modulating DC function. Vignali DAA, Collison LW, Workman CJ, How regulatory T cells work, *Nature Reviews Immunology*, 8, 523-532, 2008, Springer Nature. *Reproduced with permission from Springer Nature*.

Tregs in autoimmunity

Tregs play a critical role in preventing unwanted inflammation that can lead to autoimmunity. In patients with autoimmune disease, Treg function is hindered or significantly reduced. Defects in Treg function have been described in most autoimmune diseases including type I diabetes (T1D), inflammatory bowel disease (IBD), psoriasis, multiple sclerosis (MS), and rheumatoid arthritis (RA)[95]. Patient-derived autoreactive T cells have a lower activation threshold but were not shown to be resistant to Treg suppression[119]. Thus, autoimmunity can be attributed, in part, to Treg dysfunction. Loss of function has been correlated with decreased Foxp3; however, genomic data of patients with MS, T1D, and RA did not reveal a genetic mutation in *FOXP3*[119].

The role of reduced Treg function in autoimmunity provides therapeutic potential to enhance Treg suppressive activity. Multiple therapies are being investigated to expand Tregs and increase suppressive function. Clinical trials testing the use of low dose IL-2 to promote Treg expansion have shown an increase in Tregs in GVHD patients (NCT00529035)[120] and improvement of hepatitis C-induced vasculitis (NCT00574652)[121]. Another therapeutic approach utilizes autoantigens to expand antigen-specific Tregs to induce tolerance[114]. Lastly, adoptive cell transfer of Tregs is being investigated as an effective therapy for autoimmunity and GVHD.

An example of utilizing Treg cell transfer to treat autoimmunity is in amyotrophic lateral sclerosis (ALS), a neurodegenerative autoimmune disease that destroys motoneurons[122]. As the disease enters a rapidly progressing phase, Treg numbers are significantly reduced, potentially due to loss of Foxp3 expression[122]. A phase I trial for the treatment of ALS tested the safety and tolerability of autologous Tregs that were

expanded *ex vivo* and re-infused into patients (NCT03241784). Results of the trial showed infusions were safe and slowed disease progression rates in early and late stages of ALS[123]. Challenges of autologous cell transfer include isolation of large quantities of Tregs, survival of *ex vivo* expanded and transferred cells, loss of activation and suppressive activity, and lack of antigen specificity that may be required[114]. Future studies may require the use of non-autologous Tregs, since patients with autoimmune diseases have a very limited number of Tregs to isolate.

Tregs in tumor immunity

Treg immune suppression is a double-edged sword. While Tregs are crucial for immune tolerance and suppressing inflammation, these cells can impede immunosurveillance in the context of tumors[107]. Since a main function of Tregs is to suppress effector T cells, this consequently limits functional infiltrating antitumor immune responses. Tregs can recognize self-antigens through their TCR. Since tumor cells express self-antigen, Tregs are more easily activated than effector T cells[110]. Recognition of self-antigens increases Treg-mediated tolerance within the tumor microenvironment. However, both antigen-specific and polyclonal (TCR-activated) Tregs exert suppressive function in an antigen-independent manner[124].

Tregs are recruited to the tumor microenvironment through the production of chemokines, increased inflammatory cytokines and expression of self-antigens. Tumor cells and infiltrating macrophages both express CCL22, a chemoattractant that is recognized by CCR4[125]. Expression of CCL22 signals to CCR4-expressing Tregs to migrate to the site of inflammation by direct trafficking to specific tissues[53]. It has been

shown that blocking CCL22 can reduce Treg trafficking, suggesting a potential target for antitumor therapy[126].

Tregs that have accumulated in the tumor microenvironment or draining lymph nodes can recognize tumor-associated self-antigens, leading to Treg proliferation and expansion[125]. Tregs require ligand-specific activation through APCs at the tumor site but do not require recognition of antigen[100,124]. Production of TGF-β by tumor cells can also induce Foxp3$^+$ Tregs in the periphery[125]. The recruitment, activation and expansion of Tregs dampens antitumor responses.

Tregs suppress a variety of immune cells including T, B, NK and dendritic cells. Effector T cells are activated through the TCR that recognizes TAAs presented by MHC molecules on APCs, and require a co-stimulatory signal along with MHC-TCR interactions to be activated and expanded. As discussed, Tregs can inhibit effector T cell activation and diminish antitumor activity by a number of mechanisms.

In cancer, Treg function is enhanced and these cells are recruited by the chronic inflammatory environment in tumors to suppress antitumor responses, favoring tumor progression. Treg-mediated immunosuppression promotes tumor escape of the immune system, which has been associated with unfavorable outcomes for patients[53]. Curiel et al., showed that adoptive transfer of human tumor Tregs into tumor-bearing mice resulted in accumulation of Tregs in tumor tissue, suppression of T cell immunity, and allowed increased tumor growth *in vivo*[126]. Moreover, Antony et.al, demonstrated that transfer of Treg-depleted CD4$^+$CD25$^-$ T cells in mice induced tumor regression and long-term survival[127]. These studies demonstrate that Tregs are potent mediators of immune suppression and enhance tumor progression.

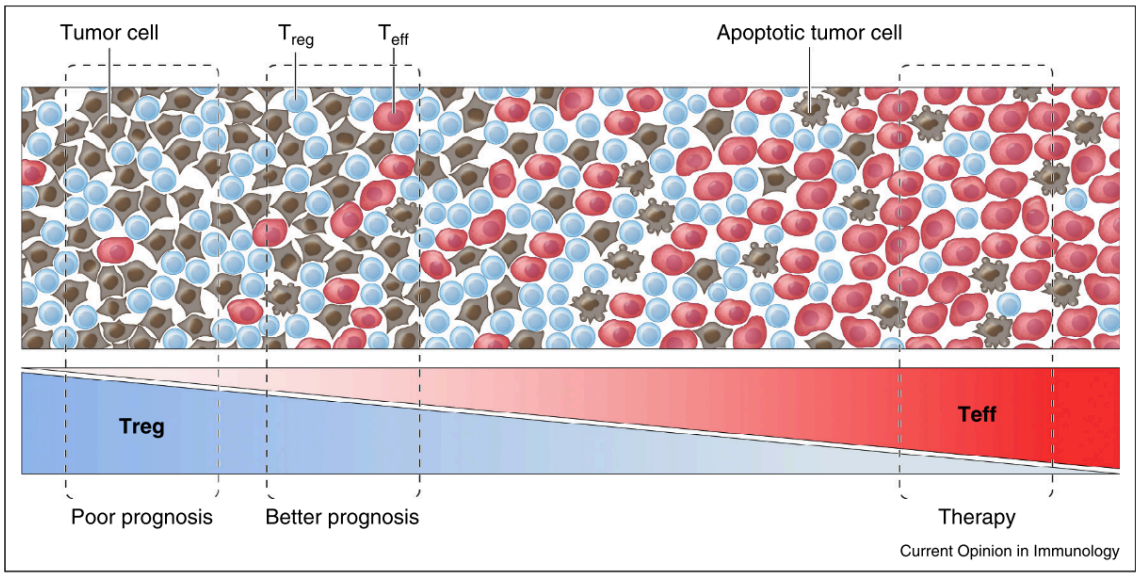

Figure 4. The balance between effector T cells (Teff) and Tregs in the tumor microenvironment influneces immune responses. High Treg:Teff ratios are typically present in solid tumors, leading to poor outcomes. Lower Treg:Teff ratios are associated with better prognosis. An increase in the number of Teff cells through therapuetic manipulation of Treg:Teff ratios results in increased apoptosis of tumor cells. Tregs (blue), effector T cells (red), tumor cells (brown). Reprinted from *Current Opinion in Immunology*, 33, Roychoudhuri R, Eil RL, Restifo NP, The interplay of effector and regulatory T cells in cancer, 101-111, 2015, with permission from Elsevier.

Tregs are implicated in numerous cancers and especially in solid tumors. Low Treg to effector T cell ratios correlate with favorable prognosis in a number of human tumors including breast, ovarian, lung, renal, pancreatic and colorectal carcinomas[50]. Many tumors have been shown to have a considerable number of tumor-infiltrating Tregs and decreased $CD8^+$ T cells[110]. Increased Tregs in the tumor microenvironment negatively correlates with patient survival and response to immunotherapy[110]. Therefore, the balance between antitumor T cells and Tregs in the tumor microenvironment influences the efficacy of immune responses and antitumor therapies (Figure 4). Targeting Treg function and activating antitumor T cells may enhance the efficacy of

cancer immunotherapies[124]. Blocking Tregs by attenuating their suppressive activity or reducing the overall number of Tregs, thus increasing the ratio of effector T cells, would allow for increased antitumor immunity and response to other therapies.

There is a high clinical and scientific need to study Treg function to better understand and characterize mechanisms of Treg suppression of effector T cells. The exact mechanism of Treg-mediated immune suppression in tumors is unclear. The development of therapeutics that specifically target human Tregs is hindered by their low abundance in blood (<1%) and high heterogeneity (mixed populations). Isolation of Tregs is an obstacle as it relies on expression of a cell surface protein[128]. Since they lack a specific cell surface molecule that distinguishes these cells from other T cell subtypes, this makes these cells difficult to study and functionally characterize. Tregs also hinder the therapeutic efficacy of current immunotherapies. Identification of a Treg-specific cell surface molecule that mediates suppression would provide a key target for immunomodulation, in conjunction with current immunotherapies, and offer a cell-specific method to differentiate this population.

In Chapter 2, titled "Identification of a $CD4^+$ T cell line with Treg-like activity," a $CD4^+$ T cell line (MoT cells) was characterized and found to be phenotypically similar to and exhibit cell contact-dependent suppressive activity like Tregs derived from peripheral blood. Suppression by PBMC-derived Tregs and MoT cells was found to be independent of soluble cytokines and known immune checkpoint pathways, providing evidence for an uncharacterized suppressive mechanism.

In Chapter 3, titled "Generation and characterization of a monoclonal antibody that binds to Galectin-1", Galectin-1 (Gal-1) was investigated as a potential cell surface

suppressive molecule. Proteomic analysis of the cell surface-ome found Gal-1 to be expressed on both MoT cells and Tregs, while absent on Jurkat cells. It was hypothesized that cell surface-bound Gal-1 mediates MoT suppression of $CD4^+$ T cells. To test this, monoclonal antibodies to Gal-1 were generated and characterized for binding and functional activity.

In Chapter 4, titled "Characterization of monoclonal antibodies (mAbs) that bind to MoT cells," monoclonal antibodies were generated to the MoT cell surface and tested for binding and functional activity. Since MoT cells and Tregs mediate suppression by direct cell-contact, it was hypothesized that these cells express one or more molecules on the cell surface that mediates suppressive function. Monoclonal antibodies that bound to MoT cells and not Jurkat were expanded and tested for the ability to block suppressive function.

In Chapter 5, titled "Construction and characterization of anti-PD-L1 chimeric antigen receptor T cells that selectively kill PD-L1-positive tumor cells," an anti-PD-L1 scFv CAR T cell lentiviral construct was designed and T cells were infected with lentivirus to express the scFv. These CAR T cells were expanded and tested for the ability to kill PD-$L1^+$ human and murine kidney and lung tumor cells. CAR T cell killing was restricted to PD-$L1^+$ cells and did not kill non-malignant cells.

Chapter 6, "Discussion," summarizes the implications of the previous chapters, including characterizing and targeting Treg suppressive activity, developing ACTs and checkpoint blockade immunotherapies, and future direction of the research.

CHAPTER 2

IDENTIFICATION OF A $CD4^+$ T CELL LINE WITH TREG-LIKE ACTIVITY

Originally published in *Human Immunology,* January 2022, Volume 83, Issue 4

Thai H. Ho*, Kirsten Pfeffer*, Glen J. Weiss, Yvette Ruiz, Douglas F. Lake

*co-first authors

Abstract

Regulatory T cells (Tregs) suppress adaptive immunity and inflammation. Although they play a role in suppressing anti-tumor responses, development of therapeutics that target Tregs is limited by their low abundance, heterogeneity, and lack of specific cell surface markers. We isolated human PBMC-derived $CD4^+$ $CD25^{high}$ $Foxp3^+$ Tregs and demonstrate they suppress stimulated $CD4^+$ PBMCs in a cell contact-dependent manner. Because it is not possible to functionally characterize cells after intracellular Foxp3 staining, we identified a human T cell line, MoT, as a model of human $Foxp3^+$ Tregs. Unlike Jurkat T cells, MoT cells share common surface markers consistent with human PBMC-derived Tregs such as: CD4, CD25, GITR, LAG-3, PD-L1, CCR4. PBMC-derived Tregs and MoT cells, but not Jurkat cells, inhibited proliferation of human $CD4^+$ PBMCs in a ratio-dependent manner. Transwell membrane separation prevented suppression of stimulated $CD4^+$ PBMC proliferation by MoT cells and Tregs, suggesting cell-cell contact is required for suppressive activity. Blocking antibodies against PD-L1, LAG-3, GITR, CCR4, HLA-DR, or CTLA-4 did not reverse the suppressive activity. We show that human PBMC-derived Tregs and MoT cells suppress stimulated $CD4^+$ PBMCs in a cell contact-dependent manner, suggesting that a

Foxp3^{+} Treg population suppresses immune responses by an uncharacterized cell contact-dependent mechanism.

Introduction

Regulatory T cells (Tregs) play a critical role in maintaining immune tolerance to self-antigens and eliminating autoreactive cells in T cell development (natural/thymic Treg), in peripheral tissue after infection [129,130], during inflammation, and in cancer [50,125]. Tregs were first described as CD4^{+} cells that inhibited autoreactive T cells and expressed high levels of CD25 [8]. Although they play a role in autoimmunity and cancer immunosurveillance, the development of therapeutics that target human Tregs *in vivo* is limited by the low abundance, the heterogeneity of Tregs in human peripheral blood mononuclear cells (PBMCs), and the lack of specific cell surface markers that readily allow identification or enrichment of live cells so that functional studies can be performed.

Characterization of Tregs that are thymic-derived or peripherally-induced is challenging due to mixed subpopulations upon isolation, lack of a classifiable cell surface marker, and differences in their specificity and secretion of cytokines/chemokines [128,131]. Tregs produce immunosuppressive cytokines including IL-10 [132], TGF-β [50], IL-35 [133] and are found circulating in peripheral blood and in multiple tissue types [134]. Tregs can be isolated from human peripheral blood and expanded *in vitro* with the addition of IL-2, TGF-β and/or the inhibition of mTOR and PI3K with single antigens, but mixed populations result [135–137]. Tregs are characterized by CD4^{+}CD25^{high} expression; most, but not all, express Foxp3. In addition, cells that express intermediate levels of CD25 can

express low or high levels of Foxp3 [128]. Treg subpopulations are known to modulate TH1, TH2 and TH17 responses [134] via cell-to-cell contact mechanisms [105], and through the production of chemokines, cytokines, and metabolites [138]. Peripherally induced $CD4^+$ $CD25^{high}$ $Foxp3^+$ Tregs appear to modulate peripheral immune tolerance by expressing high levels of cytokines IL-10, TGF-β, IFN-γ, IL-5, and low levels of IL-2 [139]. Helios, a transcription factor, is expressed in all $CD4^+CD8^-Foxp3^+$ thymocytes, but is restricted to a subpopulation of peripheral $Foxp3^+$ T cells [103]. Treg populations, like other immune cell populations, are highly heterogenous.

To address a clinical and basic science need to better characterize Tregs and to study the molecular interactions between Tregs and activated T cells, we purified, expanded and characterized $CD4^+$ $CD25^{high}$ $Foxp3^+$ Tregs from human donor PBMCs and then identified a human T-lymphoblastoid cell line (MoT) that was previously derived from spleen cells from a patient with a T-cell variant of hairy-cell leukemia that is $CD4^+$ $CD25^{high}$ $Foxp3^+$, and has Treg-like activity [140]. Phenotypically, MoT cells and human Tregs share common surface markers such as: CD4, CD25, glucocorticoid induced TNF receptor (GITR), lymphocyte activation gene (LAG-3), programmed death receptor ligand 1 (PD-L1), and C-C Motif Chemokine Receptor 4 (CCR4). We demonstrate that $CD4^+$ $CD25^{high}$ $Foxp3^+$ MoT cells suppress CD3/CD28-stimulated $CD4^+$ T cell proliferation in a manner similar to $CD4^+$ $CD25^{high}$ $Foxp3^+$ PBMC-derived Tregs. Tregs can suppress effector T cells in a cell-cell contact dependent manner [125] and perform cell-contact dependent killing of target cells [141]. Without the presence of APCs, cell-cell contact is required for suppression of $CD4^+$ T cell proliferation by human $CD4^+$ $CD25^{high}$ $Foxp3^+$ Tregs. Cell-cell contact is essential for MoT-mediated suppression; transwell

membrane separation abrogates the suppressive activity of MoT cells. To further characterize MoT cells, we tested blocking antibodies against known immunomodulatory pathways: PD-L1, LAG-3, GITR, CCR4, HLA-DR, or CTLA-4. None of them inhibited the suppressive activity of MoT cells. Furthermore, neither MoT cells nor PBMC-derived $CD4^+$ $CD25^{high}$ cells could be inhibited by standard antibodies suggesting that one or more uncharacterized cell surface suppressive molecules may exist.

Materials and Methods

Cell lines

Tregs were isolated from whole PBMCs using EasySep Human $CD4^+CD127^{low}CD25^+$ Regulatory T Cell Isolation Kit (Catalog # 18063; Stemcell Technologies). Isolated Tregs were expanded up to four weeks. Tregs were stimulated every 7 days with the addition of soluble anti-CD3/CD28 at 1ug/ml and 2.5ug/ml, respectively, with the addition of 500 IU/ml rhuIL-2 every 2-3 days. PBMC-derived Tregs were used for staining and suppression assays 3-5 days after the 2nd or 3rd stimulations. MoT cells were a gift from the late David Golde and are also deposited in ATCC (ATCC CRL-8066; Manassas, VA, USA). They are a human T-lymphoblast cell line derived from spleen cells from a patient with a T-cell variant of hairy-cell leukemia [140]. Jurkat cells (ATCC TIB-152) are a human T-lymphocyte cell line from a patient with acute T cell leukemia. MoT and Jurkat cells were maintained in DMEM (Gibco; Grand Island, NY, USA) supplemented with 5% heat-inactivated fetal bovine serum (Atlanta Biologicals; Norcross, GA, USA). Cell lines underwent short tandem repeat validation (Promega; Madison, WI, USA) to confirm their identities.

Flow cytometry

MoT, Jurkat and PBMC-derived Tregs, at 5 x 10^5 cells per 12x75 mm flow tube were washed twice in PBS, blocked in flow cytometry staining buffer (5% FBS/PBS) for 1 hour at room temperature then incubated individually in staining buffer with each antibody specific to the following markers: Alexa Fluor 700-conjugated CD3 (eBioscience clone UCHT1), FITC-conjugated CD4 (eBioscience clone RPA-T4), PE-conjugated CD25 (eBioscience clone BC96), PE-conjugated GITR (eBioscience clone eBioAITR), Alexa Fluor 700-conjugated LAG-3 (eBioscience clone 3DS223H), PE-conjugated CTLA-4 (BD Biosciences clone BN13), PD-1 (Pembrolizumab), PD-L1 (Atezolizumab), Alexa Fluor 647-conjugated CCR4 (BioLegend clone L291H4), PE-conjugated TCR alpha/beta (eBioscience clone IP26), PE-conjugated TCR gamma/delta (eBioscience clone B1.1), Alexa Fluor 647-conjugated Foxp3 (BioLegend clone 259D), Alexa Fluor 647-conjugated Helios (BioLegend clone 22F6), Alexa Fluor 647-conjugated Granzyme A (BioLegend clone CB9) and FITC-conjugated Granzyme B (BioLegend clone GB11), each for 1 hour at room temperature protected from light. For Foxp3 staining, cells were fixed and permeabilized with the Foxp3 Transcription Factor Buffer Staining Set (eBioscience) then subsequently stained to detect intracellular Foxp3. For Helios staining, cells were fixed and permeabilized with True-Nuclear Transcription Factor Buffer Set (BioLegend) then stained to detect intracellular Helios. For Granzyme A and Granzyme B staining, cells were fixed and permeabilized with BD Cytofix/Cytoperm (BD Biosciences) to detect intracellular Granzyme A and Granzyme B. Cells were washed three times in 5% FBS/PBS and analyzed on BD FACSCelesta

(BD Biosciences). Fluorescence was quantified and expressed as mean fluorescence intensity (MFI).

Co-culture suppression assays

After IRB approval at Arizona State University (protocol #0601000548), peripheral blood was collected from healthy donors. Ficoll-Paque Plus gradient separation of the buffy coat was performed from peripheral blood. $CD4^+$ cells were purified using EasySep Human $CD4^+$ T Cell Isolation Kit (Catalog # 17952; Stemcell Technologies). Cells were allowed to rest overnight in 10% FBS/DMEM at 37°C, 5% CO_2. The following day, purified $CD4^+$ T cells were counted, labeled with CFSE dye (Carboxyfluorescein succinimidyl ester, Catalog #10009853; Cayman Chemical) according to the manufacturer's instructions, washed 3 times in 10% FBS/DMEM, counted and then plated in 10% FBS/DMEM at $2x10^5$ cells per well in a 48-well plate pre-coated with anti-CD3 clone OKT3 antibody at 5.0 ug/mL per well. Co-stimulatory anti-CD28 (eBioscience clone CD28.6) at 2.5 ug/mL final concentration was added at the time of CFSE-labeled cell addition. PBMC-derived Tregs were plated in X-VIVO 15 with 10% huAB serum at $2x10^5$ cells per well ($4x10^5$ cells per well in some experiments).

Two-fold serial dilutions of MoT, Jurkat cells or human PBMC-derived Tregs were added to CD3/CD28-stimulated $CD4^+$ PBMC, starting at $1.5x10^5$ MoT, Jurkat cells and PBMC-derived Tregs (figures show the ratio of stimulated $CD4^+$ PBMC:Treg cells). Final volume per well was 1 mL. Cells were incubated together for 5 days at 37°C in 5% CO_2. To prove that MoT cells did not consume all the nutrients, media was changed daily. On day 5 of culture, cells were collected into individual flow tubes, washed twice

in 5% FBS/PBS and placed on ice prior to analysis by flow cytometry (BD FACSCelesta).

Antibody blocking experiments

In experiments to determine if IL-2 consumption by MoT cells or PBMC-derived Tregs was involved in suppression, anti-IL-2R Mab (R&D Systems; clone 22722) was pre-incubated with MoT cells or PBMC-derived Tregs for 30 minutes, washed three times to remove excess antibody, then added to $CD4^+$ PBMCs.

In experiments to determine if anti-human IL-10R (R&D Systems; clone 37607), atezolizumab (anti-PD-L1), mogamulizumab (anti-CCR4), anti-LAG-3, anti-HLA-DR, anti-CTLA-4 or anti-GITR Mabs could attenuate the suppression of MoT cells or PBMC-derived Tregs, thereby restoring $CD4^+$ PBMC proliferation, the Mabs were pre-incubated with MoT cells for 30 minutes, then they were added to $CD4^+$ PBMCs. Note: IL-10R Mab was tested for function by neutralization of IL-1β inhibition by IL-10 (R&D Systems).

Results

Characterization of $CD4^+$ $CD25^{high}$ $Foxp3^+$ Tregs from human PBMC in a co-culture suppression assay

Previous studies have identified functionally distinct subsets of human $Foxp3^+$ Tregs cells in healthy donors. We purified $CD4^+$ $CD25^{high}$ $CD127^{lo}$ T cells from 6 different human PBMC donors (age/gender: 25/M, 67/M, 68/F, 55/M, 52/F, 39/F) and expanded them with anti-CD3, anti-CD28, and 500 IU/ml recombinant human IL-2

(rhIL-2). Tregs make up approximately 10% of the CD4+ T cell population[125]. Starting with $1x10^8$ PBMCs, on average, we isolated $1x10^6$ cells or 1% of the starting population. We expanded the isolated Treg population to $2x10^7$ cells by the end of the 3rd stimulation. Representative Foxp3 staining demonstrates that the majority of the pre-expansion cell population is $Foxp3^+$, while some heterogeneity exists post expansion (Appendix B, Supplemental Figure 1).

A hallmark of Tregs is their ability to functionally suppress activated T cell proliferation. To confirm that the $CD4^+$ $CD25^{high}$ $Foxp3^+$ T cells possess suppressive activity, we co-cultured these cells for 5 days with CFSE-labeled CD3/CD28-stimulated $CD4^+$ cells purified from healthy donor PBMCs. Stimulated $CD4^+$ PBMC proliferation was monitored over the 5 day time-course (Appendix B, Supplemental Figure 2). $CD4^+$ $CD25^{high}$ $Foxp3^+$ T cells inhibited proliferation of stimulated PBMCs in a PBMC:Treg ratio-dependent manner (Figure 5). Suppressive activity of $CD4^+$ $CD25^{high}$ $Foxp3^+$ Tregs was lost as they were diluted out of the co-culture. Only one proliferative peak of stimulated, CFSE-labeled cells at a 1:2 ratio of stimulated PBMC:Tregs was observed compared to 7 proliferative peaks (cell doublings) in the absence of Tregs. Two-fold dilutions of human Tregs in the co-culture at 1:1 and 1:1/2 stimulated T cells:Tregs resulted in 3 and 4 proliferative peaks of CD3/CD28-stimulated T cells, respectively.

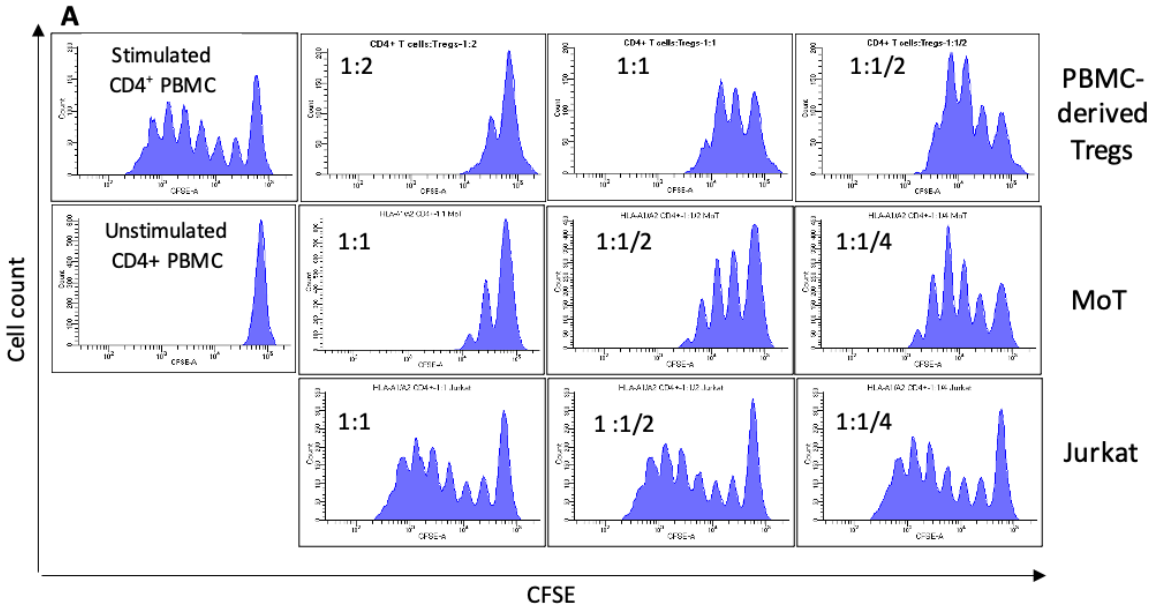

Figure 5. Five-day CFSE-labeled cell proliferation assays demonstrate that CD4$^+$ CD25^{high} Foxp3$^+$ PBMC-derived Tregs and MoT cells suppress CD3/CD28 stimulated CD4$^+$ PBMCs in a cell ratio-dependent manner. (A) PBMC-derived Tregs (top row), MoT (middle row) and Jurkat cells (bottom row) were two-fold serially diluted keeping the same number of CD4$^+$ PBMC. This stimulation induces cell division such that with every cell division, half the cell-associated CFSE dye is divided between the parent and daughter cells. The dividing cells shift left in the flow cytometry histogram. Each peak to the left of the initial peak (far right) represents one cell division. Although we observed variations in the number of cell divisions from independent human PBMC donors (N=6; age/gender: 25/M, 52/F, 55/M, 39/F, 67/M, 68/F), we consistently observed suppression of proliferation by PBMC-derived Tregs and MoT cells that is not seen by Jurkat. Representative data is shown from 6 different donors. (Individual donors are depicted in Appendix B, Supplemental Figure 3).

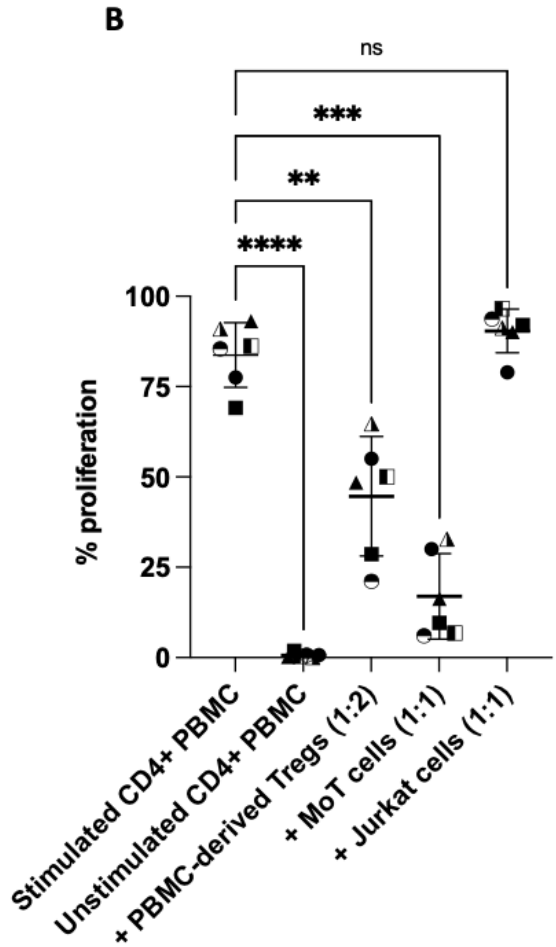

B) Average percent proliferation for all biological replicates (N=6) of stimulated, unstimulated $CD4^+$ PBMC, and stimulated $CD4^+$ PBMC co-cultured with PBMC-derived Tregs, MoT or Jurkat cells. Each donor is represented by a shape and the data is paired by donor. Statistical analysis run on the mean percent proliferation. Significance determined by one-way ANOVA; **, $p<0.005$; ***, $p<0.0005$; ****, $p<0.0001$; ns=not significant.

MoT cells suppress PBMC proliferation similar to CD4$^+$ CD25^{high} Foxp3$^+$ T cells

The majority of the PBMC-derived Treg populations from 6 different human donors were Foxp3$^+$ (Appendix B, Supplemental Figure 1). Since the primary obstacle in functional characterization of human Tregs is that they need to be permeabilized to detect Foxp3 (or Helios) transcription factors to prove they are Tregs, we searched for, and identified a CD4$^+$ CD25^{high} Foxp3$^+$ T cell line and tested it in the suppression assay [142]. MoT cells (CD4$^+$ CD25^{high} Foxp3$^+$) were compared with another CD4$^+$ acute T cell leukemia cell line, Jurkat (CD4$^+$ CD25$^-$ Foxp3$^-$),[143] for the ability to suppress PBMC proliferation similar to PBMC-derived CD4$^+$ CD25^{high} Foxp3$^+$ T cells. To determine if MoT cells have suppressive activity, we co-cultured MoT or Jurkat cells with CD3/CD28-stimulated CD4$^+$ cells purified from healthy donor PBMCs. MoT cells, but not Jurkat cells, inhibited proliferation of stimulated CD4$^+$ PBMCs (Figure 5). Like PBMC-derived Tregs, suppressive activity of MoT cells decreased as they were titrated out of the co-culture in a cell ratio-dependent manner. In contrast, Jurkat cells have no suppressive activity even at the highest ratio of 1:1. Preliminary experiments indicated that MoT cells as a monoclonal cell line are more suppressive than heterogenous PBMC-derived Tregs. Therefore, twice as many PBMC-derived Tregs (1:2) were required to obtain similar suppressive activity as the MoT cell line (1:1), keeping the number of CD4+ PBMC consistent.

MoT cells express known Treg cell surface markers

MoT cells were derived from a patient with a T-cell variant of hairy-cell leukemia [140]. As shown in Figure 6, MoT cells express surface markers consistent with human

Tregs such as CD4, CD25, GITR, LAG-3, programmed death receptor ligand 1 (PD-L1), and C-C Motif Chemokine Receptor 4 (CCR4). MoT cells express Foxp3 and weakly express Helios, a transcription factor expressed in thymic-derived Tregs, that differentiates them from peripherally-induced Tregs [103]. They do not express PD-1 or CTLA-4, and despite being $CD4^+$, they do not express CD3 or a T cell receptor (TCR). They also do not express granzymes A and B (Appendix B, Supplemental Figure 4).

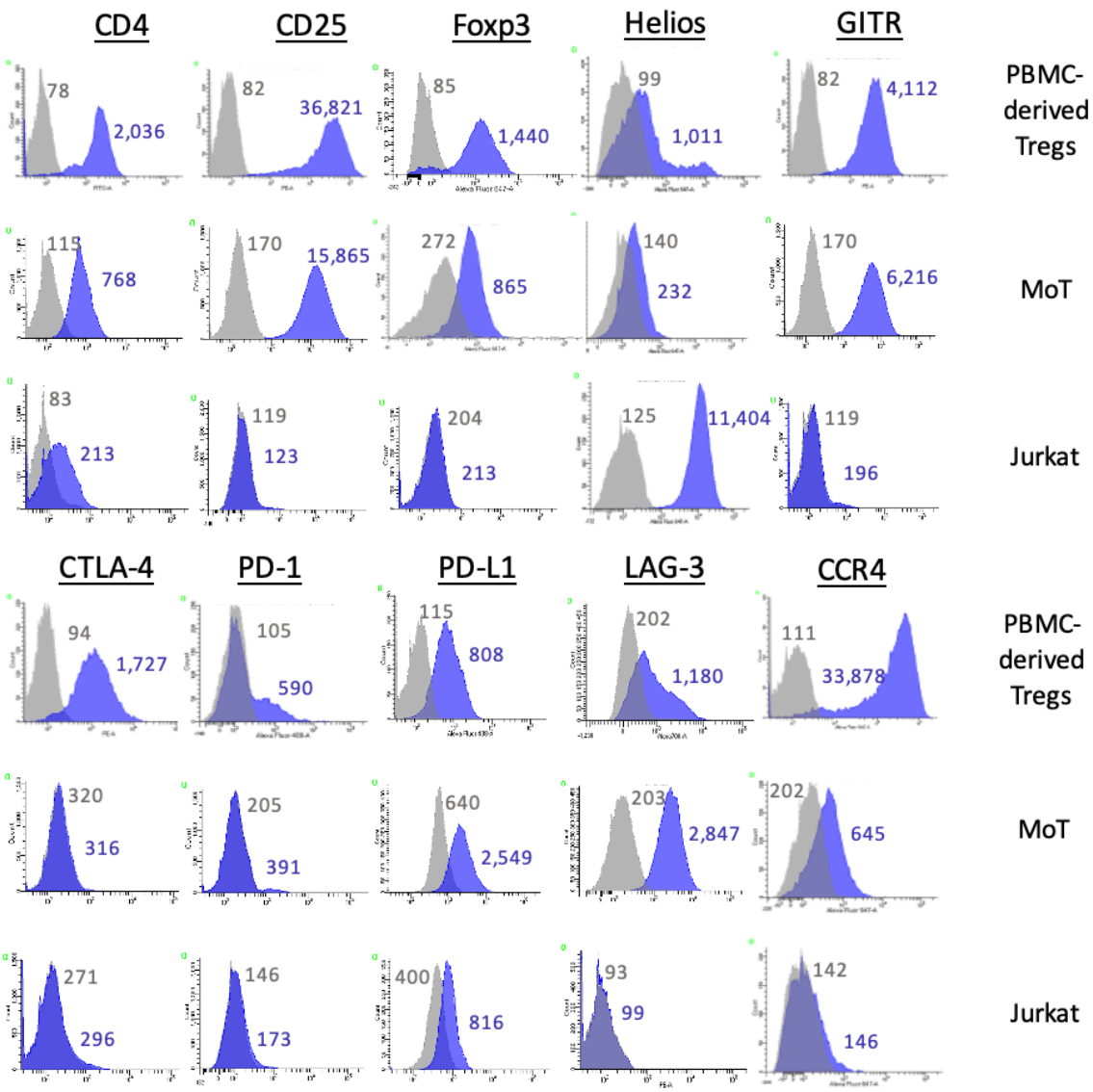

Figure 6. MoT, but not Jurkat cells, demonstrate a $CD4^{+}$ $CD25^{high}$ $Foxp3^{+}$ Treg-like phenotype. MoT were assessed for cell surface and intracellular markers by flow cytometry and compared to Jurkat and PBMC-derived Tregs: CD4, CD25, Foxp3, Helios, GITR, CTLA-4, PD-1 PD-L1, LAG-3, and CCR4. For each histogram, mean fluorescence intensity of isotype controls is in gray on the left and specific Mab staining is shown on the right (blue histogram). MFI values are indicated on the graph.

Since MoT cells express the IL-2 receptor (CD25), we were concerned that they may act as an IL-2 sink and sequester the IL-2 produced by CD3/CD28 stimulated $CD4^+$ PBMCs, thereby leading to suppression of CD3/CD28 stimulated $CD4^+$ proliferation. Therefore, we pre-incubated an IL-2 receptor blocking antibody (anti-human-IL-2R alpha; R&D Systems MAB223 clone 22722) with PBMC-derived Tregs or MoT cells prior to adding them to the stimulated $CD4^+$ PBMC. PBMC-derived Tregs and MoT cells were washed three times in PBS to ensure removal of excess receptor blocking antibody that would affect $CD4^+$ PBMC proliferation. Figure 7A panel a shows 6 cell divisions in CD3/CD28 stimulated $CD4^+$ cells. When PBMC-derived Tregs or MoT cells were co-cultured with CD3/CD28 stimulated $CD4^+$ PBMCs, PBMC-derived Tregs and MoT cells suppressed cell division to two peaks (panels 7b and 7e). When IL-2 receptor was blocked on PBMC-derived Tregs or MoT cells (panels 7c and 7f), they remained predominately suppressive. Comparing panels, 7a (6 peaks) and f (3 peaks) indicate that MoT cells are not sequestering IL-2 from CD3/CD28-stimulated $CD4^+$ PBMC. If MoT cells were sequestering IL-2, blocking of the IL-2 receptor would lead to complete restoration of 6 cell divisions in CD3/CD28 stimulated $CD4^+$ cell, as IL-2 would be available for PBMC to proliferate. This experiment suggests that MoT suppression is mainly independent of IL-2. To further convince ourselves that MoT cells were not stealing IL-2 from CD3/CD28-stimulated $CD4^+$ PBMC, we performed a separate experiment showing that addition of exogenous, supraphysiological doses of up to 1000 IU/ml of rhIL-2 to the CD3/CD28-stimulated $CD4^+$ PBMC:MoT mixture does not reverse MoT suppression (Figure 8). Physiological concentration of IL-2 in human peripheral blood is between 9.4-15.9 pg/ml[144]. Addition of up to 1000 units of rhIL-2

equates to a 10,000-fold excess of IL-2. We performed these experiments with PBMC-derived Tregs and found that neither blocking the endogenous IL-2 receptor (Figure 7) nor adding exogenous supraphysiological levels of rhIL-2 (Figure 8) reversed Treg-mediated suppression of $CD4^+$ PBMC.

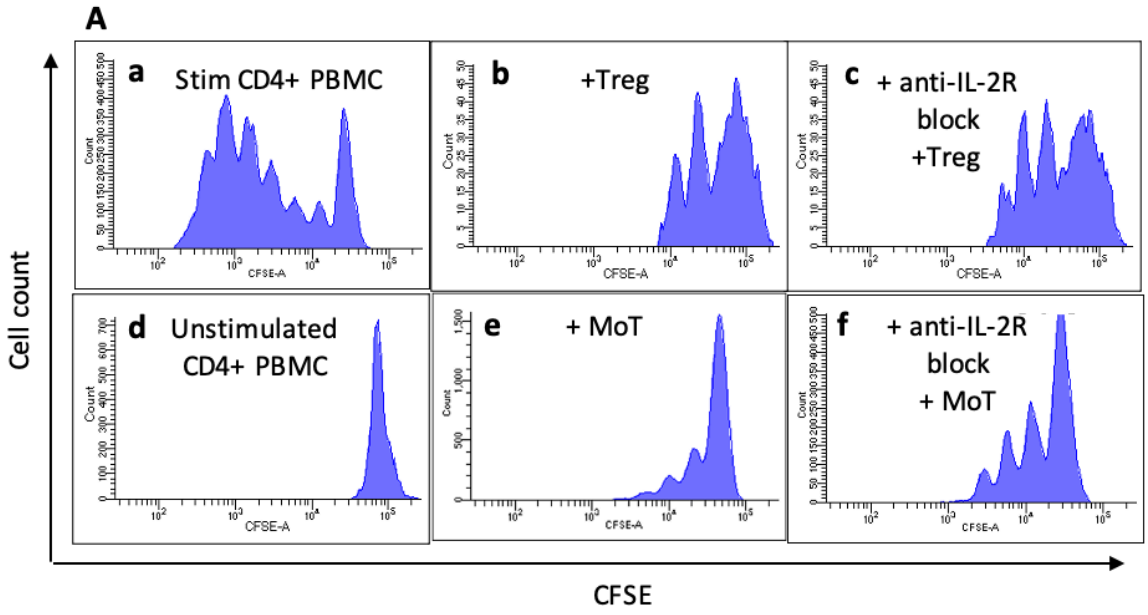

Figure 7. (A) **Blocking IL-2 receptor using anti-human-IL-2R alpha does not restore CD3/CD28-activated CD4$^+$ PBMC proliferation.** (a) shows 6 proliferative peaks of CD4$^+$ PBMC activated by anti-CD3/CD28 stimulation. (b) PBMC-derived Tregs co-incubated with anti-CD3/CD28 activated CD4$^+$ PBMC (1:2). (c) shows 3 proliferative peaks when IL-2 receptor-blocked PBMC-derived Tregs are co-incubated with anti-CD3/CD28 activated CD4$^+$ PBMC. (d) Unstimulated CD4+ PBMC. (e) MoT cells co-incubated with anti-CD3/CD28 activated CD4$^+$ PBMC (1:1). (f) shows 3 proliferative peaks when IL-2 receptor-blocked MoT cells are co-incubated with anti-CD3/CD28 activated CD4$^+$ PBMC. Representative data is shown (N=3).

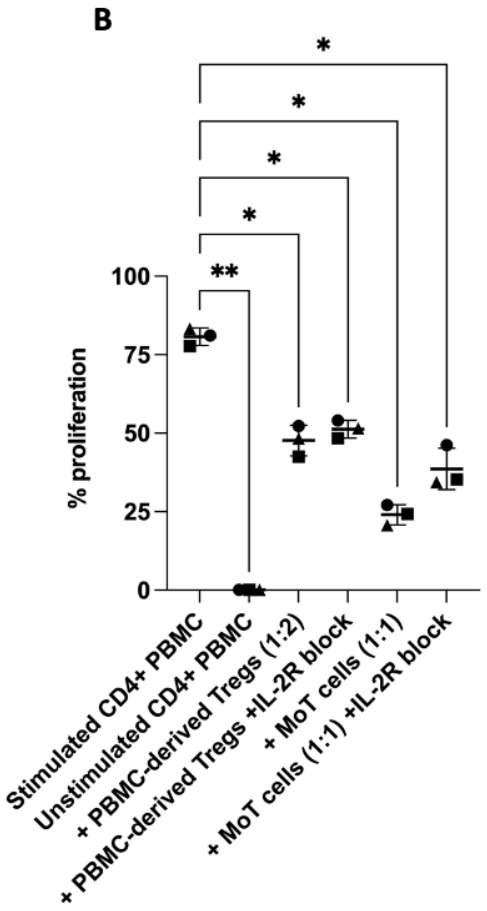

(B) Average percent proliferation for all replicates (N=3) of stimulated, unstimulated $CD4^+$ PBMC, and stimulated $CD4^+$ PBMC co-cultured with PBMC-derived Tregs or MoT cells. Each donor is represented by a shape. Statistical analysis run on the mean percent proliferation, paired by donor. Significance determined by one-way ANOVA; *, $p<0.05$; **, $p<0.005$; ns=not significant.

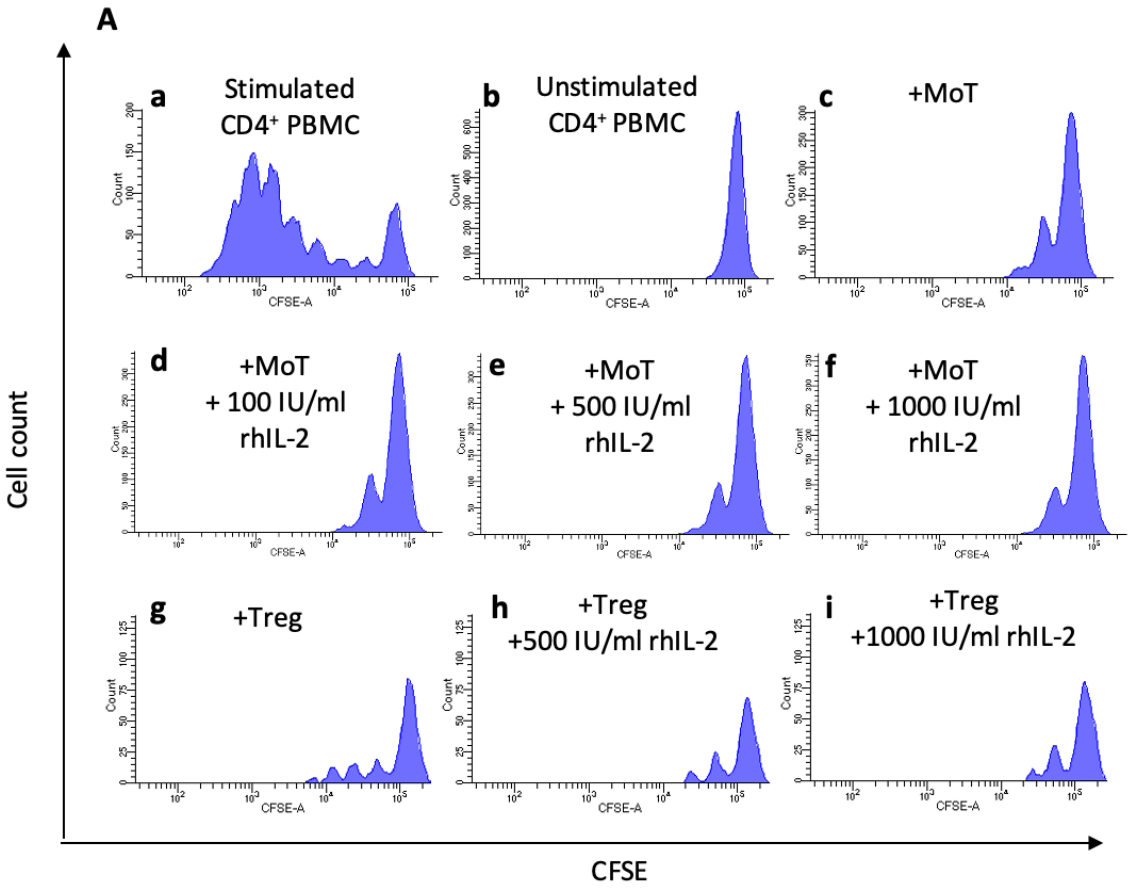

Figure 8. (A) **Supraphysiological levels of exogenous rhIL-2 does not reverse MoT suppression of CD3/CD28-activated CD4$^+$ PBMC proliferation.** (a) shows ~7 proliferative peaks of CD4$^+$ PBMC activated by anti-CD3/CD28 stimulation to the left of the farthest right peak. (b) CFSE-labeled CD4$^+$ PBMC with no stimulation. (c) shows suppression of CD3/CD28 activated CD4$^+$ PBMC proliferation when co-incubated with MoT cells (1:1). Panels d-f show suppression of stimulated CD4$^+$ PBMC by MoT cells independent of increasing doses of rhIL-2 (100, 500 and 1000 IU/mL). (g) shows suppression of CD3/CD28 activated CD4$^+$ PBMC proliferation when co-incubated with PBMC-derived Tregs (1:2). Panels h-i show suppression of stimulated CD4$^+$ PBMC by PBMC-derived Tregs independent of increasing doses of rhIL-2. Representative data is shown (N=3).

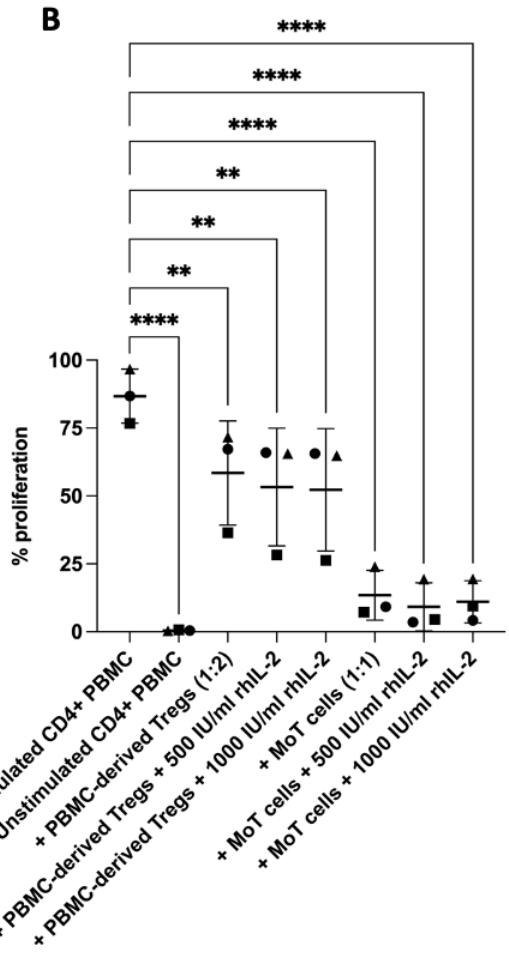

(B) Average percent proliferation for all replicates (N=3) of stimulated, unstimulated $CD4^+$ PBMC, and stimulated $CD4^+$ PBMC co-cultured with PBMC-derived Tregs or MoT cells. Each donor is represented by a shape. Statistical analysis run on the mean percent proliferation, paired by donor. Significance determined by one-way ANOVA; **, $p<0.005$; ****, $p<0.0001$.

Although both MoT and Jurkat have a similar doubling time, we wanted to ensure that MoT cells were not depleting the co-culture of nutrients. An experiment was performed in which media in the co-culture was changed daily for 5 days (data not shown). No significant difference in suppression of $CD4^+$ PBMC proliferation by MoT cells was observed between daily media change and no media change.

Cell to cell contact is required for both PBMC-derived Tregs and MoT Treg suppressive activity

To determine if suppressive cytokines or other soluble paracrine factors might be responsible for the inhibition of proliferation observed in the co-culture assay, we performed an experiment in which MoT cells were separated from CD3/CD28-stimulated T cells by a transwell membrane. Figure 9A shows 6 cell division peaks in CD3/CD28-stimulated $CD4^+$ PBMC, but when PBMC-derived Tregs or MoT cells were added, they suppressed the stimulated $CD4^+$ PBMC (panels 9b and 9e). When PBMC-derived Tregs were separated from stimulated $CD4^+$ PBMC by a Millipore 0.4 μm transwell membrane, they were unable to suppress as shown by at least 5 peaks of stimulated $CD4^+$ PBMC in panel 9c. We observed similar cell contact-dependent suppression by MoT cells. In Figure 9 panel f, MoT cells were not suppressive when separated from stimulated $CD4^+$ PBMC, similar to PBMC-derived Tregs. Although suppression is contact-dependent, we were still concerned that a soluble factor might be involved, so we performed a cytokine array to determine what suppressive cytokines were expressed and upregulated by MoT cells and PBMC-derived Tregs when co-cultured with $CD4^+$ PBMCs (Appendix B, Supplemental Figure 5). However, we did not observe an increase in suppressive

cytokines when MoT cells or PBMC-derived Tregs were co-cultured with responder cells. We observed expression of IL-10 but not TGF-β. Since IL-10 is highly expressed by both MoT cells and PBMC-derived Tregs, we blocked the IL-10 receptor on $CD4^+$ PBMCs (anti-human-IL-10R alpha; R&D Systems MAB274 clone 37607). When IL-10R was blocked, suppression was not reversed (Figure 10). Our data demonstrates that cell-to-cell contact, not a soluble factor, is required for MoT and PBMC-derived Treg suppressive activity since suppression does not occur when MoT cells or PBMC-derived Tregs are separated from CD3/CD28-stimulated $CD4^+$ PBMCs by a transwell membrane or when IL-10 activity is blocked.

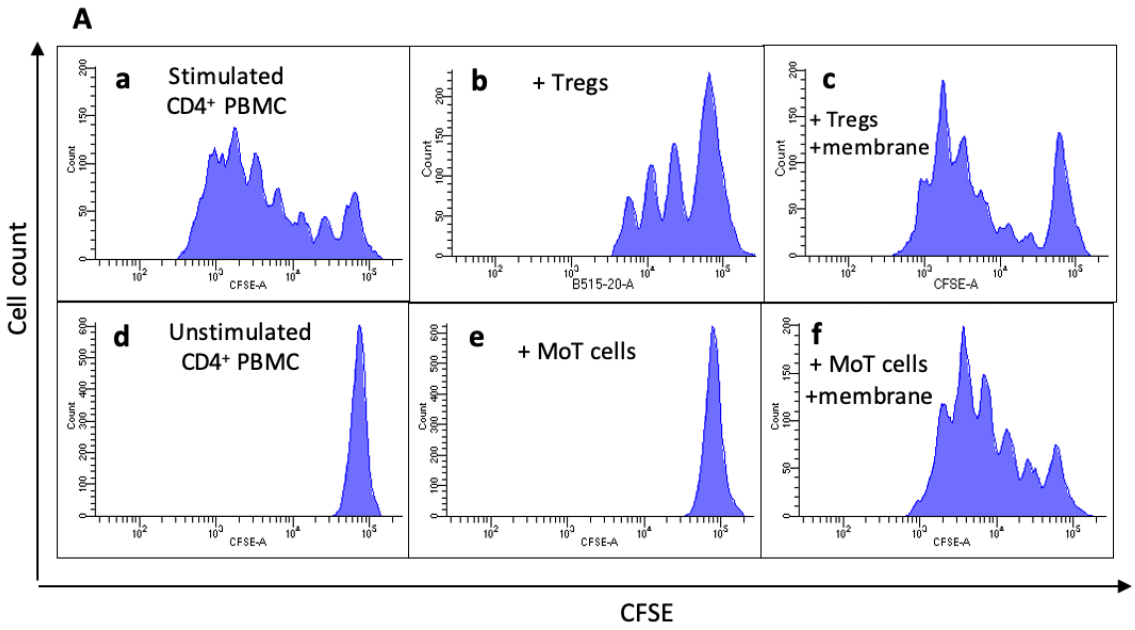

Figure 9. (A) **Cell-cell contact is required to functionally suppress proliferation of CD4$^+$ PBMC.** (a) Stimulated CD4$^+$ PBMC. (b) Stimulated CD4$^+$ PBMC + PBMC-derived Tregs (1:2). (c) Stimulated CD4$^+$ PBMC + PBMC-derived Tregs separated by Millipore membrane. (d) Unstimulated CD4$^+$ PBMC. (e) Stimulated CD4$^+$ PBMC + MoT cells (1:1). (f) Stimulated CD4$^+$ PBMC + MoT cells separated by Millipore membrane. Representative data is shown (N=3).

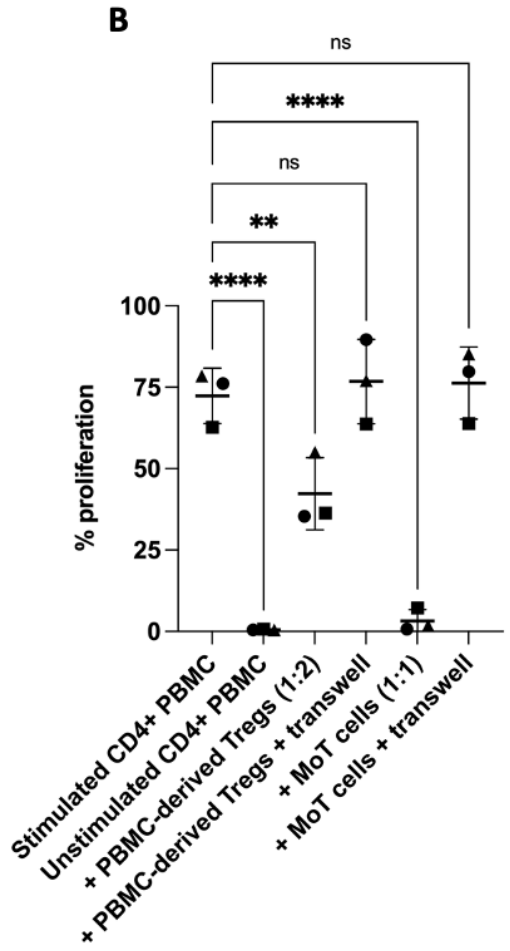

(B) Average percent proliferation for all replicates (N=3) of stimulated, unstimulated $CD4^+$ PBMC, and stimulated $CD4^+$ PBMC co-cultured with PBMC-derived Tregs or MoT cells. Each donor is represented by a shape. Statistical analysis run on the mean percent proliferation, paired by donor. Significance determined by one-way ANOVA. **, $p<0.005$; ****, $p<0.0001$; ns=not significant.

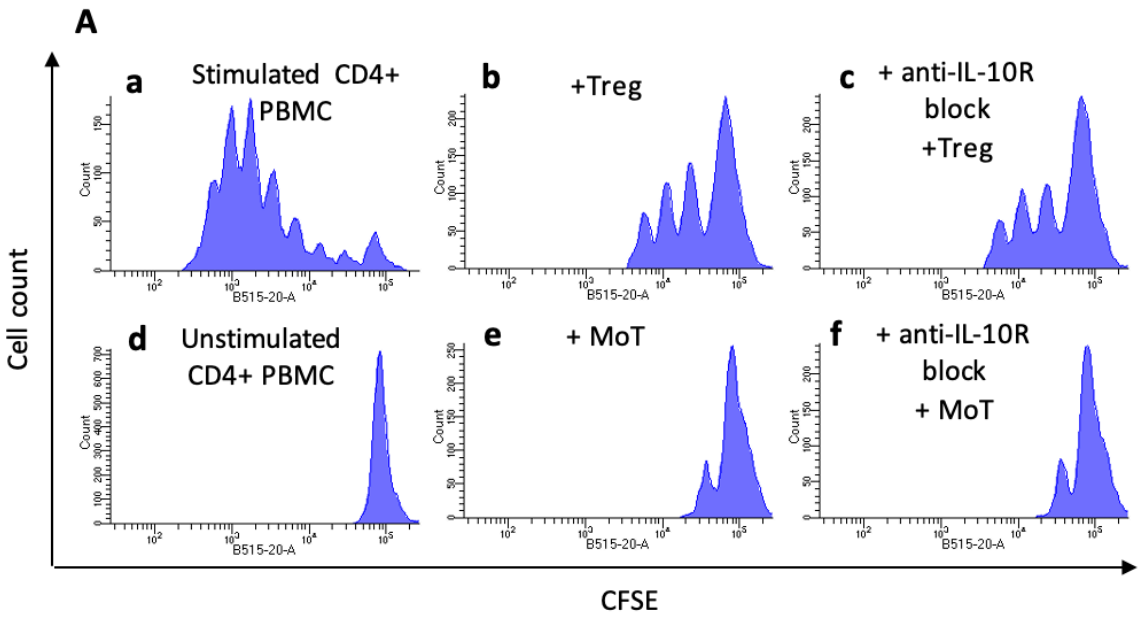

Figure 10. (A) **Blocking IL-10 receptor using anti-human-IL-10R alpha does not restore CD3/CD28-activated CD4$^+$ PBMC proliferation.** (a) shows 7 proliferative peaks of CD4$^+$ PBMC activated by anti-CD3/CD28 stimulation. (b) PBMC-derived Tregs co-incubated with anti-CD3/CD28 activated CD4$^+$ PBMC (1:2). (c) shows 3 proliferative peaks when IL-10 receptor-blocked anti-CD3/CD28 activated CD4$^+$ PBMC are co-incubated with PBMC-derived Tregs. (d) Unstimulated CD4+ PBMC. (e) MoT cells co-incubated with anti-CD3/CD28 activated CD4$^+$ PBMC (1:1). (f) shows 1 proliferative peak when IL-10 receptor-blocked anti-CD3/CD28 activated CD4$^+$ PBMC are co-incubated with MoT cells. Note: IL-10R Mab was tested for function by neutralization of IL-1β inhibition by IL-10 (R&D Systems). Representative data is shown (N=3).

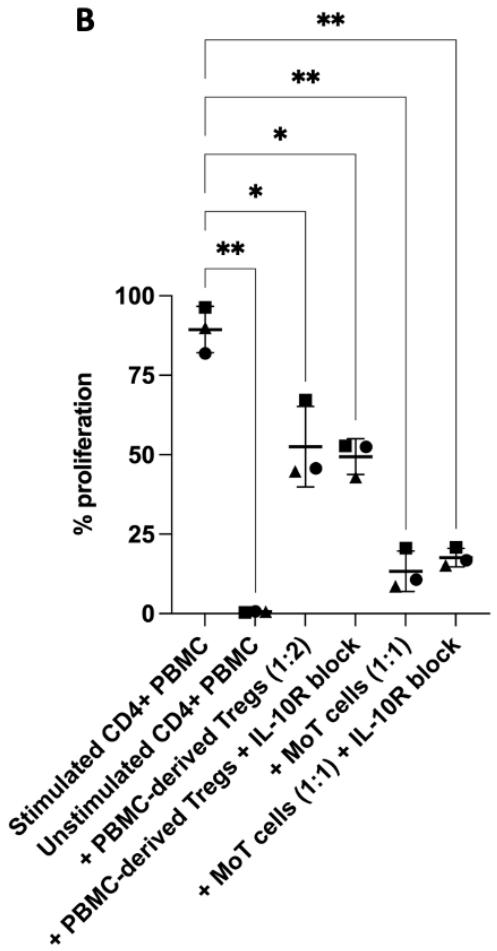

(B) Average percent proliferation for all replicates (N=3) of stimulated, unstimulated $CD4^+$ PBMC, and stimulated $CD4^+$ PBMC co-cultured with PBMC-derived Tregs or MoT cells. Each donor is represented by a shape. Statistical analysis run on the mean percent proliferation, paired by donor. Significance determined by one-way ANOVA; *, $p<0.05$; **, $p<0.005$.

Immune checkpoint inhibitors do not attenuate MoT suppressive activity

To determine if FDA approved and research grade immune checkpoint inhibitors attenuate the MoT Treg suppressive activity, we tested clinical grade anti-PD-L1 *(*atezolizumab), clinical grade anti-CTLA-4 (ipilimumab), anti-CCR4 (mogamulizumab), anti-GITR agonist, anti-LAG-3, and anti-HLA DR monoclonal antibodies (Mabs) for the ability to reverse MoT suppression (Figure 11). Since MoT cells are strong suppressive cells, we used a ratio of 1:1/2 to provide a better opportunity for the blocking antibodies to reverse the suppression. CCR4 was previously reported to be present in Tregs [83]. Although CTLA-4 is not expressed on MoT cells, ipilimumab was tested in case of expression on stimulated $CD4^+$ PBMCs. Since Treg suppression is thought to be mediated via the TCR, MHC II was blocked. None of the Mabs including anti-GITR, anti-CCR4, anti-PD-L1, anti-CTLA-4 or anti-HLA DR reversed MoT cell-mediated suppression of $CD4^+$ PBMC. The same blocking Mabs did not interfere with PBMC-derived Treg-mediated suppression (Appendix B, Supplemental Figure 6). Additionally, a suppression assay was performed with an antibody blocking Fas-FasL interaction, and reversal of suppression was not observed (data not shown). These results suggest, but do not completely prove that the mechanism of MoT cell suppression is not mediated via the PD-1/PD-L1 axis, CCR4, GITR or Fas-FasL mechanisms. Despite expressing CD4, MoT cells do not express CD3 or a TCR (Appendix B, Supplemental Figure 4), further supporting that suppressive activity is independent of TCR-peptide-MHC interactions. Note: antibodies were incubated with $CD4^+$ stimulated cells alone and did not inhibit proliferation (data not shown).

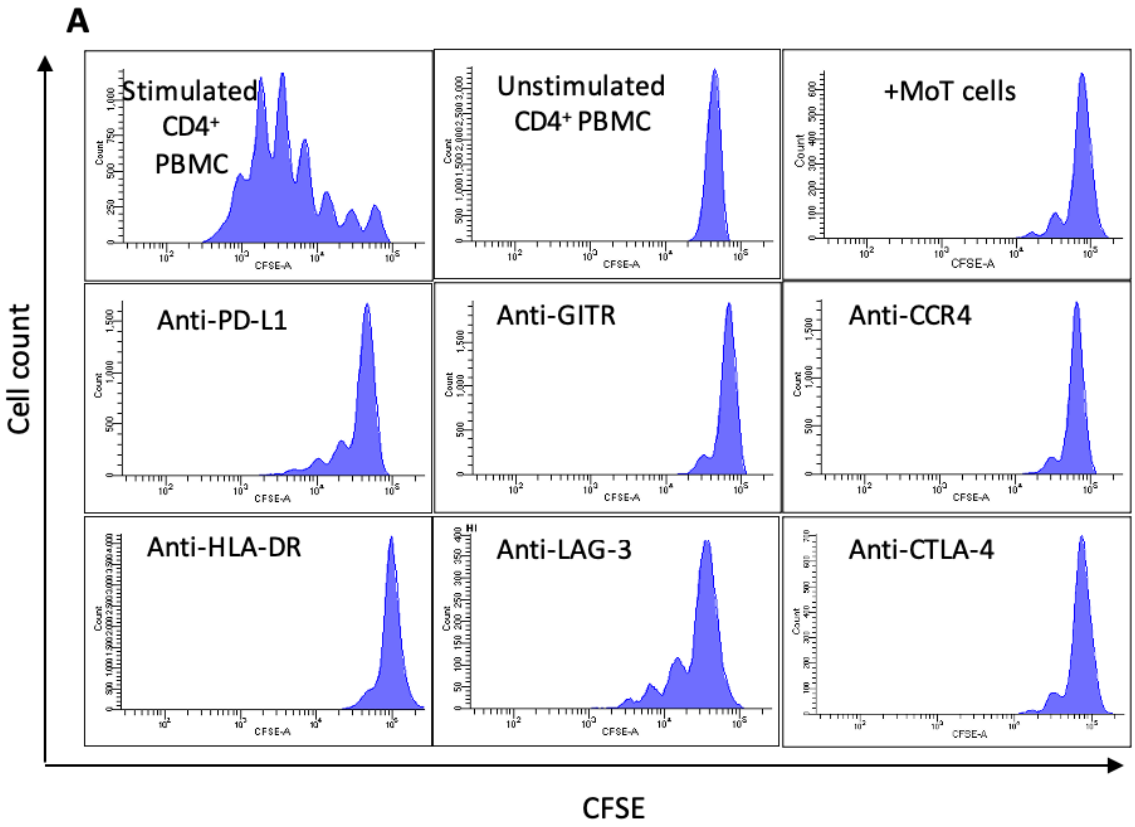

Figure 11. Anti-PD-1/PD-L1 axis, GITR, CCR4 and TCR-MHC interactions are not involved in suppression of CD4$^+$ PBMC proliferation by MoT cells. (A) Anti-GITR, anti-CCR4 (mogamulizumab), anti-PD-L1 (atezolizumab), anti-HLA-class II, anti-LAG-3 blocking, and ipilimumab was used as an anti-CTLA-4 blocking Mab. CD3/CD28-stimulated CD4$^+$ PBMC were co-incubated with MoT cells at a 1:1/2 ratio. Blocking antibodies were used at 10 μg/ml final concentration. Representative data is shown (N=3).

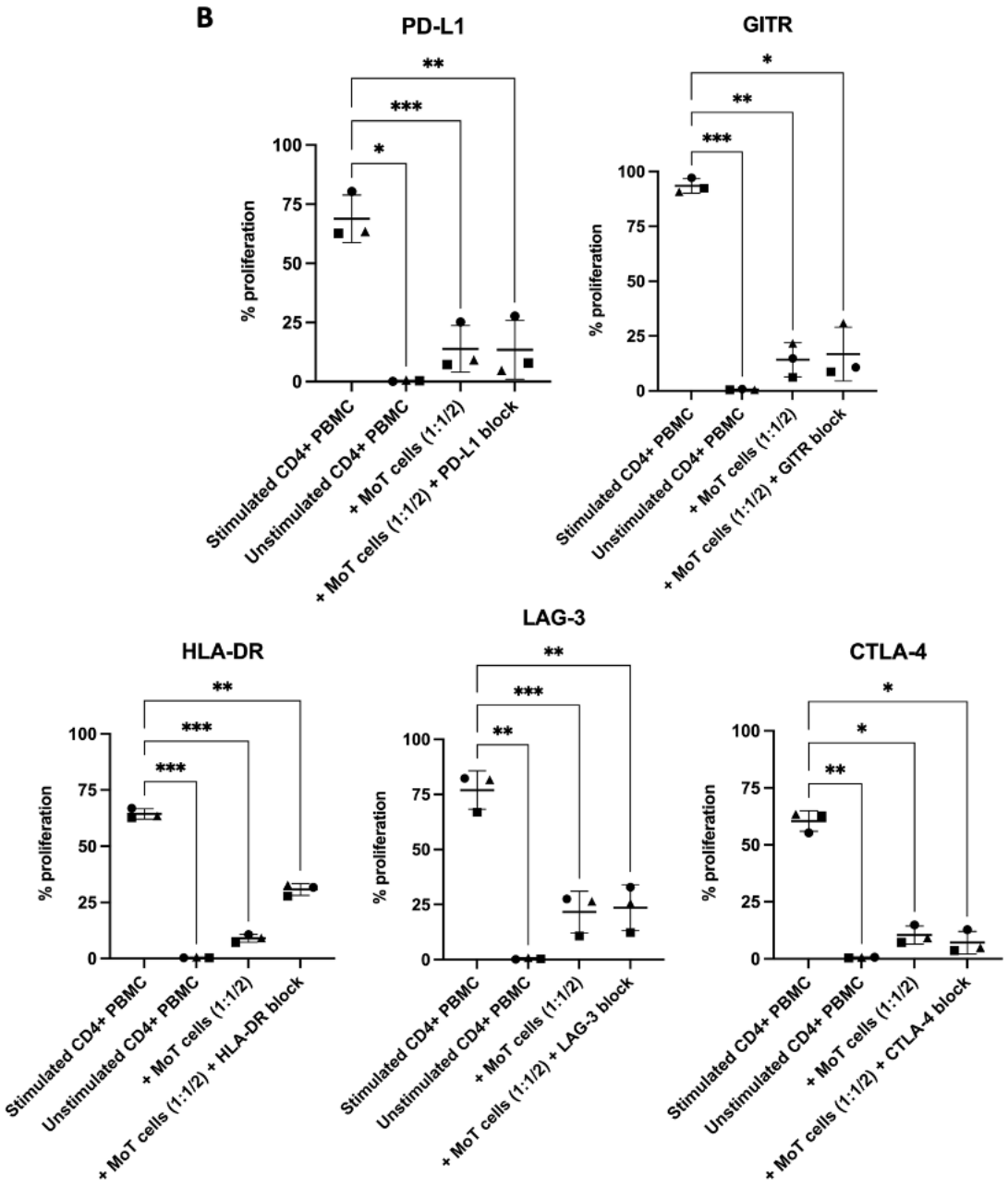

(B) Average percent proliferation for all replicates (N=3) of stimulated, unstimulated $CD4^+$ PBMC, and stimulated $CD4^+$ PBMC co-cultured with MoT cells. Each donor is represented by a shape. Statistical analysis run on the mean percent proliferation, paired by donor. Significance determined by one-way ANOVA *, $p<0.05$; **, $p<0.005$; ***, $p<0.0005$; ****, $p<0.0001$.

MoT cells induce apoptosis of CD4$^+$ PBMCs

To begin to determine a mechanism of suppression of CD3/CD28-activated CD4$^+$ PBMC proliferation by MoT cells and PBMC-derived Tregs, we performed an annexin V/propidium iodide (PI) experiment and evaluated the results by flow cytometry (Figure 12). This experiment allows for visualization of early and late apoptosis, as well as dead cells. Progression through the apoptotic pathway was assessed over the course of the five-day assay. In Figure 12A, viable CD4+ PBMCs are Annexin V/PI negative (lower left quadrant), Annexin V single positive cells (lower right quadrant) indicate cells undergoing early apoptosis, and Annexin V and PI double positive cells indicate cells in late apoptosis (upper right quadrant). The presence of these 3 distinct phenotypes within the CD4+ PBMC population suggests apoptosis is being induced in activated CD4+ PBMC when stimulated with anti-CD3/CD28.

Although stimulated responder cells undergo apoptosis, co-incubation with MoT cells and PBMC-derived Tregs hastens apoptosis over the course of the five-day assay. Figure 12 suggests that MoT cells not only inhibit CD4+ PBMC proliferation but also induce apoptosis. By 24 hours of co-culture with MoT cells, the mean CD4+ PBMC population (32.6%) is Annexin V (+), and by day 5 almost half of the mean total population is undergoing early (36%) or late apoptosis (11.1%) compared to stimulated cells alone (21.1% and 2.2%, respectively). This result suggests that MoT cells ultimately induce CD4$^+$ PBMC cell death and clearly enter into an Annexin V-positive and PI-negative state (early apoptosis) prior to cell death at an earlier timepoint in the co-incubation compared to stimulated cells alone. A population of stimulated CD4$^+$ PBMC also undergo apoptosis when co-incubated with PBMC-derived Tregs.

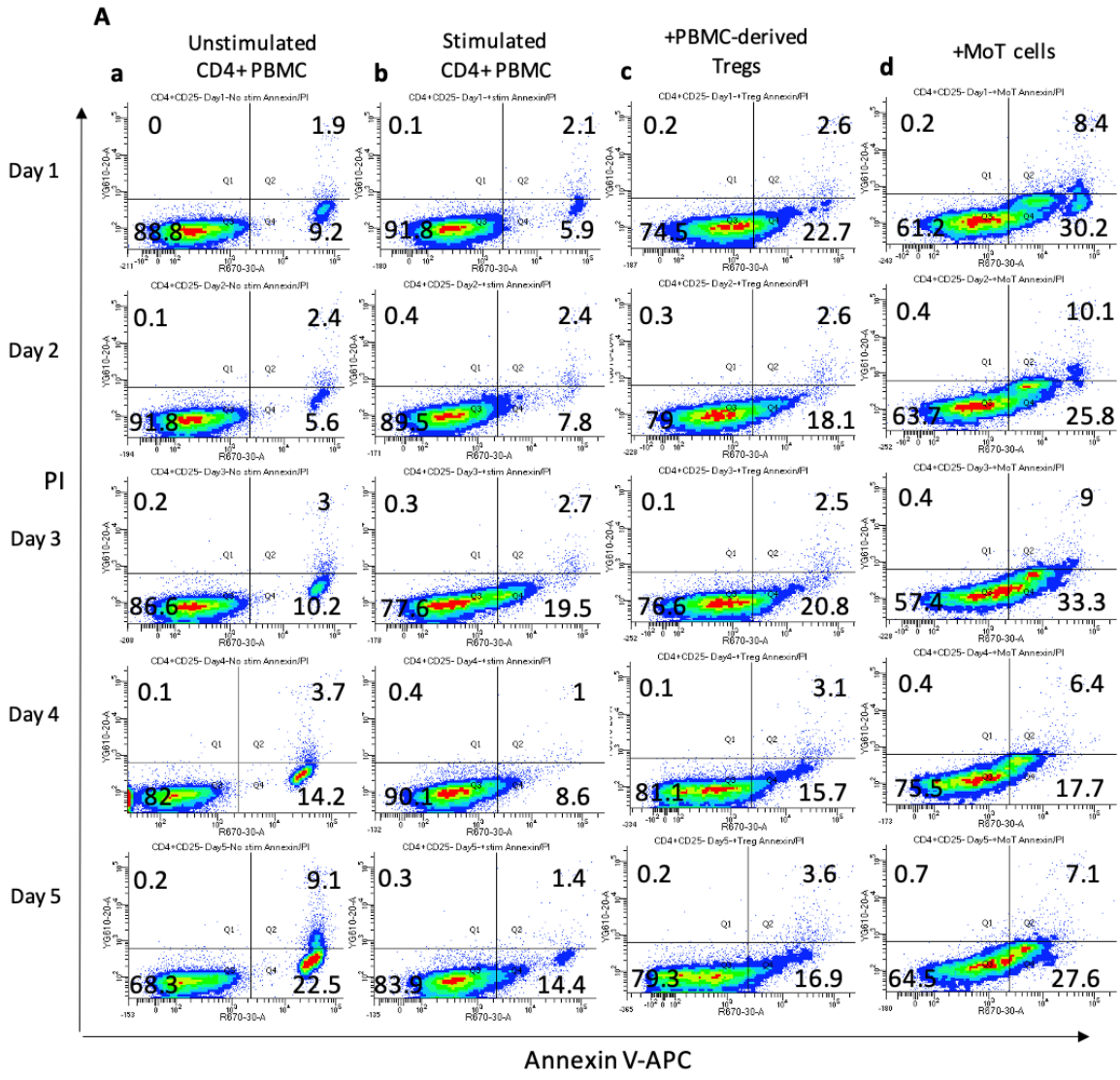

Figure 12. MoT cells induce apoptosis (lower right quadrant representing CD4+, Annexin V+ population) early in the co-incubation. CD4+ PBMC were labeled with CFSE prior to stimulation with anti-CD3 and anti-CD28. (A) Contour plots show Annexin V/PI staining of CFSE-gated CD4+ PBMC over the five-day assay. (a) Unstimulated CD4+ PBMC. (b) anti-CD3/CD28-stimulated CD4+ PBMC. (c) CD4+ PBMC co-incubated with PBMC-derived Tregs (1:2). (d) CD4+ PBMC co-incubated with MoT cells (1:1). Representative data is shown (N=3).

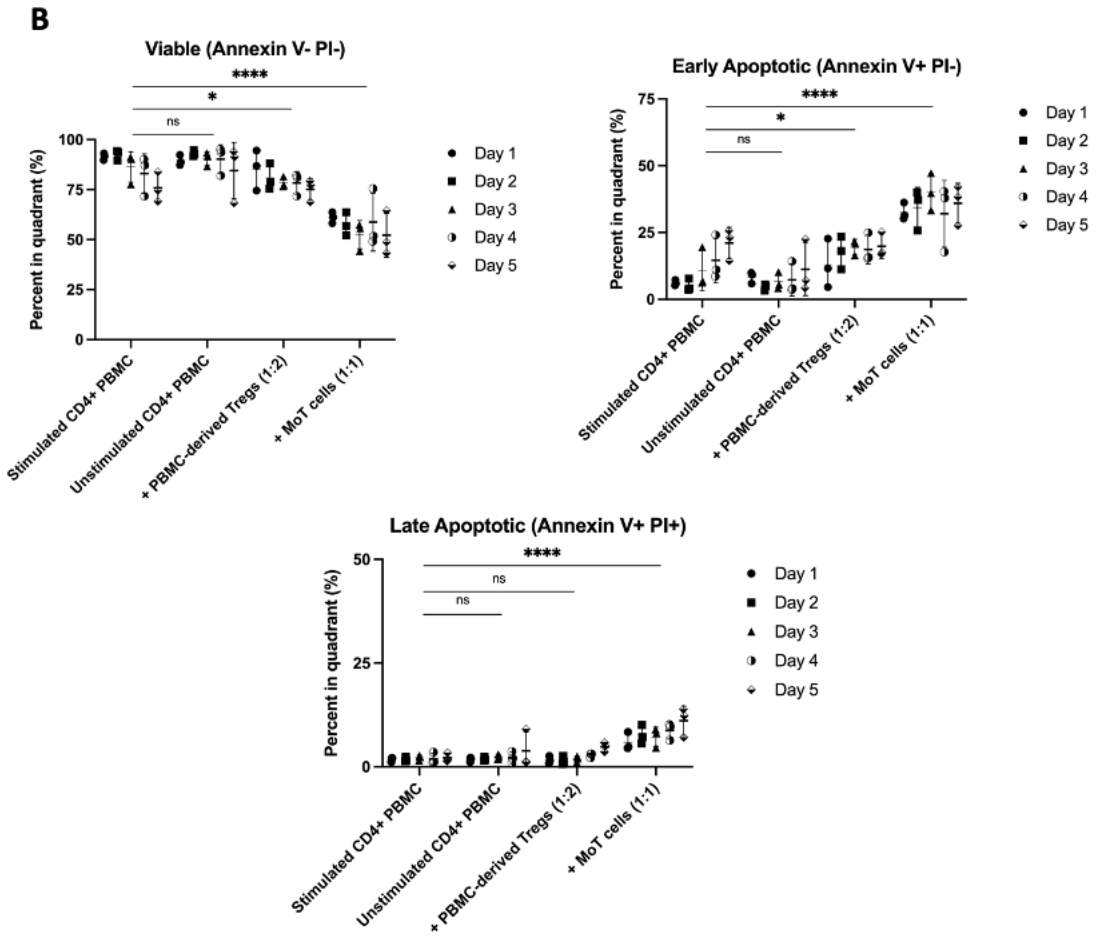

(B) Percent of cells in each quadrant per day for all samples (N=3) of stimulated, unstimulated $CD4^+$ PBMC, and stimulated $CD4^+$ PBMC co-cultured with PBMC-derived Tregs or MoT cells. Statistical analysis run on mean percent calculated for viable (Annexin V- PI-), early apoptotic (Annexin V+ PI-), and late apoptotic (Annexin V+ PI+) cells over the 5 day time-course. Significance determined by two-way ANOVA; *, $p<0.05$; ****, $p<0.0001$; ns=not significant.

Reverse transcriptase inhibitor AZT does not reverse the suppression of MoT cells

ATCC indicates that MoT cells carry three copies of HTLV-II genome, one replication competent and two defective. To address the possibility that MoT cells suppress $CD4^+$ CD3/CD28-simulated T cells by transferring and/or infecting activated $CD4^+$ PBMCs with HTLV-II, the suppression assay was performed in the presence of azidothymidine (AZT). Even if HTLV-II virus entered $CD4^+$ T cells, AZT inhibits reverse transcriptase and prevents viral RNA from being reverse transcribed into DNA and integrating into T cell genomes. Treatment of MoT cells with AZT, however, does not cure them of infection because reverse transcriptase has already integrated the pro-viral DNA into the genome of MoT cells. It is possible, however, that an HTLV-II gene such as Tax could be driving the expression of either an HTLV-II protein or another cellular protein capable of mediating Treg-like activity (Appendix B, Supplemental Figure 7).

Discussion

The study of regulatory T cells is limited by the low prevalence of Tregs in peripheral blood, their heterogeneity upon isolation and characterization, and primarily by the lack of a cell surface molecule that would allow purification of Tregs for functional characterization alone and in the presence of other purified cell populations. Therapies that boost Treg function could inhibit pathologic immune cell function in autoimmune disease [145], decrease graft rejection in solid organ transplants [146], and decrease graft-vs-host disease in allogeneic bone marrow transplants [147]. Conversely, suppression of Tregs may also enhance the anti-tumor response with immune checkpoint

therapies and has been shown to increase the anti-tumor activity of $CD8^+$ CTL [148]. However, no FDA approved therapies exist that specifically either enhance or suppress Treg activity, although a phase II clinical trial is recruiting to expand Tregs to treat type 1 diabetes [149].

These challenges hinder development of therapies that specifically target Tregs. We observed that the majority of PBMC-derived Tregs, expanded from human PBMC are $CD4^+$ $CD25^{high}$ $Foxp3^+$. Since it is not possible to sort and functionally characterize T cells that have been permeabilized for Foxp3 staining, we studied a $CD4^+$ $CD25^{high}$ $Foxp3^+$ MoT cell line in a co-culture suppression assay which demonstrates MoT cells, like PBMC-derived Tregs, inhibits proliferation of stimulated $CD4^+$ PBMCs. Mechanisms of Treg-mediated suppression include the production of soluble suppressive factors and indirect suppression of CD4+ T cells via targeting APCs, while a subset of CD4+$CD25^{high}$ Tregs suppress CD4+CD25- responder cell activation via cell-cell contact [142]. In our *in vitro* suppression assays, we assessed MoT and Treg cell-contact dependent suppression. Separation of MoT cells and PBMC-derived Tregs from stimulated $CD4^+$ PBMC by a transwell insert did reverse suppression; this strongly suggests a cell-to-cell contact mechanism of MoT suppression. As $CD4^+$ $CD25^{high}$ $Foxp3^+$ PBMC-derived Tregs or MoT cells were titrated out of the co-culture, $CD4^+$ PBMCs regained the ability to proliferate as shown in Figure 5. Daily media changes ensured MoT cells and PBMC-derived Tregs were not depleting the co-culture of nutrients (data not shown).

Since MoT cells and PBMC-derived Tregs have an IL-2 receptor, we were initially concerned they were "sponging up" any IL-2 produced by activated $CD4^+$ T cells, having the effect of suppressing their proliferation. To address this possibility, we

pre-incubated MoT cells and PBMC-derived Tregs with an IL-2 receptor blocking antibody prior to washing away excess blocking Mab and adding the IL-2 receptor-blocked cells to activated $CD4^+$ PBMC. If MoT cells and PBMC-derived Tregs were scavenging IL-2 produced from activated $CD4^+$ T cells, blocking the IL-2 receptor would have restored the proliferative capacity of $CD4^+$ T cells such that the number of cell divisions would look similar to activated $CD4^+$ T cells alone. We did not observe this. MoT cells and PBMC-derived Tregs suppressed activated $CD4^+$ PBMCs even in the presence of an IL-2 receptor blocking antibody. To further demonstrate that MoT and PBMC-derived Treg suppression is not dependent on a lack of IL-2 for $CD4^+$ T cell proliferation, we added exogenous rhIL-2 to the suppression assay (Figure 8). In the absence of MoT cells or PBMC-derived Tregs, $CD4^+$ T cells from the donor used in this experiment divided at least 7 times over 5 days. Addition of 100, 500, and 1000 IU/ml of rhIL-2 did not overcome MoT or PBMC-derived Treg suppression of $CD4^+$ T cell division.

Several limitations should be considered when evaluating our study. First, we did not identify a cell surface protein on MoT cells or PBMC-derived Tregs responsible for the suppressive Treg-like activity. Our data indicates that the suppressive properties of MoT cells and PBMC-derived Tregs do not appear to be due to soluble factors like cytokines. Despite our data showing a cell-to-cell contact dependence for Treg suppression, we evaluated a prominent suppressive cytokine, IL-10, secreted by both MoT cells and PBMC-derived Tregs. We did not observe reversal of suppression when IL-10 receptor was blocked, indicating that IL-10 is not responsible for suppression. Since PBMC-derived Tregs are a polyclonal population, compared to monoclonal, there

are likely multiple other soluble suppressive molecules. The suppression we observed does not require known pathways such as PD-L1 or CTLA-4 axes since neither atezolizumab nor ipilimumab reversed suppression mediated by MoT cells or PBMC-derived Tregs on $CD4^+$ T cells. Both atezolizumab and ipilimumab used in our study were from clinical grade stocks of antibodies used for the therapeutic treatment of patients. Since MoT cells are infected with HTLV-II, a suppressive molecule could be due to HTLV-II, but since PBMC-derived Tregs appear to mediate the same type of suppression, the suppressive molecule could also be lineage-specific and/or expressed at a certain stage of lymphocyte development. Alternatively, HTLV-II genes could be driving the expression of either an HTLV-II protein or another cellular protein capable of mediating Treg-like activity.

Second, since MoT cells are allogeneic to all PBMC donors used in this study it is possible that some T cell receptor recognition by stimulated $CD4^+$ PBMC of allo-MHC on MoT cells influenced their suppressive activity. However, we performed allogeneic suppression assays with PBMC-derived Tregs and observed the same suppressive effect as MoT-mediated suppression and autologous Treg suppression (data not shown, available upon request). Therefore, suppressive capacity of MoT cells and PBMC-derived Tregs overcomes any potential allogeneic stimulation.

Third, CD3/CD28 stimulation is variable among human donors. Six different PBMC donors were used in this study. The proliferative capacity after CD3/CD28 activation of each donor is slightly different. Some T cells double 8 times in 5 days while others double 5 or 6 times. Additionally, some donor PBMC are more easily suppressed by MoT cells, while some are less easily suppressed. However, activated $CD4^+$ PBMCs

from 6 different PBMC donors were all suppressed by MoT cells (Appendix B, Supplemental Figure 2).

Fourth, we did not detect TCR or CD3 expression on MoT cells. This suggests that the suppression observed is not a trogocytosis-mediated phenomenon [141]. MHC II blockade had no impact on suppression, further supporting that the suppressive activity is independent of TCR-peptide-MHC interactions. One possibility is that MoT are of NK origin that kill allogeneic cells. We think this is unlikely because MoT cells do not express granzymes and suppression is not reversed by blocking Fas-FasL interaction. Although MoT cells are leukemia cells, they could still represent an uncharacterized sub-population of suppressive/regulatory lymphocytes. We are currently interrogating PBMC-derived $CD4^+$ $CD25^{high}$ $Foxp3^+$ T cells to determine if there is a population of $Foxp3^+$ cells that lacks TCR/CD3.

Tregs can limit antitumor responses and the presence of Tregs in solid tumors can impact clinical prognosis. Although current cancer therapies such as cyclophosphamide, sunitinib, idelalisib [150], and sorafenib can modulate Treg suppressive activity, these therapies are not Treg specific and likely impact anti-tumor T cells. Thus, there is a growing clinical need to selectively target Tregs in tumors while preserving anti-tumor T cell activity and peripheral immune homeostasis.

Immune checkpoint inhibitors such as anti-PD-L1, -CCR4, -LAG-3, -CTLA-4, or -GITR did not attenuate MoT Treg suppressive activity. Herein, we demonstrated that human PBMC-derived $CD4^+$ $CD25^{high}$ $Foxp3^+$ Tregs and MoT cells suppress CD3/CD28-stimulated $CD4^+$ PBMCs in a cell contact-dependent manner, suggesting that a $CD4^+$ $CD25^{high}$ $Foxp3^+$ Treg population in peripheral blood may play a role in suppressing

$CD4^+$ T cell-mediated immune responses by an unknown cell contact-dependent mechanism. Although MoT cells and PBMC-derived Tregs induce apoptosis, they may do so by different mechanisms. Both are driving stimulated $CD4^+$ PBMC toward apoptosis but it is unclear if induction of apoptosis is the major mechanism of suppression. Other mechanisms may involve T cell fratricide, autophagy, and other caspase-dependent cell death. Further studies are required to identify the cell surface marker(s) that suppresses $CD4^+$ T cell proliferation. Transcriptional and epigenetic profiling of Treg and MoT should be performed in future studies to investigate the suitability of MoT cells as a model of Tregs. At this point, it is unclear if the mechanisms of suppression by MoT cells and PBMC-derived Tregs are the same. We are actively investigating potential cell surface molecules and pathways. Characterization of a novel suppressive marker on Tregs and related cell types could lead to functional cellular and molecular studies of Tregs with the goal of harnessing them for therapy.

Summary Sentence: Human $Foxp3^+$ Tregs and a Treg-like cell line suppress $CD4^+$ PBMC proliferation by cell-to-cell contact, independent of known checkpoint inhibitors, suggesting an uncharacterized suppressive mechanism.

Acknowledgments

Support was provided by Gloria A. and Thomas J. Dutson Jr. Kidney Research Endowment, Novartis, and an ASU-Mayo Seed grant to THH and DFL. THH is supported by the Gerstner Family Career Development Award and the National Cancer Institute (R01CA224917). Opinions, interpretations, conclusions, and recommendations

are those of the author and are not necessarily endorsed by the funding agencies. The funding agencies had no role in the study design.

Author contributions

THH, GJW and DFL designed and interpreted all experiments.

YR and KP performed all experiments.

Disclosures

THH has received research funding from Novartis and has served on advisory boards for Exelixis, Genentech, EMD-Serono, Ipsen, Cardinal Health, Surface Therapeutics, and Pfizer. GJW is an employee of SOTIO and former employee of Unum Therapeutics-both outside of submitted work, reports personal fees from MiRanostics Consulting, Paradigm, Angiex, IBEX Medical Analytics, Spring Bank Pharmaceuticals, Pfizer, IDEA Pharma, GLG Council, Guidepoint Global, Ignyta, Circulogene, Genomic Health-all outside this submitted work; has received travel reimbursement from Cambridge HealthTech Institute, GlaxoSmith Kline, and Tesaro-outside of this submitted work; had ownership interest in MiRanostics Consulting, Unum Therapeutics, Exact Sciences, and Circulogene-outside the submitted work; and has a patent for methods and kits to predict prognostic and therapeutic outcome in small cell lung cancer issued, outside the submitted work. The other authors declare no conflicts of interest.

Supplemental Data

Supplemental data for Chapter 2 in Appendix B.

CHAPTER 3

GENERATION AND CHARACTERIZATION OF A MONOCLONAL ANTIBODY THAT BINDS TO GALECTIN-1

Originally published in *Protein Expression and Purification,* May 2023, Volume 210

Kirsten Pfeffer, Thai H. Ho, Francisca J. Grill, Yvette Ruiz, Douglas F. Lake

Abstract

Galectin-1 is a β-galactoside-binding lectin that has been implicated as a suppressive molecule in cancer and autoimmune diseases. Gal-1 has known immunomodulatory activity and was found to be expressed on regulatory T cells, leading to the potential for targeted immunotherapies. Anti-Gal-1 monoclonal antibodies were generated in this study using classical hybridoma techniques. MAb 6F3 was found to bind to Gal-1 by Western blot and ELISA. Flow cytometry was used to determine cell surface and intracellular binding of mAb 6F3 to Gal-1 in PBMC-derived Tregs and tumor cells, including Treg-like cell lines. These results suggest mAb 6F3 may be used to further study Gal-1 protein expression and function.

Introduction

Galectin-1 (Gal-1) is a 14.5kDa protein encoded by *LGALS1* gene belonging to a family of conserved lectins that bind to β-galactoside-containing glycoproteins. These lectins share conserved carbohydrate recognition domains (CRD) that are responsible for binding to β-galactoside[151]. Gal-1 functions as a homodimer, contains one CRD and can be found both intra- and extracellularly. Although it does not contain a canonical signal sequence, it is known to be secreted and bind to cell surfaces, but the exact mechanism is unknown[152]. Intra- and extracellular Gal-1 have distinct functions. Extracellular Gal-1 predominately exists as a homodimer and functions by binding carbohydrate moieties containing β-galactoside, while the function of intracellular Gal-1 does not require carbohydrate binding[151]. Intracellular Gal-1 can be found in the cytosol and nucleus and plays a role in signal transduction and transcription to enhance cell proliferation[153,154]. Extracellular Gal-1 homodimers mediate cell-cell interactions by binding to cell surface receptors via β-galactosides which induces cross-linking due to bivalent binding activity[155,156]. These interactions with cell surface glycoproteins induce signaling pathways that modulate cell proliferation[153]. Extracellular Gal-1 has been shown to exert strong immunosuppressive activity, specifically targeting and inducing apoptosis of activated T cells[157,158], making it a potential biological target for immunotherapy.

The immunomodulatory activity of Gal-1 has been implicated in numerous cancers[155,159,160] and autoimmune diseases[158]. Gal-1 expression and subsequent secretion has been found to be upregulated in tumors compared to normal cells, influencing tumor progression via immunosuppression, and by promoting cell adhesion, apoptosis and angiogenesis[155,161]. Increased expression of Gal-1 is found in highly invasive and poorly

differentiated tumors and correlated with poor patient prognosis[151,155,161]. The potential role of Gal-1 in immune suppression and cancer progression makes it a significant protein of interest.

Evidence of the role of Gal-1 in tumorigenesis has led to an increased interest in investigating novel approaches to inhibit its function. Targeting strategies include using oligosaccharides, synthetic peptides, small molecules and monoclonal antibodies that specifically block the CRD and prevent Gal-1-glycan interactions[153]. Several Gal-1 inhibitors are currently under development. OTX008 compound was derived from a peptide that was shown to inhibit Gal-1 and reduces tumor growth and angiogenesis *in vivo*[153]. An allosteric inhibitor is being evaluated that targets both Gal-1 and Gal-3[162]. Neutralizing mAbs targeting Gal-1 are also being investigated. An anti-Gal-1 neutralizing antibody was developed and shown to block Gal-1-induced apoptosis[159,163]. Another anti-Gal-1 neutralizing mAb is currently being tested in tumor models for immunomodulatory activity[164].

We became interested in Gal-1 as it has been identified on human $CD4^+$ $CD25^{high}$ $FoxP3^+$ Tregs and may play a role in Treg cell expansion and suppressive activity[162,165]. Previously, we found that human $CD4^+$ $CD25^{high}$ $FoxP3^+$ regulatory T cells (Tregs) suppress $CD4^+$ PBMCs by an uncharacterized cell contact-dependent mechanism[166]. However, Tregs are difficult to purify and expand due to high heterogeneity and lack of a Treg-specific cell surface molecule. To study Tregs, we identified a human Treg-like cell line that is phenotypically similar and suppresses activated $CD4^+$ PBMCs[166]. However, the mechanisms of Treg-mediated immune suppression are not fully understood. *In vitro*, Tregs suppress via cell-cell contact and suppression is not reversed by blocking cytokines

or immune checkpoint pathways that are known to play a role in Treg suppression *in vivo*[165,166]. Proteomic analysis by our group found Gal-1 to be expressed on Tregs.

To aid in the study of Gal-1 mediated suppression by Tregs and tumor cells, we developed a non-neutralizing, non-blocking monoclonal antibody against Gal-1. This antibody may be useful in research and/or diagnostic settings for the study of Gal-1–T cell interactions and immunosuppression. Herein, we describe the generation and characterization of a Gal-1 specific monoclonal antibody compatible with flow cytometry and intracellular staining.

Materials and Methods

Cell lines

Tregs were isolated using EasySep Human CD4+CD127^{low}CD25+ Regulatory T Cell Isolation Kit from whole PBMCs. MoT cells were a gift from the late David Golde (ATCC CRL-8066; Manassas, VA, USA) and are a CD4+ human T-lymphoblast cell line derived from a patient with a T-cell variant of hairy-cell leukemia[140]. Jurkat cells (ATCC TIB-152) are a human T-lymphocyte cell line from a patient with acute T cell leukemia. MT-2 cells (RRID:CVCL_2631) are a T cell line established by co-incubation with HTLV-I-infected leukemic cells from a patient with adult T cell leukemia. MT-4 cells (RRID:CVCL_2632) are a T cell line derived from co-incubation with cells from a patient with adult T cell leukemia. H9 cells (HTB-176) are a human cutaneous T-lymphocyte line isolated from a patient with lymphoma. MDA-MB-231 (ATCC HTB-26) is a human triple-negative breast adenocarcinoma (TNBC) cell line and MCF7 (ATCC HTB-22) is a human non-invasive breast cancer cell line[167]. All cell lines were

maintained in DMEM (Gibco; Grand Island, NY, USA) supplemented with 5% heat-inactivated fetal bovine serum (Atlanta Biologicals; Norcross, GA, USA). Cell lines underwent short tandem repeat validation to confirm their identities (University of Arizona Genetics Core).

Production and purification of recombinant Galectin-1

Human Galectin-1 expression plasmid (Galectin-1 cDNA ORF Clone, Human, C-His tag in pCMV3), was purchased from Sino Biological (Catalog #HG10290-CH) and transfected into FreeStyle 293F cells (Catalog #R79007; Thermo Fisher). Transfected 293F cells were grown shaking at 37°C, 8% CO_2 for seven days. Cell supernatants were harvested by centrifugation and recombinant Gal-1 (rGal-1) was purified by nickel column via C-terminal 10X histidine tag. Purified protein was concentrated and dialyzed in 1X phosphate-buffered saline (PBS) with an Amicon filter unit (Sigma), quantified using the Pierce BCA Protein Assay Kit (Thermo Fisher) and stored at -80°C. 10µg of protein was excised from a polyacrylamide gel after electrophoresis (SDS-PAGE) and subjected to in-gel tryptic digestion protocol for LC-MS/MS. Tryptic digest was submitted to the ASU proteomics core facility for analysis. Mass spectra were searched against a human proteome FASTA database from UniProt (Proteome ID: UP000005640) using Proteome Discoverer.

Immunization and hybridoma production

BALB/c mice were immunized by subcutaneous (SQ) injection with rGal-1 (15µg) in Magic Mouse Adjuvant (Creative Diagnostics) under an IACUC-approved

protocol at Arizona State University. Serum was collected to monitor anti-Gal-1 antibody titers by indirect enzyme-linked immunosorbent assay (ELISA). Once sufficient antibody titers were reached, a final SQ boost was given, mice were sacrificed and splenocytes were fused with myeloma cells (P3X63Ag8.653; ATCC CRL-1580) by a previously described hybridoma generation technique[168]. Briefly, splenocytes were fused with myeloma cells at a ratio of 1:2 using 50% polyethylene glycol solution (Sigma-Aldrich). The fused cells were resuspended in hypoxanthine-aminopterin-thymidine (HAT) media (Sigma-Aldrich) to select for successfully fused clones and plated at 5 x 10^4 splenocytes per well in 96-well flat bottom plates. Plates were incubated for ten days at 37°C, 5% CO_2.

Detection and purification of anti-Gal-1 monoclonal antibodies

Mouse antisera and hybridoma supernatants were screened by indirect ELISA for anti-Gal-1 IgG antibodies. Briefly, streptavidin at 10 μg/ml was coated onto a 96-well high-binding plate at 37°C for 1 hour, washed three times with 1X PBS + 0.05% Tween-20 (PBST) and blocked in 1% bovine serum albumin (BSA) in PBS for 1 h. Next, biotinylated rGal-1 was added to the plate at 1 μg/ml in 1% BSA/PBS and allowed to bind overnight at 4°C. To monitor antibody titers, mouse antisera was two-fold serially diluted starting at 1:2,000, added to the plate, and incubated for 1 h at room temperature. To test hybridoma supernatants, undiluted cell supernatant was added to the plate and incubated for 1 h at room temperature. To detect primary antibody bound to rGal-1, plates were washed with PBST three times and incubated with HRP-conjugated Goat Anti-Mouse IgG, Fcγ fragment specific antibody (Jackson ImmunoResearch) at 1:10,000

dilution for 1 h at room temperature. Plates were then washed with PBST four times and TMB substrate was added to develop for 15 minutes. The reaction was stopped with 0.16 M sulfuric acid, and absorbance was measured at 450 nm. Positive wells were subcloned by limiting dilution and re-screened after ten days using the same procedure. Positive subclones were cultured in DMEM (Gibco; Grand Island, NY, USA) supplemented with 10% heat-inactivated fetal bovine serum (Atlanta Biologicals; Norcross, GA, USA). Monoclonal antibodies were purified from hybridoma supernatants by Protein A chromatography (MabSelect; Cytiva). Multiple mAbs against rGal-1 were identified, but mAb 6F3 performed well in several assays.

Western blotting

rGal-1 was subjected to SDS-PAGE under non-reducing conditions using 15% polyacrylamide gels at 130 V for 1 h (Bio-Rad) and subsequently stained with Coomassie Blue dye. For Western blot analysis, proteins were transferred to PVDF membranes at 90V for 1 h. Membranes were then blocked in 5% BSA/PBS overnight at 4°C. Next, anti-Gal-1 6F3 at 5 μg/ml was added and incubated with the membrane for 1 h at room temperature, then washed three times in Tris-buffered saline + 0.1% Tween-20 (TBST). After washing, secondary antibody (peroxidase conjugated goat anti-mouse IgG, Fcγ fragment specific; Jackson ImmunoResearch) was added at 1:10,000 and incubated for 1 h at room temperature. Membranes were then washed four times with TBST followed by addition of KPL TrueBlue Peroxidase Substrate (Sera Care) and developed for 10 minutes.

Indirect ELISA

To evaluate mAb 6F3 binding by ELISA, biotinylated rGal-1 was bound to streptavidin (SA-bound) as described above. Then, the plates were washed three times with PBST and blocked in 1% BSA/PBS for 1 h. To test binding, mAb 6F3 was added at 16 μg/ml and diluted two-fold in 1% BSA/PBS for 1 h. The plates were washed three times with PBST and then incubated with HRP-conjugated Goat Anti-Mouse IgG, Fcγ fragment specific antibody (Jackson ImmunoResearch) at 1:10,000 dilution for 1 h at room temperature. Plates were then washed with PBST four times and developed for 15 minutes with TMB substrate. The reaction was stopped with 0.16 M sulfuric acid, and absorbance was measured at 450 nm.

Flow cytometry

2 x 10^5 cells per 12x75 mm flow tube were washed twice in PBS and blocked in flow cytometry staining buffer (5% FBS/PBS) for 1 h at room temperature. Next, primary antibody anti-Gal-1 mAb 6F3 or anti-Gal-1 mAb control (Galectin-1 Monoclonal Antibody, clone 6C8.4-1; Invitrogen) was added at 2 μg/100 μl for 1 h at room temperature. Cells were washed two times in 5% FBS/PBS and secondary antibody was added (PE-conjugated Goat Anti-Mouse Ig; BD Pharmingen) at 1:50 for 1 h at room temperature. Next, cells were washed three times in 5% FBS/PBS and analyzed on CytoFlex LX flow cytometer (Beckman Coulter). For intracellular staining, cells were fixed and permeabilized with True-Nuclear Transcription Factor Buffer Set (BioLegend) then stained as described above to detect intracellular Gal-1. For Treg staining, biotinylated mAb 6F3 was used and detected with AlexaFluor 555-conjugated

streptavidin (Invitrogen). Fluorescence was quantified and expressed as difference in geometric mean fluorescence intensity (ΔMFI) between the primary antibody staining and secondary alone control.

Results

Production and purification of recombinant Galectin-1

Recombinant human Gal-1 was produced using pCMV3 mammalian expression plasmid. After purification, rGal-1 was separated by SDS-PAGE and stained with Coomassie blue stain (Figure 13A). Bands were observed at the expected molecular weight of monomeric (~14.5kDa) and dimeric (~30kDa) Gal-1. Further analysis using mass spectrometry confirmed the identity of these bands as Gal-1, accession no. P09382 (Figure 13B).

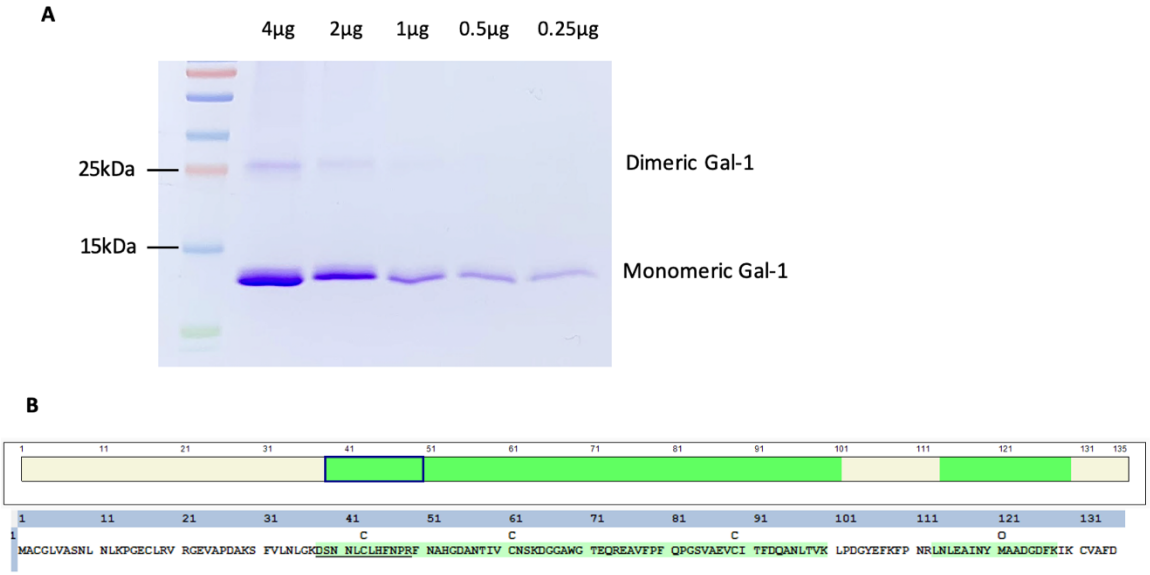

Figure 13. (A) **Coomassie blue stain of rGal-1.** (B) **Peptide mapping of rGal-1 by mass spectrometry.** Tryptic digest of the expected bands (~14.5 and ~30 kDa) were analyzed by LC-MS and results show 58.52% coverage of Gal-1. High confidence peptides are highlighted in green. Amino acids with carbamidomethylation and oxidation sites are designated as C and O, respectively.

Anti-Gal-1 mAb binds specifically to recombinant Galectin-1

Mice were immunized with rGal-1, followed by generation of hybridomas. Anti-Gal-1 IgG antibodies were detected in spent hybridoma supernatants by ELISA (described above). Clone 6F3 was identified by screening supernatants for binding to rGal-1 and purified by Protein A affinity chromatography. Western blot analysis was performed to evaluate binding of purified mAb 6F3 to rGal-1 (Figure 14).

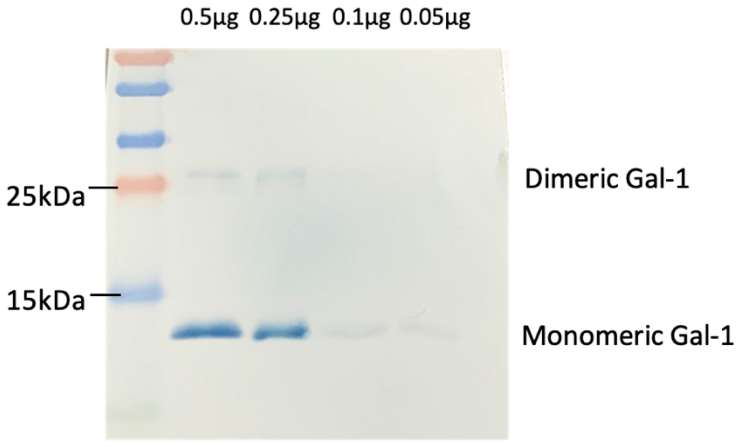

Figure 14. Anti-Gal-1 mAb 6F3 binds to target recombinant Gal-1 on Western blot. rGal-1 was separated by SDS-PAGE (15%) and transferred to PVDF membrane. Membrane was probed with mAb 6F3, followed by detection with HRP-conjugated anti-mouse IgG secondary antibody. TrueBlue Peroxidase Substrate was used to visualize bands.

Since immobilization of protein on plastic can sterically hinder the ability of antibody to bind antigen[169], we tested the binding ability of mAb 6F3 to SA-bound biotinylated rGal-1 by ELISA (Figure 15). Control antigen (CTRL) was used as a negative control. HL antigen, derived from the *Coccidioides* fungus, was used as a control recombinant protein and was produced in 293F cells under the same conditions as rGal-1. This protein was chosen due to its similar molecular weight ~17kDa and because it contains a C-terminal his-tag.

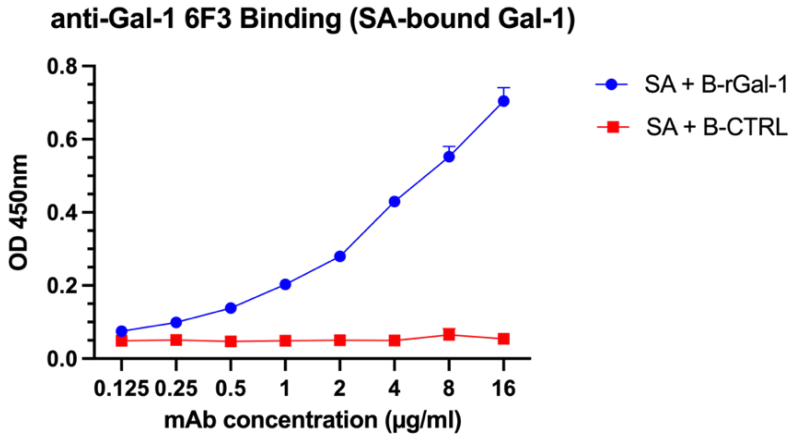

Figure 15. MAb 6F3 binds to SA-bound rGal-1 by ELISA. Serial dilutions of mAb 6F3 were incubated with rGal-1 immobilized by SA on ELISA plates. HRP-conjugated anti-mouse IgG Fcγ fragment specific secondary antibody was used to detect the interaction. Mean and standard deviation are plotted from three independent experiments.

To further support that mAb 6F3 specifically binds to rGal-1, a competition ELISA was performed (Figure 16). MAb 6F3 was pre-incubated with rGal-1 at molar fold-excess of antigen starting at 200:1 and two-fold serially diluted. When rGal-1 was allowed to pre-incubate with mAb 6F3, we observed reduced binding to SA-bound rGal-1 in a dose-dependent manner. Pre-incubation of mAb 6F3 with control antigen had no effect on binding.

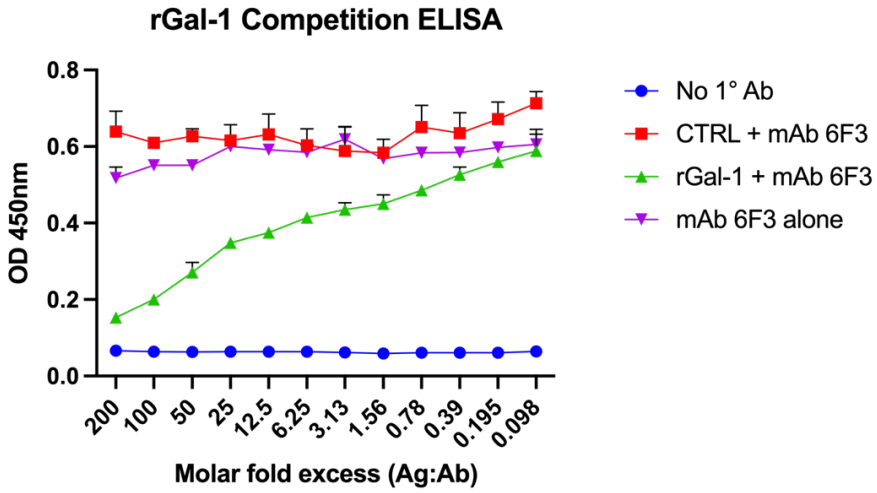

Figure 16. MAb 6F3 binding is specific for Gal-1. Competition ELISA was performed by pre-incubation of Ag:Ab at molar-fold excess. CTRL antigen was HL from the *Coccidioides* fungus. Ag:Ab was incubated before adding to SA-bound rGal-1-coated plate. Mean and standard deviation are plotted from three independent experiments.

Since Galectins -3 and -9 are also implicated in immune modulation, are known to be secreted, and interact with T cell surface proteins[162,170,171], we tested mAb 6F3 for cross-reactivity. We found neither mAb 6F3 or the commercial mAb show cross-reactivity by ELISA (Appendix C, Supplemental Figure 1).

Anti-Gal-1 mAb binding to cell surface and intracellular Gal-1 detected by flow cytometry

Gal-1 has been found to be expressed on Tregs and may play a role in Treg-mediated suppression of inflammatory T cells[165]. We previously characterized a Treg-like cell line, MoT cells, which expresses Treg-associated markers and suppresses CD4+ T cell proliferation, similarly to human Tregs isolated from peripheral blood[166]. Therefore, we wanted to evaluate mAb 6F3 binding to Gal-1 on PBMC-derived Tregs and MoT cells. We found that mAb 6F3 binds to Tregs and MoT cell surface but not to Jurkat cells, a non-suppressive T cell line (Figure 17A). In contrast, a commercially available anti-Gal-1 mAb bound poorly to MoT cells and also demonstrated minor non-specific binding on Jurkat cells. We also evaluated other Treg-like cell lines: MT-2[142], MT-4 and H9. MAb 6F3 detected intracellular Gal-1 in Tregs, MoT, MT-2, and MT-4 but not H9 cells. Since Gal-1 has been implicated in metastatic breast cancer[154], we also evaluated mAb 6F3 binding to MDA-MB-231 (highly aggressive) and MCF7 (non-metastatic) breast cancer cell lines. MAb 6F3 detected higher levels of intracellular Gal-1 in MDA-MB-231 compared to MCF7. In contrast, we observed shifts of all cell lines relative to the secondary control when using the commercial mAb. We then wanted to evaluate the ability of mAb 6F3 to detect endogenous versus recombinant Gal-1 on the cell surface. Briefly, Jurkat cells (Gal-1-negative) were pre-incubated with rGal-1 at increasing concentrations to allow rGal-1 to bind to the cell surface. After incubation, the cells were washed to remove unbound rGal-1 and subsequently surface stained with mAb 6F3 as described. Commercially available Gal-1 mAb was used as a control. MAb 6F3 was able

to detect rGal-1 bound to Jurkat cells suggesting that Jurkat cells do not produce Gal-1 but possess the β-galactoside carbohydrate (Figure 17B).

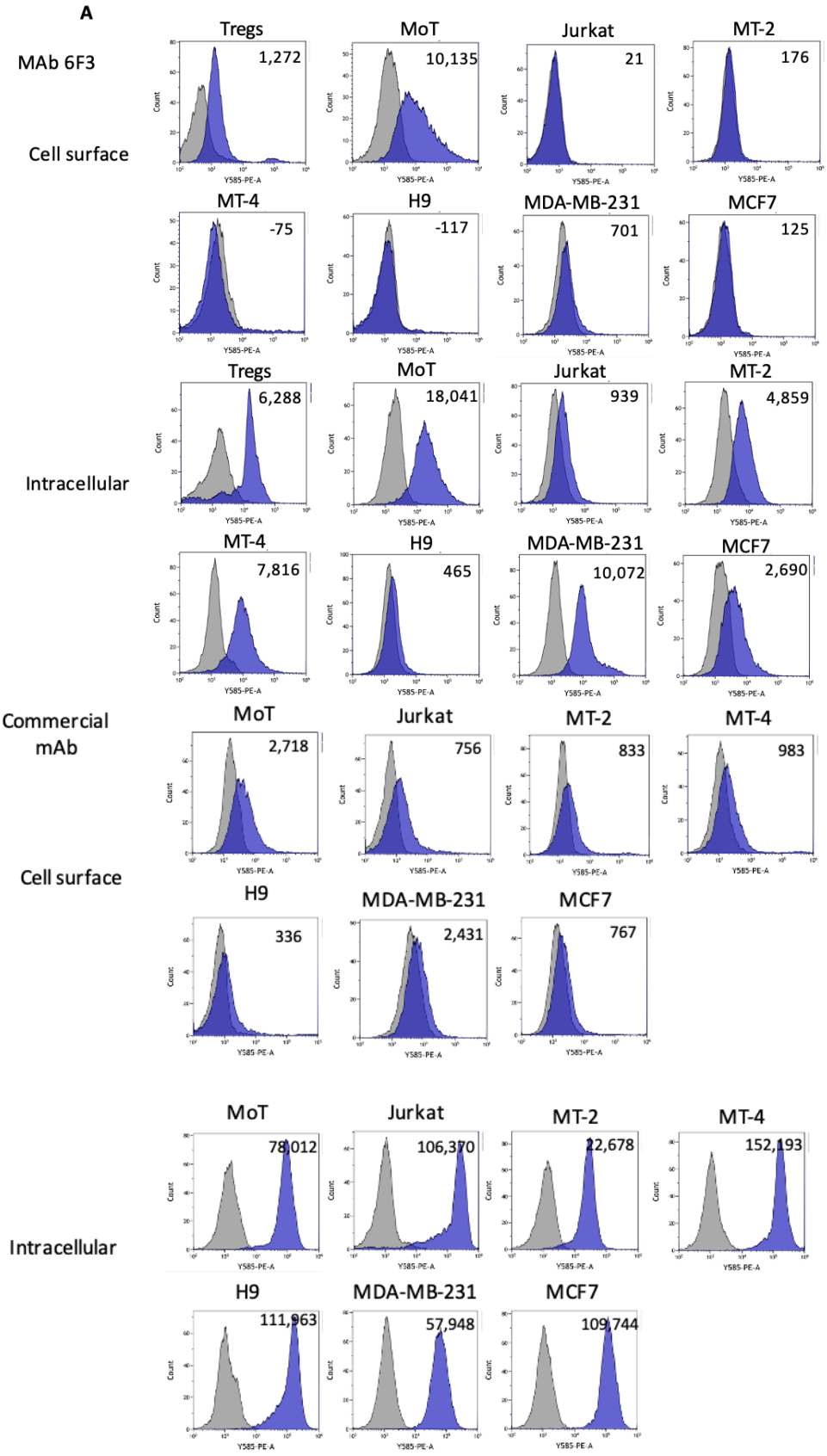
A
MAb 6F3
Cell surface
Tregs
1,272
MoT
10,135
Jurkat
21
MT-2
176
MT-4
-75
H9
-117
MDA-MB-231
701
MCF7
125
Intracellular
Tregs
6,288
MoT
18,041
Jurkat
939
MT-2
4,859
MT-4
7,816
H9
465
MDA-MB-231
10,072
MCF7
2,690
Commercial mAb
Cell surface
MoT
2,718
Jurkat
756
MT-2
833
MT-4
983
H9
336
MDA-MB-231
2,431
MCF7
767
Intracellular
MoT
78,012
Jurkat
106,370
MT-2
22,678
MT-4
152,193
H9
111,963
MDA-MB-231
57,948
MCF7
109,744
Count
Y585-PE-A

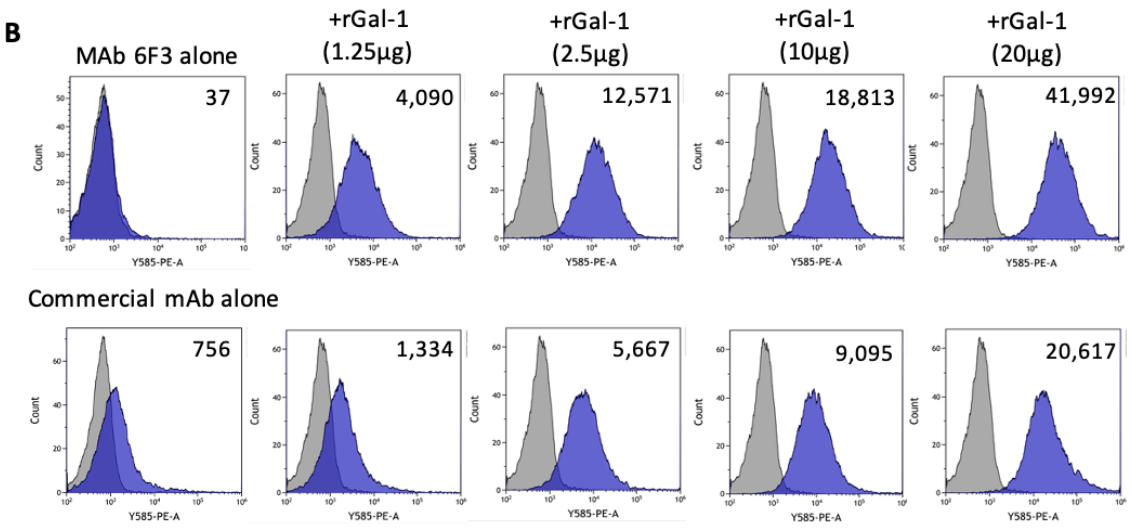

Figure 17. (A) **Anti-Gal-1 mAb 6F3 binds to cell surface and intracellular Gal-1 by flow cytometry.** (B) MAb 6F3 detects rGal-1 bound to cell surface. MAb 6F3 staining (blue histogram) and secondary alone (gray histogram) are shown. Cell surface and intracellular staining was performed for each cell type. For each histogram, ΔMFI values are indicated on the graph.

Discussion

In this study, mAbs against Gal-1 were generated by fusion of B cells from mice immunized with rGal-1 to mouse myeloma line P3X63. Anti-Gal-1 IgG antibodies were detected in the resulting hybridoma supernatants. MAb 6F3 was isolated and found to bind to rGal-1 by Western blot (Figure 14). In Figures 15 and 16, we show mAb 6F3 is specific for rGal-1 by indirect and competition ELISA techniques. MAb 6F3 does not demonstrate cross-reactivity with other galectins (Appendix C, Supplemental Figure 1).

MAb 6F3 was used to detect cell surface and intracellular Gal-1 in Tregs, T cell lines and breast cancer lines by flow cytometry analysis. Interestingly, mAb 6F3 detects Gal-1 on the cell surface of PBMC-derived Tregs and MoT cells but not on other Treg-like or other T cell lines (Figure 17A). MAb 6F3 also detected higher levels of intracellular Gal-1 in MDA-MB-231 compared to MCF7. This finding supports Gal-1 expression in highly invasive, metastatic breast cancer as has been reported[155]. In comparison, the commercial mAb showed positive intracellular staining of all cell lines, even in Gal-1 negative/low cells. Mab 6F3 detected low and high concentrations of rGal-1 in a dose-dependent manner on the cell surface of a Gal-1-negative cell line (Figure 17B).

The generation of mAb 6F3 provides a new tool in studying Gal-1 function and interactions with other proteins. Gal-1 is known to interact with several binding partners including extracellular matrix proteins, cell surface glycoproteins, cytoplasmic and nuclear proteins. Flow cytometry showed that mAb 6F3 has the ability to bind to tumor cells and human Tregs. This is significant as Gal-1 is known to bind to the cell surface and interact with ECM proteins, integrins, and T cell glycoproteins[172]. MAb 6F3 can also

detect intracellular Gal-1 (Figure 17A), which can be used as a tool when studying interactions between Gal-1 and other intracellular proteins. Gal-1 has been shown to interact with and influence the function of nuclear proteins FoxP3[154] and Genim4[151,153] and cytoplasmic protein Ras[151,153]. These proteins that have significant biological functions in cell growth signaling pathways, RNA splicing, and gene activation.

Gal-1 promotes an immunosuppressive environment by increasing the number of Tregs[162] and inducing T cell apoptosis, although the mechanism of Gal-1-mediated apoptosis is not well understood[161,173]. Development of an anti-Gal-1 mAb can be used to evaluate Gal-1 function, including Gal-1-mediated apoptosis of T cells. We tested mAb 6F3 in a suppression assay to determine if it reversed Gal-1-mediated Treg suppression as previously suggested[165] and found that it did not block suppressive activity (Appendix C, Supplemental Figure 2). This led to the conclusion that mAb 6F3 either does not block Gal-1 activity or Gal-1 is not mediating Treg cell contact-dependent suppression. A previously published[163] neutralizing mAb was not available upon request for comparison. Herein, we demonstrate that mAb 6F3 may be used to evaluate Gal-1 expression in different tumor cell types and study its function in the context of cancer and other immune diseases.

Funding

This work was supported by NIH grants R01 CA224917 (THH) and CA271503 (THH).

Author Contributions

THH and DFL conceptualized research.

KP, FJG, and YR performed all experiments.

KP wrote the paper with revision by THH, FJG, YR, and DFL.

Acknowledgments

We would like to thank Alexa Roeder at Arizona State University for providing the control antigen used in our ELISAs.

Declaration of Competing Interest

THH has received research funding from Novartis and has served on advisory boards for Exelixis, Genentech, EMD-Serono, Ipsen, Cardinal Health, Surface Therapeutics, and Pfizer. The other authors declare no conflict of interest.

Supplemental Data

Supplemental data for Chapter 3 in Appendix C.

CHAPTER 4

CHARACTERIZATION OF MONOCLONAL ANTIBODIES THAT BIND TO MOT CELLS

Abstract

Regulatory T cells can suppress activated T cell proliferation by direct cell-contact, although the exact mechanism is poorly understood. Identification of a Treg-specific cell surface molecule that mediates suppression would offer a unique target for cancer immunotherapy to inhibit Treg immunosuppressive function or deplete Tregs in the tumor microenvironment. In this study, whole cell immunization using a Treg-like cell line (MoT cells) was performed to generate monoclonal antibodies that bound cell surface proteins in their native conformations. From the 105 hybridomas that bound to the MoT cell surface, 32 exhibited functional activity in a suppression assay. Most of the mAbs blocked MoT suppressive activity, but a few appeared to enhance MoT suppressive activity. Characterization of one anti-MoT mAb, 12E7, exhibited strong binding to MoT/Treg cell surface, was subsequently found to bind to CD44, and demonstrated the ability to reverse MoT-mediated suppression.

Introduction

The primary target for cancer immunotherapies are membrane-bound and/or soluble proteins that modulate or affect immune cell function. Immune checkpoint molecules are expressed on the cell surface of activated immune cells to help maintain homeostasis. Activated T cells upregulate these inhibitory molecules to abrogate T cell responses and minimize tissue damage[49,74]. Tumor cells utilize these checkpoint pathways to prevent immune cells from effectively killing[61]. The goal of cancer immunotherapy is to target and block immune checkpoints, taking the brakes off the immune system to boost anti-tumor response[174].

Current FDA-approved immune checkpoint therapies utilize monoclonal antibodies that target cell surface proteins. Immune checkpoint-targeted mAbs can be agonistic to enhance co-stimulation or antagonistic to block inhibitory pathways[72,74]. Most mAbs approved for cancer therapy do not target the tumor directly but target infiltrating lymphocytes to increase endogenous antitumor T cell activity[74]. Compared to traditional therapies, checkpoint inhibitors have been shown to elicit durable antitumor responses and less off-target effects, with some patients achieving long-term remission[49,77].

Effective, long-term responses to immune checkpoint therapies are dampened by Treg immunosuppression. Tregs infiltrate the tumor microenvironment, where these cells hinder the antitumor immune response[74,113]. The exact mechanism of Treg immune suppression is still being investigated, although Tregs are known to suppress by direct cell-cell contact[115,166,175]. Tregs can suppress effector T cells by producing anti-inflammatory cytokines (IL-10, IL-35, TGF-β), sequestering growth factor IL-2, or

through modulating APC function[112,115,176,177]. Cell contact-dependent suppressive mechanisms are mediated through direct interactions between Tregs and target T cells which can include granzyme/perforin killing, cytolysis, delivery of immunosuppressive metabolites, and membrane-bound suppressive cytokines (TGF-β)[112,116,117,178]. The role of TGF-β remains controversial as it can play a role *in vivo* but is not required for *in vitro* suppression[112,179]. Identification of a mAb that can specifically target and block Treg suppressive function may be utilized as an additional immune checkpoint therapy, in conjunction to existing immune checkpoint inhibitors, to increase host antitumor responses.

A method to study and identify functional cell surface molecules is to generate mAbs by whole cell immunization techniques[180–182]. Large, diverse mAb libraries that recognize cell surface proteins can be generated by immunizing mice with whole, intact target cells[182]. In contrast to genomic and proteomic techniques, this approach retains physiological conformation and post-translational modifications of cell surface proteins[182]. These mAbs can then be used in a variety of applications such as isolation of specific cell types and inhibition of a specific cell function. The first mAb to be FDA-approved for the treatment of B cell non-Hodgkin lymphoma (NHL), rituximab, was generated by immunizing BALB/c mice with a human lymphoblastoid cell line and targets CD20 antigen expressed on B cells[183,184]. Whole cell immunization is a promising approach that can be utilized for discovery and characterization of Treg-specific suppressive molecule(s) that are expressed on the cell surface.

An advantage of immunizing with whole, intact cells is that antibodies can recognize glycosylations and other post-translation modifications (PTMs) of cell surface

proteins produced in the cell of interest. Glycosylation is the post-translational addition of oligosaccharides to proteins mediated by specific enzymes[185]. Oligosaccharides are added to the extracellular portion of a membrane-bound glycoprotein. Glycosylation is an important protein modification as it promotes proper folding, ensures stability and can impact protein function[186]. It is estimated that 50-70% of all eukaryotic proteins are glycosylated[187]. Most glycosylated membrane proteins are *N*-glycosylated (asparagine-linked), while some are *O*-glycosylated (carbohydrate attached to side chain of serine or threonine residues)[188]. Mammalian *N*-linked glycoproteins are typically membrane-bound or secreted. These cell surface glycoproteins mediate extracellular events including cell adhesion, cell-cell interactions and signaling[188].

Glycans influence T cell development, activation, differentiation and function[174,188]. Some glycoprotein immune functions include discrimination of self/non-self, migration, homing, TCR activation and differentiation into effector cells[186]. Like effector T cells, Tregs also have glycosylated cell surface proteins. In general, T cell glycosylation patterns have been widely studied and distinct patterns have been shown between T cell subsets and different activation states[186]. Since Tregs are understudied, little is known about Treg-specific protein glycosylation. Expression of *N*-glycans on Tregs have been correlated with suppressive function and expression of immunosuppressive proteins[186]. It has been shown that *N*-glycosylation also contributes to Treg adherence and migration[185]. Studying the *N*-glycan profile of Tregs and how glycans influence protein activity may have clinical implications for targeting glycosylated proteins that contribute to immunosuppressive function.

Identification and characterization of a cell surface protein that mediates suppression is significant for the study of Tregs and targeting Tregs in clinical applications. Our studies demonstrated that suppression of $CD4^+$ PBMC by human Tregs and MoT cells (Treg-like cell line) is mediated by direct cell-cell contact *in vitro*[166]. It was hypothesized that cell contact-dependent suppression is mediated by one or more suppressive molecules on MoT/Treg cell surface. To address this hypothesis, monoclonal antibodies against the suppressive cell line (MoT) were generated to identify a Treg protein that plays a role in suppression.

Materials and Methods

Cells and cell lines

Tregs were isolated using EasySep Human $CD4^+CD127^{low}CD25^+$ Regulatory T Cell Isolation Kit from whole PBMCs. MoT cells were a gift from the late David Golde (ATCC CRL-8066; Manassas, VA, USA) and are a $CD4^+$ human T-lymphoblast cell line derived from a patient with a T- cell variant of hairy-cell leukemia[189]. Jurkat cells (ATCC TIB-152) are a human T-lymphocyte cell line from a patient with acute T cell leukemia which served as a $CD4^+$, non-suppressive cell line. MT-2 cells (RRID:CVCL_2631) are a T cell line established by co-incubation with HTLV-I-infected leukemic cells from a patient with adult T cell leukemia. MT-4 cells (RRID:CVCL_2632) are a T cell line derived from co-incubation with cells from a patient with adult T cell leukemia. H9 cells (ATCC HTB-176) are a human cutaneous T-lymphocyte line isolated from a patient with T cell lymphoma. Daudi cells (ATCC CCL-213) are a B cell lymphoblast cell line derived from a patient with Burkitt's Lymphoma. MDA-MB-231 (ATCC HTB-26) is a

human triple-negative breast adenocarcinoma (TNBC) cell line and MCF7 (ATCC HTB-22) is a human non-invasive breast cancer cell line[167]. Renca (ATCC CRL-2947) is an epithelial kidney cell line derived from a male mouse with renal cortical adenocarcinoma. All cell lines were maintained in DMEM (Gibco; Grand Island, NY, USA) supplemented with 5% heat-inactivated fetal bovine serum (Atlanta Biologicals; Norcross, GA, USA). Cell lines underwent short tandem repeat validation to confirm their identities (University of Arizona Genetics Core).

Whole cell immunization and hybridoma production

MoT cells were washed in sterile PBS and resuspended at $5x10^6$ cells/ml. BALB/c mice were immunized by intraperitoneal (IP) injection with whole MoT cells ($1x10^6$ cells) in sterile 1X PBS under an IACUC-approved protocol at Arizona State University. Serum was collected to monitor anti-MoT titers by surface staining MoT cells and analyzed by flow cytometry. Once sufficient titers were reached, a final IP boost was given ($2x10^6$ cells), mice were sacrificed and splenocytes were fused with myeloma cells (P3X63Ag8.653; ATCC CRL-1580) by a previously described hybridoma generation technique[168]. Fused cells were incubated for ten days at 37°C, 5% CO_2.

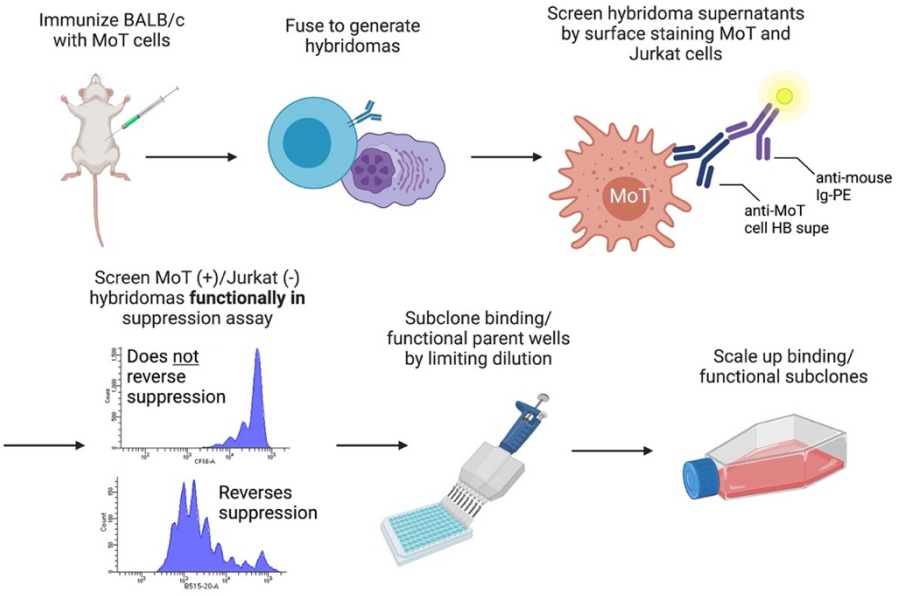

Figure 18. Whole cell immunization, generation and screening of functional anti-MoT antibodies. (Created using Biorender.com)

Detection of binding and functional anti-MoT monoclonal antibodies

Mouse antisera and hybridoma supernatants were screened by surface staining for anti-MoT antibodies. Briefly, $1x10^5$ MoT or Jurkat cells (non-suppressive control cell line) per well were plated in 96-well U-bottom plates and blocked in 5% FBS/PBS for 1 h at room temperature. Next, antisera (4-fold serial diluted starting at 1:20,000) or undiluted hybridoma supernatants (50 µl/well) were added to cells and incubated for 1 h at room temperature. Cells were then washed 2X in 5% FBS/PBS. To detect primary antibody bound to MoT cell surface, cells were incubated with secondary antibody (PE-conjugated Goat Anti-Mouse Ig; BD Pharmingen) for 1 h at room temperature. Cells were washed 3X and analyzed on CytoFlex LX flow cytometer (Beckman Coulter).

To identify functional anti-MoT antibodies that reverse the suppressive property of MoT cells, hybridoma supernatants were tested in a 96-well suppression assay (Figure 19). Briefly, CFSE-labeled $CD4^+$ responder cells were plated with MoT cells at 1:1/16 (responder to suppressor ratio) in 96-well flat-bottom plates and stimulated with anti-CD3/CD28 antibodies. 100 µl of anti-MoT hybridoma supernatants were added and incubated for five days at 37°C, 5% CO_2. After five days, cells were analyzed on CytoFlex LX flow cytometer. Binding and functional hybridomas were subcloned by limiting dilution and re-screened by surface staining after ten days. Positive subclones were cultured in DMEM supplemented with 10% FBS. Monoclonal antibodies were purified from hybridoma supernatants by Protein A (MabSelect) chromatography. Multiple mAbs were identified, but mAb 12E7 performed well in several assays.

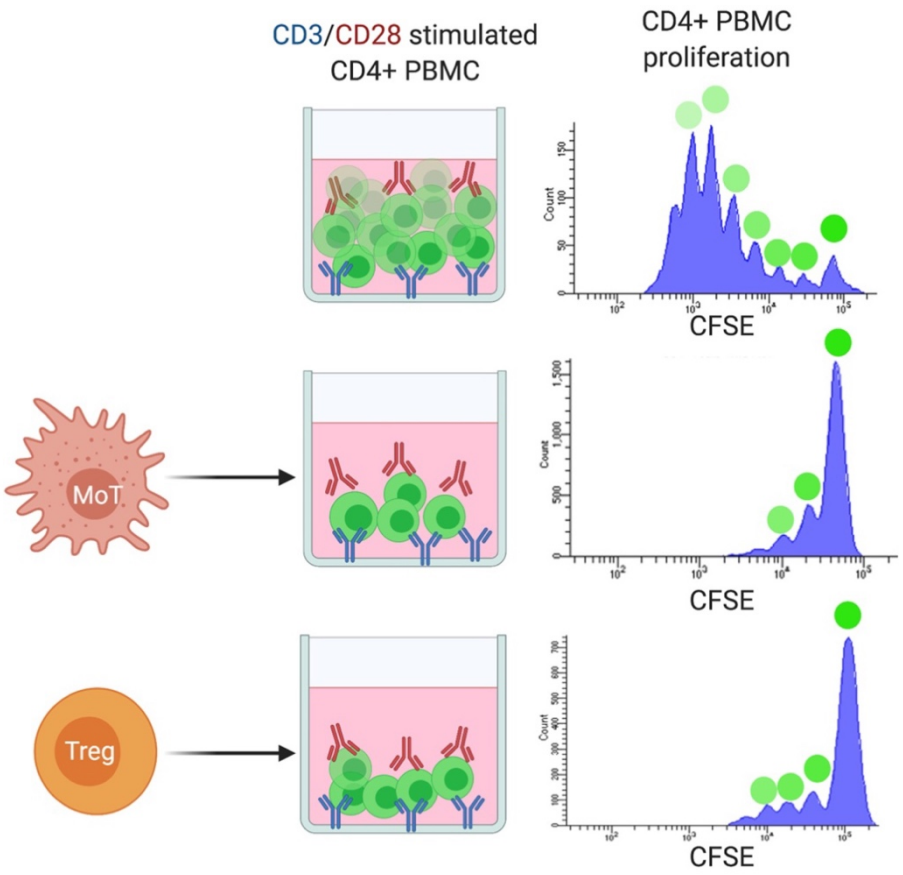

Figure 19. Five-day *in vitro* suppression assay measured by proliferation of CFSE-labeled CD4$^+$ PBMC responder cells. CD4$^+$ PBMC are labeled with CFSE followed by stimulation with plate-bound anti-CD3 and soluble anti-CD28. As responder cells proliferate, the cells lose half of the membrane associated fluorescent dye, resulting in 5-7 proliferative peaks. When suppressor cells are added (MoT cells or PBMC-derived Tregs), responder cell proliferation is reduced to 0-4 proliferative peaks. Each peak to the left of the main peak (right) represents one responder cell division.

Immunoprecipitation and mass spectrometry to identify antigen

$1x10^7$ live MoT cells were incubated with anti-MoT mAb 12E7.A4 (200 µg) in 0.1% FBS/PBS for 1 h at room temperature, end-over-end rotation. After incubation, cells were lysed in IP lysis buffer with protease inhibitor (87787; Pierce). Lysate was added to MabSelect resin (Cytiva) and incubated for 1 h at room temperature with end-over-end rotation. The column was washed four times in 1X PBS, then eluted with 100mM sodium citrate, pH = 3 and neutralized with 1M Tris, pH = 9. Elutions 1-5 were combined and concentrated by acetone precipitation. Briefly, 100% acetone was pre-chilled to -20°C and 4x the elution volume of acetone was added dropwise, on ice. The mixture was vortexed and incubated at -20°C for 1 h. Precipitated protein was pelleted at 15,000 x g for 10 minutes at 4°C. The pellet was resuspended in SDS-PAGE loading dye followed by SDS-PAGE. For mass spectrometry analysis, an SDS-PAGE gel slice corresponding to the location of a single band visualized by western blotting with mAb 12E7 was excised and subjected to in-gel tryptic digestion protocol for LC-MS/MS. The tryptic digest was submitted to the ASU proteomics core facility for analysis. Mass spectra from the proteins in the gel slice were searched against a human proteome FASTA database from UniProt (Proteome ID: UP000005640) using Proteome Discoverer.

Western blotting

Whole cell lysate (15 µg) or rCD44 (0.3 µg) (12211-H08H; Sino Biological) was subjected to SDS-PAGE using 10% polyacrylamide gels at 135 V for 1 h (Bio-Rad). For western blot analysis, proteins were transferred to PVDF membranes at 90V for 1.5 h.

After transfer, membranes were blocked in 1% BSA/TBST overnight at 4°C. Primary antibodies, Anti-MoT clone 12E7 at 5 µg/ml, anti-CD44 pAb (3578; Cell Signaling) anti-CD44 mAb (clone IM7, biotin; STEMCELL Technologies) or anti-PD-L1 (clone E1L3N; Cell Signaling) at 1:1,000 were incubated with the membrane for 1 h at room temperature, then washed three times in TBST. Next, secondary antibody was added at 1:10,000 (AP-conjugated) or 1:50,000 (HRP-conjugated) and incubated for 1 h at room temperature, then washed four times with TBST. Membranes were developed using 1-Step NBT/BCIP Substrate Solution (Thermo Scientific) or SuperSignal West Pico Chemiluminescent Substrate (Thermo Fisher) according to the manufacturer's instructions and imaged on Azure 600 instrument (Azure Biosystems).

Indirect ELISA

To evaluate mAb 12E7 binding by indirect ELISA, rCD44 @ 0.5 µg/ml was coated onto a 96-well high-binding plate at 4°C overnight. The plate was washed three times with PBST and blocked in 1% BSA/PBS for 1 h at room temperature. To test binding, anti-MoT mAbs or anti-CD44 mAb were added at 20 ng/ml and diluted two-fold in 1% BSA/PBS for 1 h. The plates were then washed three times and incubated with HRP-conjugated goat anti-mouse IgG Fcγ (Jackson ImmunoResearch) or HRP-conjugated streptavidin (BD Biosciences) at 1:10,000 dilution for 1 h. After incubation, plates were washed four times and developed with TMB for 10 minutes. 0.16M sulfuric acid was added to stop the reaction and absorbance was measured at 450 nm.

De-glycosylation of cell lysate and whole cells

To cleave *N*- and *O*-linked oligosaccharides from glycoproteins, cell lysate or live cells were treated with PNGase F amidase or *O*-Glycosidase. For cell lysate, 20 µg lysate was combined with 2 µl of 10X GlycoBuffer, and H_2O. 2 µl of PNGase F (P0704S, New England Biolabs) or *O*-Glycosidase (P0733S, New England Biolabs) was added to cleave *N*- and *O*-linked glycans, respectively, under non-denaturing conditions. The reactions were incubated at 37°C overnight. For live cells, irradiated MoT cells (2000 RADS) were resuspended at $1x10^6$ cells/ml in pre-warmed 1% BSA/PBS. Cells were plated at $2x10^5$ cells/well in 96-well flat bottom plate and 400 U/well of PNGase F was added (glycerol-free P0705S, New England Biolabs). Cells were incubated for 2 h at 37°C, 5% CO_2. Cells were washed and resuspended in complete media. For no enzyme controls, cell lysate or MoT cells were incubated under the same conditions without PNGase F or *O*-glycosidase.

Results

Anti-MoT hybridomas were generated to MoT cell surface proteins by immunizing mice with live human MoT cells. By day 33, immunized mice generated high titer antibodies to MoT cell surface proteins, as monitored by surface staining (Figure 20). After one primary immunization and two boosts, splenocytes were isolated and fused to myeloma cells to generate hybridomas. A total of 1,152 parent hybridoma wells were analyzed by flow cytometry for binding to MoT cell surfaces using Jurkat cells as non-suppressive control cell type. Positive binding mAbs were categorized into three groups based on a shift in mean fluorescence intensity (ΔMFI, MoT cell binding

fluorescence – Jurkat cell binding fluorescence): strong ≥ 100,000, moderate ≥ 30,000, and weak ≥ 10,000 MFI. Hybridoma wells that bound to MoT (+) and not to Jurkat (-) were selected for further evaluation. Wells that bound to Jurkat (>5,000 MFI) and/or did not bind to MoT (<10,000 MFI) were excluded. In total, 105 hybridoma parent wells were positive for binding to MoT cells: 33 strong, 54 moderate, and 18 weak (Appendix D, Supplemental Figure 1).

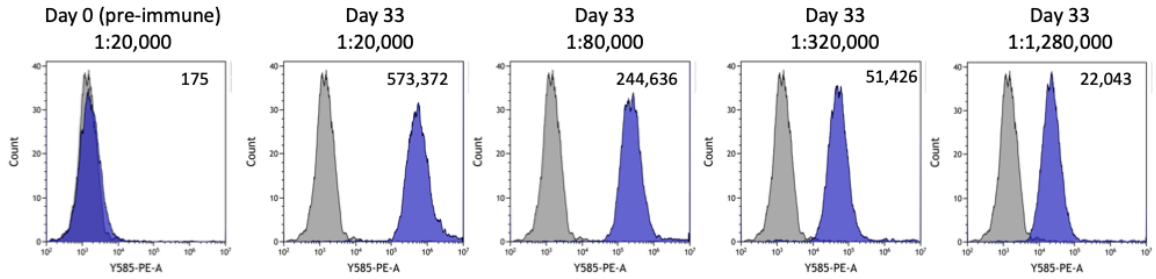

Figure 20. Generation of high titer anti-MoT antibodies by whole cell immunization. Mouse antisera was tested for anti-MoT antibodies by surface staining on Day 0 and Day 33. Antisera staining (blue histogram) and secondary alone (gray histogram) are shown. Sera dilution is indicated above each histogram. For each histogram, ΔMFI values are indicated on the graph.

Functional anti-MoT antibodies block or enhance suppressive activity

To screen for functionally blocking anti-MoT antibodies that affect MoT-mediated suppression, 96-well suppression assays were performed. The 105 hybridoma parent well supernatants that bound to MoT cell surface, MoT (+) Jurkat (-), were added to $CD4^+$ PBMC:MoT co-cultures and incubated for five days. When compared to the suppressed control (MoT co-incubated with activated $CD4^+$ cells = 3 proliferative peaks, 57.8% $CD4^+$ PBMC proliferation, the addition of hybridoma supernatants appeared to reverse suppressive activity demonstrated by responder cells to be restored (> 3 peaks, > 71% proliferation). Conversely, the addition of some hybridoma supernatants resulted in reduced responder cell proliferation (≤ 2 peaks) when incubated with MoT cells compared to the control (Figure 21).

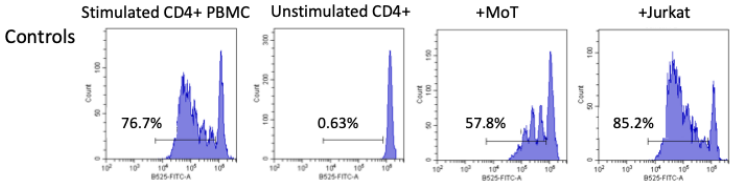

Reverses suppression

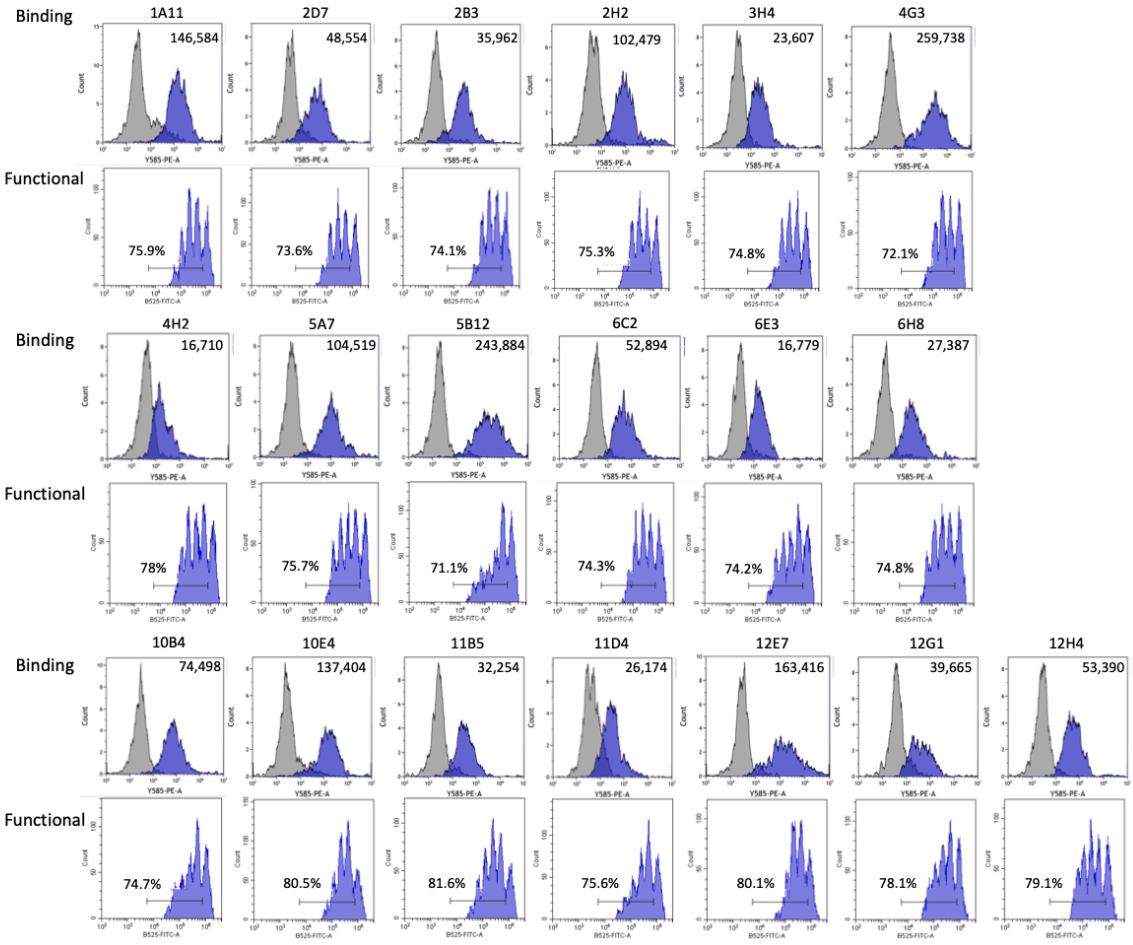

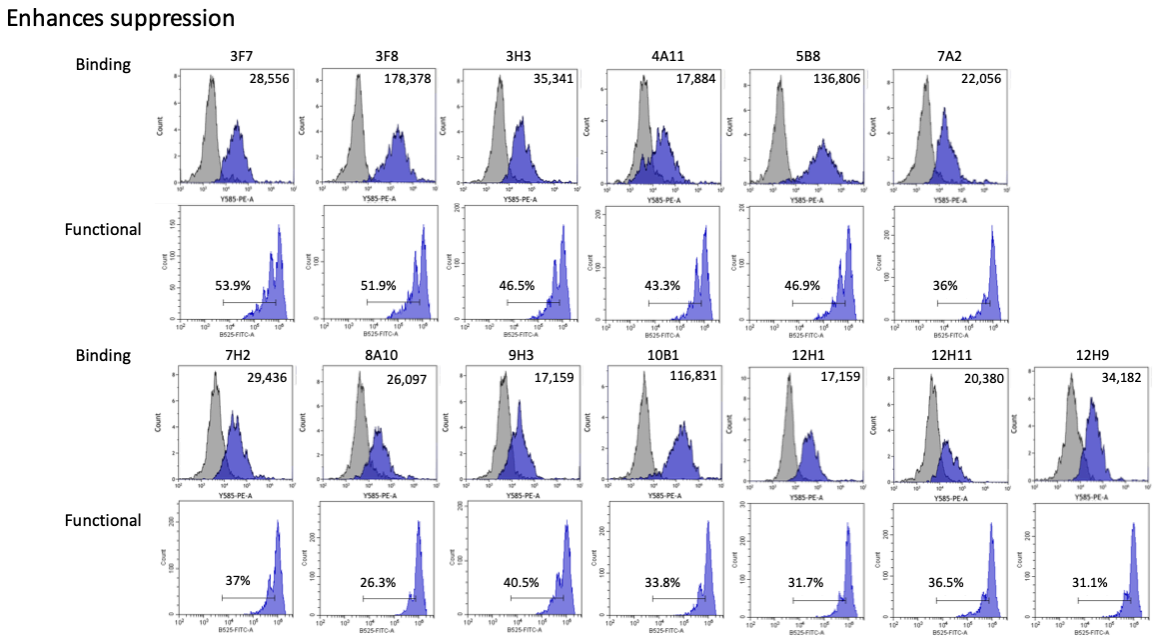

Figure 21. Binding and functional screening of anti-MoT hybridomas that bind to MoT cell surface. 105 supernatants were tested in an MoT suppression assay for functional activity. Parent wells that bound to MoT cells and reversed (blocked) or enhanced suppression are labeled as such. Binding of hybridoma supernatant staining MoT cells (blue histograms) and Jurkat cells (gray histograms) are shown. For each binding histogram, ΔMFI values are indicated on the graph. For each functional histogram, $CD4^+$ CFSE peaks are shown with % proliferation.

Anti-MoT mAbs bind to MoT cell surface by flow cytometry

Once a collection of candidate functional hybridomas was established, parent wells were subcloned by limiting dilution to isolate monoclonal antibodies. Functional hybridomas that demonstrated a reversal of suppression were chosen to further characterize based on their effect on responder cell proliferation in an MoT suppression assay (Figure 21). Subcloned mAbs were re-screened for binding to MoT cells and purified by Protein A chromatography (list of mAbs in Appendix D, Supplemental Table 1). Figure 22 shows the binding of three anti-MoT mAbs. Interestingly, mAbs 1A11 and 12E7 bind strongly to both MoT cells and PBMC-derived Tregs, while mAb 4G3 does not bind to Tregs. None of the mAbs bound to Jurkat cells.

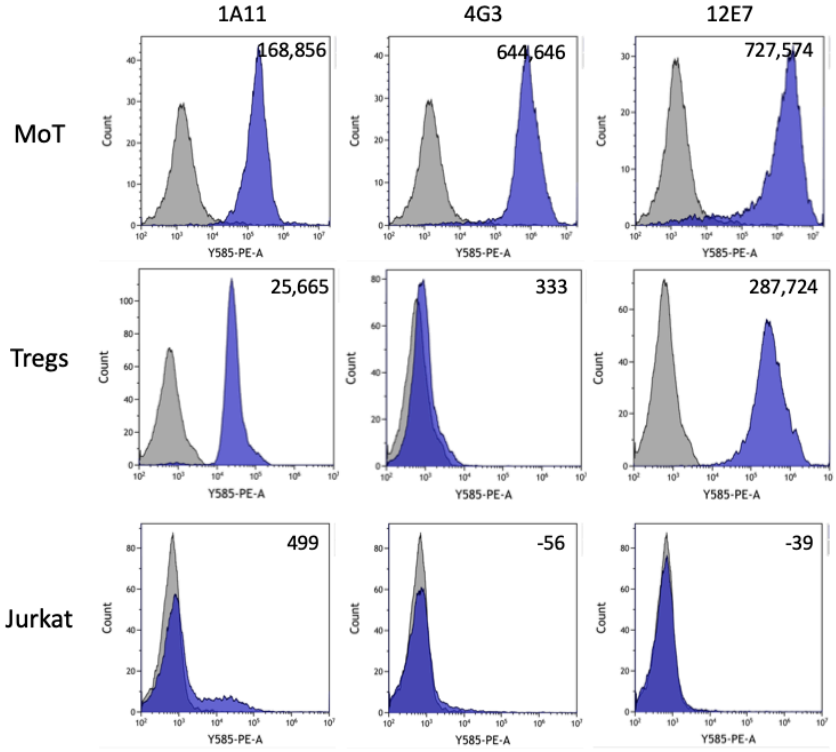

Figure 22. Anti-MoT mAbs bind to MoT cell surface by flow cytometry. MAb staining (blue histogram) and secondary alone (gray histogram) are shown. For each histogram, ΔMFI values are indicated on the graph. Designations of mAbs are shown above the columns of histograms.

Anti-MoT mAb 12E7 may block a suppressive cell surface protein

Since hybridoma parent wells were screened for the ability to reverse (or enhance) suppression, and parent wells are polyclonal, the mAbs were subcloned by limiting dilution and purified using protein A beads, then tested. Subcloned mAbs that bound to MoT cell surface were re-screened for functional activity in a suppression assay. When anti-MoT mAbs were added to the co-culture suppression assay, none affected proliferation of the responders, with the exception of mAb 12E7. Compared to the suppressive control (0 peaks, 14.1% proliferation), when mAb 12E7 was added, responder cell proliferation increased (2 peaks, 43.34% proliferation) (Figure 23). MAb 12E7 was then tested in the suppression assay at increasing doses and was found to affect suppression, even at low concentrations (Figure 24).

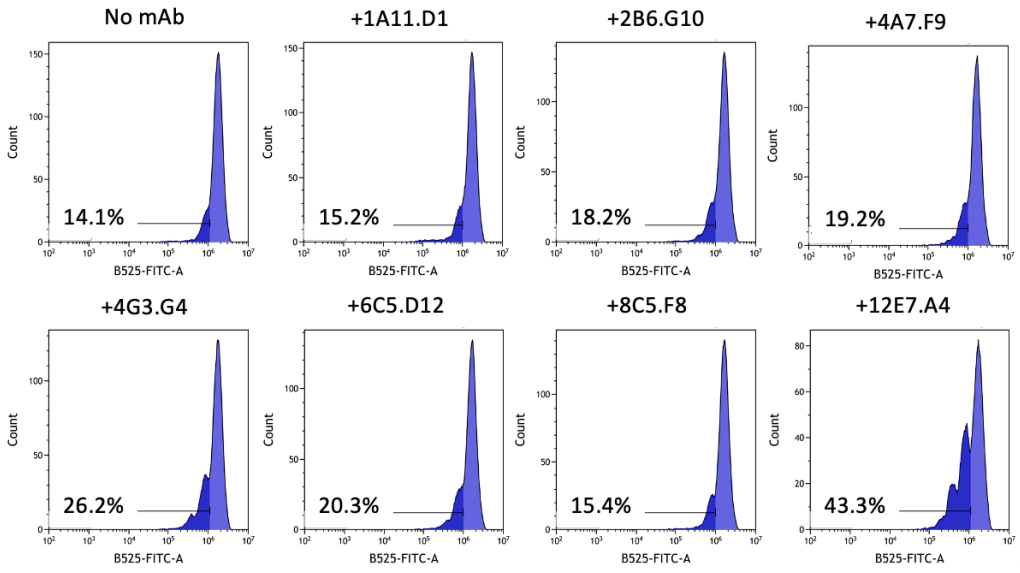

Figure 23. MAb 12E7 affects MoT-mediated suppression. MAbs were added at 20 µg/ml to $CD4^+$ PBMC:MoT co-culture wells for five days. Addition of mAb 12E7 shows 2 proliferative peaks, 43.34% proliferation, compared to no mAb control of 0 peaks, 14.1% proliferation.

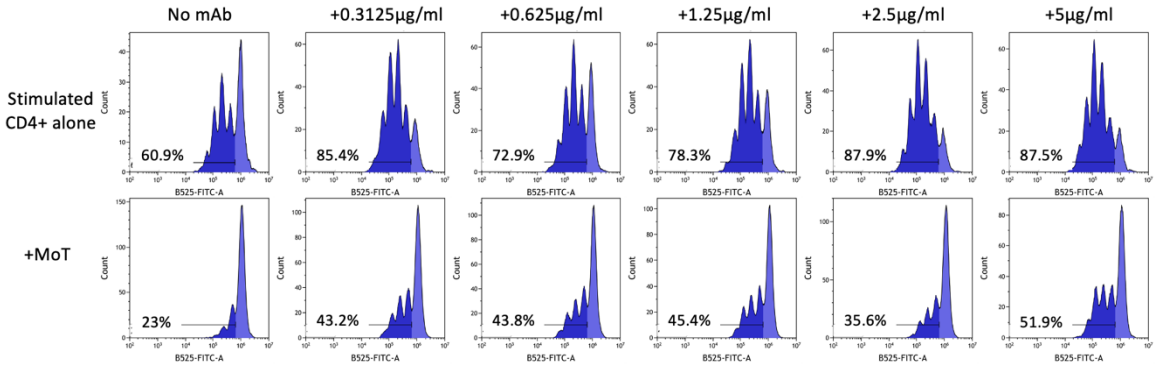

Figure 24. Addition of anti-MoT mAb 12E7 partially reverses MoT-mediated suppression of CD4$^+$ PBMC. MAb 12E7 was added to the suppression assay at increasing concentrations, indicated above each graph.

Anti-MoT mAb 12E7 binds to CD44 antigen

To begin to characterize the binding of mAb 12E7, western blot analysis was performed on Jurkat, MoT, $CD4^+$ responder and human PBMC-derived Treg whole cell lysates. It was found that anti-MoT mAb 12E7 binds to an ~80 kDa protein in MoT cells, $CD4^+$ responders, and PBMC-derived Tregs, that is not present in Jurkat (Figure 25).

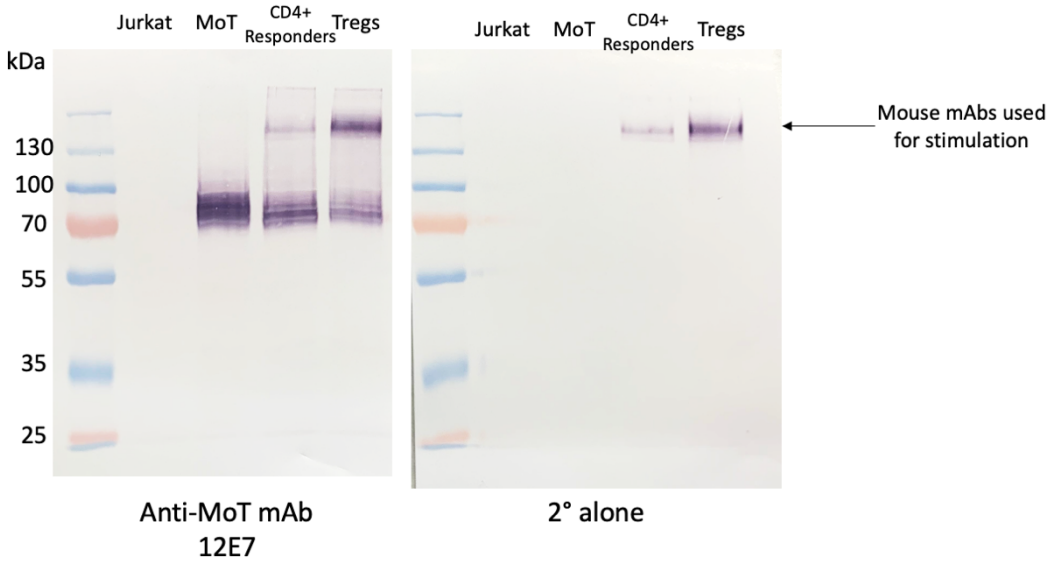

Figure 25. Anti-MoT mAb 12E7 binds to an 80 kDa protein present in MoT cells, $CD4^+$ responder cells and Tregs that is not present in Jurkat. Whole cell lysate was separated by 10% SDS-PAGE and transferred to PVDF membrane. Membrane was probed with mAb 12E7, followed by detection with AP-conjugated anti-mouse IgG secondary Ab. NBT/BCIP substrate was used to visualize bands.

To identify the antigen for mAb 12E7, an immunoprecipitation (IP) was performed using intact MoT cells. IP successfully isolated the 80 kDa target protein from whole cells (Figure 26A). However, it was not at a high enough concentration in the elution to visualize by Coomassie gel staining for downstream mass spectrometry analysis. Therefore, elutions 1-5 were combined and acetone precipitated to concentrate the protein (Figure 26B). The concentrated elutions were run on SDS-PAGE and stained with Coomassie safe stain. Although the band was still not easily visible, proteins within 70 – 100 kDa were excised and prepped for in-gel trypsin digestion followed by mass spectrometry analysis (Figure 26C).

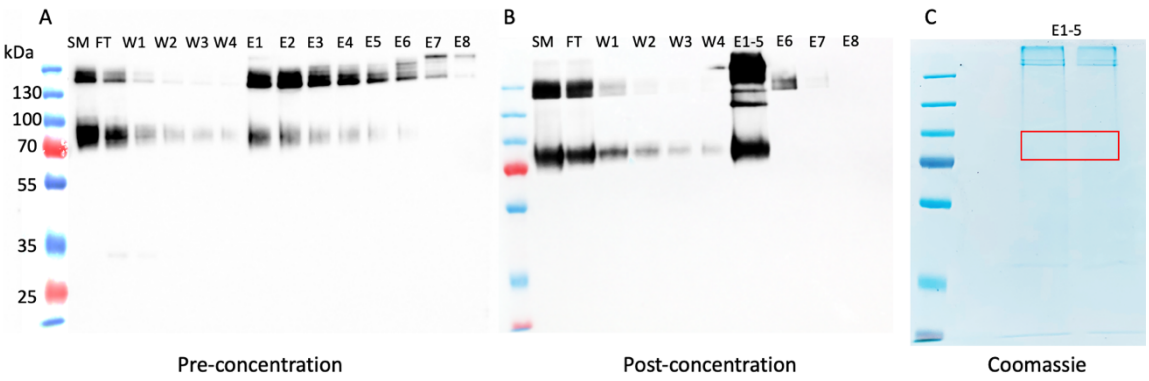

Figure 26. Immunoprecipitation of an 80 kDa protein from MoT cells using anti-MoT mAb 12E7. Western blot of IP elution profile is shown (A) pre- and (B) post-concentration of elutions by acetone precipitation. (C) Concentrated elutions were stained by Coomassie, 70 -100 kDa size proteins were excised, subjected to in-gel tryptic digest and submitted for mass spectrometry analysis. SM = starting material, FT = flow through, W = washes, E = elutions. Membranes were probed with mAb 12E7 followed by detection with HRP-conjugated anti-mouse IgG secondary Ab. Blots were developed with chemiluminescent substrate.

CD44 antigen was identified by IP and mass spectrometry analysis (Figure 27). Possible targets that are ~70-85 kDa in size and known to be on the cell surface or secreted were investigated, including heat shock proteins (HSPs) and CD44 antigen (highlighted in green).

Accession	Description	Coverage [%]	# Peptides	# PSMs	# Unique Pept	# AAs	MW [kDa]	calc. pI	Score Sequest	# Peptides (by
P11021	Endoplasmic reticulum chaperone BiP OS=Homo sapiens OX=9(	31	19	39	18	654	72.3	5.16	109.22	19
P11142	Heat shock cognate 71 kDa protein OS=Homo sapiens OX=9606	22	14	31	12	646	70.9	5.52	85.66	14
P38646	Stress-70 protein, mitochondrial OS=Homo sapiens OX=9606 G	22	14	20	14	679	73.6	6.16	55.97	14
P60709	Actin, cytoplasmic 1 OS=Homo sapiens OX=9606 GN=ACTB PE=:	24	9	16	9	375	41.7	5.48	40.04	9
P13667	Protein disulfide-isomerase A4 OS=Homo sapiens OX=9606 GN=	17	11	15	11	645	72.9	5.07	32.23	11
P29401	Transketolase OS=Homo sapiens OX=9606 GN=TKT PE=1 SV=3	24	11	15	11	623	67.8	7.66	38.56	11
P10809	60 kDa heat shock protein, mitochondrial OS=Homo sapiens OX	19	10	15	10	573	61	5.87	42.77	10
P08238	Heat shock protein HSP 90-beta OS=Homo sapiens OX=9606 GN	13	9	14	6	724	83.2	5.03	37.16	9
P04264	Keratin, type II cytoskeletal 1 OS=Homo sapiens OX=9606 GN=K	13	8	11	6	644	66	8.12	25.87	8
P68104	Elongation factor 1-alpha 1 OS=Homo sapiens OX=9606 GN=EEF	16	8	9	8	462	50.1	9.01	24.23	8
P16070	CD44 antigen OS=Homo sapiens OX=9606 GN=CD44 PE=1 SV=3	8	5	9	5	742	81.5	5.33	23.85	5
P13645	Keratin, type I cytoskeletal 10 OS=Homo sapiens OX=9606 GN=I	13	6	8	6	584	58.8	5.21	17.61	6
P07195	L-lactate dehydrogenase B chain OS=Homo sapiens OX=9606 GI	20	6	8	5	334	36.6	6.05	18.72	6
P0DMV9	Heat shock 70 kDa protein 1B OS=Homo sapiens OX=9606 GN=H	10	5	8	3	641	70	5.66	19.87	5
P60174	Triosephosphate isomerase OS=Homo sapiens OX=9606 GN=TPI	19	4	8	4	249	26.7	6.9	22.2	4
P13796	Plastin-2 OS=Homo sapiens OX=9606 GN=LCP1 PE=1 SV=6	11	6	7	6	627	70.2	5.43	17.41	6
P00338	L-lactate dehydrogenase A chain OS=Homo sapiens OX=9606 GI	13	4	7	3	332	36.7	8.27	18.39	4
Q06830	Peroxiredoxin-1 OS=Homo sapiens OX=9606 GN=PRDX1 PE=1 S	26	5	7	4	199	22.1	8.13	16.45	5
P26038	Moesin OS=Homo sapiens OX=9606 GN=MSN PE=1 SV=3	8	5	6	4	577	67.8	6.4	12.74	5
P15311	Ezrin OS=Homo sapiens OX=9606 GN=EZR PE=1 SV=4	8	5	6	4	586	69.4	6.27	12.47	5
P67936	Tropomyosin alpha-4 chain OS=Homo sapiens OX=9606 GN=TP	16	4	6	1	248	28.5	4.69	13.5	4
P06753	Tropomyosin alpha-3 chain OS=Homo sapiens OX=9606 GN=TP	15	4	6	1	285	32.9	4.72	13.54	4
P07900	Heat shock protein HSP 90-alpha OS=Homo sapiens OX=9606 G	8	5	5	2	732	84.6	5.02	13.87	5

Figure 27. Mass spectrometry hits of anti-MoT mAb 12E7 antigen immunoprecipitated from cell lysate. Proteins ~70-85 kDa in size (highlighted in red) and are known to be expressed on the cell surface and/or secreted (highlighted in green) were investigated.

Western blot analysis of whole cell lysates found that mAb 12E7 and anti-CD44 commercial pAb have a similar binding profile, supporting that mAb 12E7 recognizes CD44 (Figure 28). MAb 12E7 bound to the extracellular portion of rCD44 (Met 1-Pro 220) by non-reducing Western blot, but not a western blot from a reducing SDS-PAGE, further characterizing that the binding region falls within the first 220 amino acids of CD44 (Figure 29). Binding of CD44 under non-reducing conditions suggests recognition of a conformational epitope as disulfide bonds are still intact. Control antigen (rGal-9) was used as a negative control. Gal-9 was chosen as a recombinant protein control because it is an immunosuppressive extracellular protein, contains a his-tag and was

produced in HEK293 cells. To further support that mAb 12E7 binds to rCD44, an indirect ELISA was performed (Appendix D, Supplemental Figure 2). Serial diluted mAb 12E7 bound to plate-bound rCD44 and binding was comparable to a commercial anti-CD44 mAb. Another anti-MoT mAb, clone 1A11, was used as a negative control and does not bind to rCD44 by ELISA or western blot.

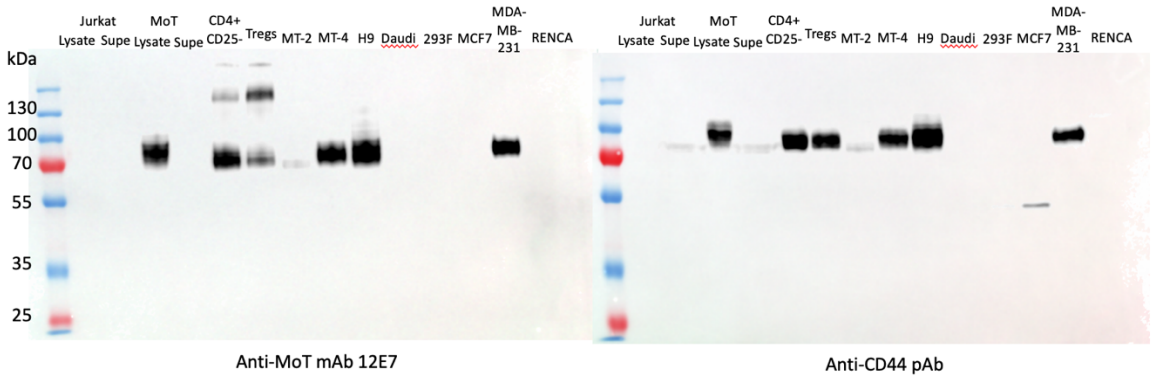

Figure 28. Binding profile of mAb 12E7 to whole cell lysates. Jurkat, MoT, MT-2, MT-4 (human T cell leukemias), $CD4^{+}CD25^{-}$ and Tregs (isolated from human PBMCs), H9 (human T cell lymphoma), Daudi (human B cell lymphoma), 293F (human embryonic kidney cells), MCF7 and MDA-MB-231 (human breast adenocarcinomas), Renca (murine kidney adenocarcinoma). CD44 antigen is expressed in tumor and T cell lysates. Whole cell lysates were separated by SDS-PAGE (10%) and transferred to PVDF membrane. Membranes were probed with anti-MoT mAb 12E7 or anti-CD44 pAb, followed by detection with HRP-conjugated anti-mouse or rabbit IgG secondary antibody. Blots were developed with chemiluminescent substrate.

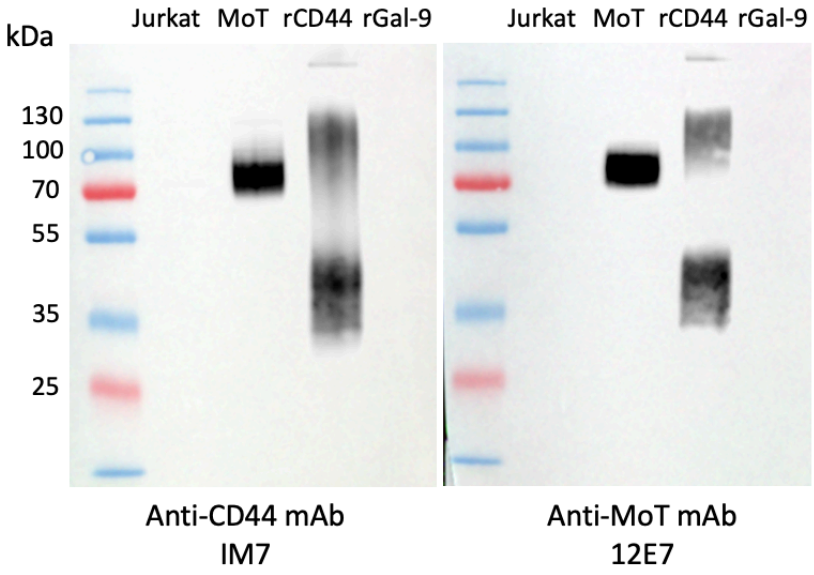

Figure 29. Anti-MoT mAb 12E7 binds to the extracellular domain of CD44 antigen. Whole cell lysates and rCD44 were separated by SDS-PAGE (10%) under non-reducing conditions and transferred to PVDF membrane. Membranes were probed with anti-CD44 mAb (clone IM7; biotin) or anti-MoT mAb 12E7, followed by detection with HRP-conjugated streptavidin or anti-mouse IgG secondary antibody. Blots were developed with chemiluminescent substrate.

To determine if glycosylation plays a role in mAb 12E7 binding, MoT cell lysate was de-glycosylated with enzymes PNGase F and O-glycosidase to cleave *N*- and *O*-glycans, respectively. De-glycosylated lysate was probed with mAb 12E7 to evaluate binding. The removal of *N*-linked glycans resulted in complete loss of mAb 12E7 binding (Figure 30). This suggests that *N*-glycans may be involved in mAb 12E7 binding epitope. Anti-PD-L1 was used as a control for de-glycosylation of a cell surface glycoprotein. Glycosylated PD-L1 shows a range of bands (45-65 kDa) while non-glycosylated PD-L1 is detected at 33 kDa.

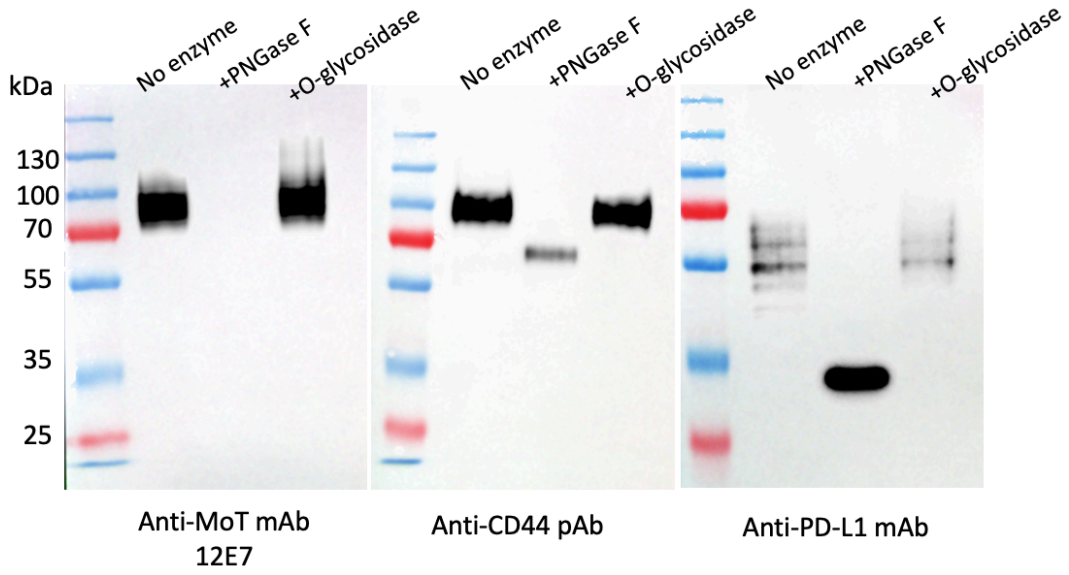

Figure 30. MAb 12E7 loses binding when MoT lysate is de-glycosylated with PNGase F enzyme. MoT cell lysate was incubated with PNGase F and O-glycosidase overnight at 37°C. De-glycosylated lysates were separated by SDS-PAGE (10%) and transferred to PVDF membrane. Membranes were probed with anti-MoT mAb 12E7, anti-CD44 pAb, or anti-PD-L1 mAb (clone E1L3N), followed by detection with HRP-conjugated anti-mouse or rabbit IgG secondary antibody. Blots were developed with chemiluminescent substrate.

Glycosylation may play a role in MoT suppressive activity

To investigate the functional role of glycosylation in MoT-mediated suppression, live cells were treated with PNGase F and subsequently used in the suppression assay. Irradiated MoT cells (iMoT) were used to reduce the production of newly glycosylated proteins generated from cell division. Incubation of PNGase F with live MoT cells resulted in de-glycosylation of *N*-linked cell surface glycoproteins. These cells were then tested in a suppression assay and resulted in reduced suppressive activity (3 peaks, 42.3% responder cell proliferation) compared to the control (1.5 peaks, 23% proliferation) shown in Figure 31. This data suggests glycosylation may be partially involved in the function of protein(s) involved in MoT suppression of $CD4^+$ PBMC.

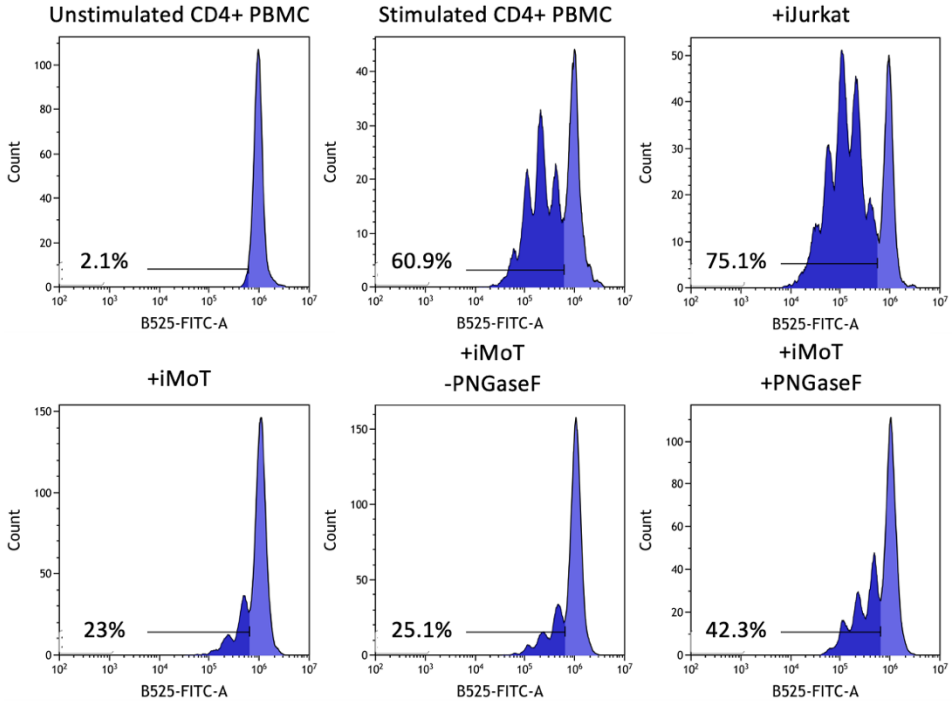

Figure 31. *N*-deglycosylated MoT cells lose suppressive potency. MoT cells were irradiated, treated with PNGase F for 2 h at 37° C, then tested in a suppression assay. PNGase F-treated iMoT cells had reduced suppressive activity compared to non-treated cells.

Discussion

Mammalian cell surfaces contain numerous membrane-bound and secreted proteins involved in a diverse range of cellular processes. Since we demonstrated that MoT cells suppress activated $CD4^+$ T cells by direct cell:cell contact, we wanted to identify and characterize cell surface proteins involved in MoT/Treg suppression. To address this we generated monoclonal antibodies to MoT cell surfaces by direct immunization of mice with intact human MoT cells. After three immunizations, mice produced high titer anti-MoT antibodies that bound to MoT cell surface by flow cytometry analysis (Figure 20). Anti-MoT antibodies were screened for binding by surface staining and functional activity in a suppression assay.

Overall, of the 105 hybridoma parent wells that bound to MoT cells, 32 had a functional effect on MoT-mediated suppression: 19 reversed and 13 enhanced suppression (Figure 21). Of these candidate hybridomas, mAb 12E7 stood out as a potential blocking mAb. It bound strongly to MoT cell and Treg cell surface, and not to Jurkat cells (Figure 22). Addition of mAb 12E7 to a suppression assay had a functional effect on MoT-mediated suppression, resulting in increased proliferation of $CD4^+$ responder cells (Figure 24). There is a possibility, however, that mAb 12E7 drives responder cell proliferation and does not actually reverse suppression by MoT cells. Since mAb 12E7 binds to Tregs and $CD4^+$ responder cells (Figure 25), it could be directly binding to and stimulating responder cell division, independently or in addition to blocking MoT cells.

IP and mass spectrometry analysis revealed that mAb 12E7 recognizes CD44 antigen, an 81 kDa transmembrane protein. CD44 is a complex cell surface adhesion

receptor that is expressed in range of human cell types, including T cells and in cancer[190]. CD44 is the receptor for hyaluronan (hyaluronic acid; HA) but also interacts with extracellular matrix (ECM) proteins[190,191]. In T cells, binding of HA to CD44 regulates diverse immune functions including T cell differentiation, activation, proliferation, adhesion and migration[190,192,193]. CD44 is required for T cell extravasation into inflamed tissues[194,195]. Activated T cells increase HA binding which allows for CD44-mediated rolling or primary adhesion[194]. Aberrant CD44 expression has been correlated with multiple malignancies and contributes to tumor formation, invasion and metastasis[190,196]. Variants of CD44 are produced by alternative splicing, resulting in distinct protein isoforms[196,197]. Expression of CD44 variant isoforms in cancer is an indicator for prognosis and clinical outcome, making it a potential anti-tumor therapeutic target[190,193,197].

Anti-MoT mAb 12E7 binds to CD44 by western blot and was found to be expressed in a variety of cell types including PBMC-derived Tregs and tumor cells (Figure 28). Thus, mAb 12E7 most likely binds to a conserved region of CD44 that is not variant or cell type-specific. MAb 12E7 binds to rCD44 (N-terminal fragment AA 1-220), indicating that its epitope is within the extracellular domain of CD44 and within the first 220 amino acids (Figure 29). MAb 12E7 binds to non-reduced CD44, indicating it recognizes a confirmational epitope due to protein disulfide interactions maintained under non-reducing conditions. When MoT lysate is de-glycosylated with PNGase F, mAb 12E7 completely loses its ability to bind to CD44, suggesting that *N*-glycans may be involved in the binding epitope of mAb 12E7 (Figure 30). Since mammalian extracellular

proteins are typically heavily glycosylated, mAbs generated to the cell surface may recognize epitopes that span protein-glycosylation junctions.

Antibodies to CD44 can modulate its function. Anti-CD44 antibodies have been previously generated that inhibit or activate T cell processes, including activation and migration[198]. Some antibodies activate CD44 by enhancing ligand binding or acting as the ligand to regulate activation[198,199]. It has been predicted that binding of these activating antibodies lead to a favorable conformation that enhances ligand recognition due to receptor cross-linking[198]. In contrast, antibodies that block CD44 function inhibit ligand binding by making the site inaccessible for HA[198]. Both blocking and enhancing anti-CD44 antibodies can modulate T cell activation and function.

CD44-targeted mAbs are being tested in preclinical and clinical studies for cytotoxic effects[190]. A study by Wessels et al. found a CD44 antibody repressed coalescence of melanoma and breast-derived tumorigenic cell lines in a 3D Matrigel model[200]. *In vitro*, coalescence between aggregates is mediated by forming cell bridges, which mirrors characteristics of tumorigenesis *in vivo*[200]. CD44 antibodies have also shown to suppress proliferation of tumor cells and induce cytotoxic effects[201,202]. CD44 is also being investigated as a tumor biomarker for drug targeting to $CD44^+$ tumors. Selective delivery of anti-tumor drugs to $CD44^+$ cells through utilizing its ligand, HA, is being tested in preclinical studies[203,204]. Modulating CD44 function and exploring CD44 as a biomarker poses a potential target for anti-tumor therapy.

To explore the role of protein glycosylation in MoT suppressive function, live MoT cells were treated with PNGase F to cleave *N*-glycans from cell surface proteins. After incubation with PNGase F, de-glycosylated MoT cells were subsequently evaluated

for suppressive activity. It was found that de-glycosylated MoT cells exhibited a reduced ability to suppress $CD4^+$ PBMC proliferation compared to cells not treated with PNGase F (Figure 31). This is supported by Cabral et. al, where they observed PNGase F-treated Tregs had reduced suppressive potency in an *in vitro* suppression assay[186]. Although a loss of suppressive potency was observed, de-glycosylation did not result in a complete reversal of suppression. This could be due to incomplete de-glycosylation as there are thousands of cell surface proteins, as well as the possible involvement of *O*-linked glycans. This data suggests that glycosylation may play a role in the function of the suppressive protein(s) that mediate MoT cell suppression.

Further studies are required to elucidate the exact function and binding epitope of mAb 12E7 and its downstream effects on MoT cell signaling. It is unclear if mAb 12E7 is inhibiting suppressive activity, directly stimulating responder cells, or physically blocking the interaction between MoT cells and $CD4^+$ PBMC. In addition to *N*-glycosylations, the involvement of *O*-glycans in MoT/Treg suppressive activity may also be evaluated. The method of whole cell immunization poses some limitations. Highly expressed, immunodominant proteins that may or may not be involved in suppression could decrease the opportunity to produce antibodies to low abundant, functional cell surface molecules[180]. Immunizing and screening against a Treg-like cell line presents the possibility of generating antibodies that bind to MoT-specific proteins that are not present in Tregs. Thus, functional antibodies are being tested for binding to Tregs and in Treg suppression assays. Furthermore, targeting one protein/mechanism may not be sufficient to completely abrogate suppression as there could be multiple inhibitory pathways that are not mutually exclusive. Additional Treg and MoT cell-targeting mAbs with

potentially greater blocking potency are being evaluated. It is possible that multiple blocking antibodies must be used in conjunction to elicit a complete blocking effect. The discovery of an antibody or antibodies that functionally block Treg-mediated suppression is immensely valuable in studying Treg function and can be explored for use in combination with existing immunotherapies to boost therapeutic outcomes.

Supplemental Data

Supplemental data for Chapter 4 in Appendix D.

CHAPTER 5

CONSTRUCTION AND CHARACTERIZATION OF ANTI-PD-L1 CHIMERIC ANTIGEN RECEPTOR T CELLS THAT SELECTIVELY KILL PD-L1-POSITIVE TUMOR CELLS

Abstract

PD-L1 has emerged as an effective, therapeutic target for anti-tumor immunotherapies. Monoclonal antibodies that bind and inhibit the PD-1/PD-L1 pathway increase the activity of cytotoxic anti-tumor T cells. CAR T cells, an adoptive T cell therapy, utilize genetically engineered T cells designed to express scFvs on the cell surface, re-directing T cells toward a specific tumor-associated antigen. The binding domains (scFv) were constructed from an anti-PD-L1 mAb and were shown to bind both human and murine PD-L1$^+$ tumor cells. A lentivirus encoding the scFv was constructed and used to transduce naive T cells to redirect their specificity to target PD-L1. Anti-PD-L1 CAR T cells were generated by expression of the scFv on the cell surface that is genetically fused to T cell signaling and co-stimulatory domains. The inclusion of these domains in the CAR design allows for activation, proliferation and survival of the engineered CAR T cells. Anti-PD-L1 CAR T cells demonstrated the ability to effectively kill PD-L1$^+$ human and mouse kidney cancer and lung cancer cells, while sparing non-malignant cells.

Introduction

Programmed cell death ligand-1 (PD-L1) has been found to be overexpressed in many cancer cell types. When PD-L1 binds to PD-1 on T cells, PD-1 acts as an off-switch to prevent activation[77]. Functionally, PD-L1 suppresses T cells by inducing an inhibitory cascade resulting in T cell apoptosis, exhaustion, and/or anergy[205]. Since tumors express PD-L1, this allows for tumor escape of anti-tumor cytotoxic T cell killing[74,206]. Tumor cells exploit this immune checkpoint by upregulating PD-L1, creating an obstacle to eliciting an effective anti-tumor response[207]. Abnormal PD-L1 expression has been reported in numerous cancer types including melanoma, lung, breast, and renal cell carcinomas[61]. Thus, inhibition of the PD-1/PD-L1 pathway using monoclonal antibodies (mAbs) has proven to be an effective cancer therapeutic strategy, with some mAbs being approved as first-line therapies[77]. There are currently three FDA-approved mAbs that target PD-L1. One anti-PD-L1 mAb, Atezolizumab, has been tested for the treatment of urothelial carcinoma, non-small cell lung cancer, triple-negative breast cancer, metastatic renal cell carcinoma and colorectal cancer, receiving its first FDA-approval for the treatment of urothelial cancer in 2016[207].

Novel targeted immunotherapies have emerged as critical and effective anti-tumor treatments. In addition to mAbs, adoptive T cell therapies have made promising strides and are increasingly being utilized in patient treatment. Chimeric antigen receptor T cells offer a fast, innovative method of generating tumor-specific cytotoxic T cells that selectively locate and kill tumor cells that express a target antigen[208,209]. A chimeric antigen receptor (CAR) is an engineered antibody (receptor) genetically fused to intracellular signaling and activation molecules. CARs are designed to be expressed on

the T cell surface, re-directing T cells to provide both antigen specificity and T cell receptor signaling capability[209], independent of restriction by major histocompatibility complex (MHC) [210,211].

A CAR consists of an extracellular single chain variable fragment (scFv) linked to intracellular signaling domains. The scFv is composed of the variable heavy and light chain regions derived from an antigen-specific monoclonal antibody (mAb) and are connected by a flexible linker. ScFvs maintain the specificity and affinity of the original mAb, and the smaller size enables efficient CAR design and expression on the T cell surface[212]. A scFv binds to native conformational epitopes of a cell surface target antigen, enhancing CAR T cell recognition and redirecting CAR T cells toward the antigen expressed on tumor cells[213]. In CAR design, the scFv is fused to a hinge and transmembrane domain that fixes CAR expression on the cell surface. CAR surface expression is vital for the efficacy of CAR T cell therapy[213]. The transmembrane domain links the scFv to co-stimulatory and intracellular signaling molecules responsible for full T cell activation[214]. The CD3ζ chain is an essential signaling molecule for T cell activation. Co-stimulatory molecules derived from T cell signaling domains include CD28 and 4-1BB; incorporation of these domains in the CAR design is crucial for full T cell activation, prolonged proliferation, lasting survival and antitumor activity[212].

The different CAR generations denote the changes in the composition of the intracellular signaling domains (Figure 32). First generation CARs include CD3ζ as the sole component of the intracellular signaling domain, but activation fails to induce adequate cytokine production, resulting in reduced proliferation and survival[212,213]. Therefore, CAR T cells require co-stimulation of the CD3ζ for full T cell activation.

Second generation CARs contain one co-stimulatory domain (CD28 or 4-1BB) while third generation CARs contain both domains. Incorporation of CD28 provides proper co-stimulation while 4-1BB increases survival of the CAR T cell[214]. An inducible caspase 9 (iCasp9) cellular "safety switch" can also be incorporated. Concerns regarding adverse effects led to the development of suicide genes that enable specific elimination of the engineered T cells[215,216]. The iCasp9 is fused to a modified FK506 binding protein (FKBP12 with F36V mutation) that dimerizes the FK506bp-Caspase 9 fusion protein in the presence of AP1903 (a chemical inducer of dimerization), causing apoptosis of the cell[215,217]. This feature allows for >90% of the CAR T cells to be eliminated after administration of a single dose of AP1903 dimerizing agent[218]. Current trials testing second and third generation CARs have shown durable responses in treating hematologic malignancies[213]. However, efficacy of CAR T cells in solid tumors continues to pose a significant challenge[219].

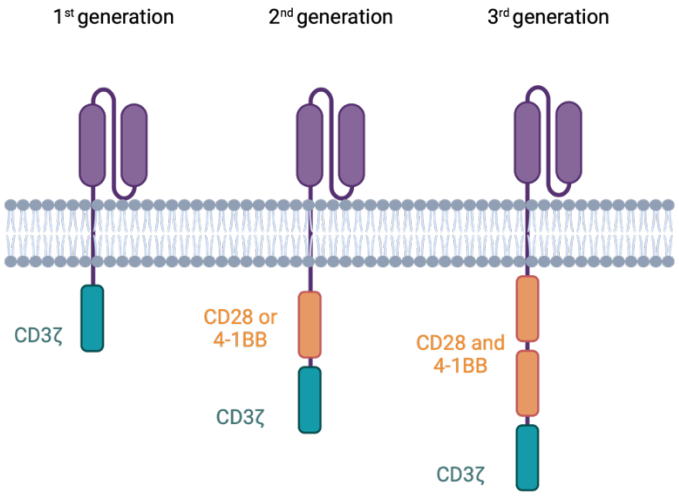

Figure 32. Generations of CAR T cells. First generation CAR T cells express an extracellular antigen binding scFv and contain intracellular CD3ζ for T cell activation via signal transduction. Second generation CAR T cells contain an additional co-stimulatory domain (CD28 or 4-1BB). Third generation CAR T cells contain two additional co-stimulatory domains (CD28 and 4-1BB). (Created using Biorender.com)

The introduction of engineered CARs into T cells for surface expression can be accomplished through different methods. One method is non-viral based DNA transfection, which is cost-effective and has a lower risk for mutagenesis[213]. Since this method has reduced gene transfer efficiency, it requires long-term culture which can be harmful to the cells[213]. The more widely employed method of inducing CAR expression uses retroviruses for the transduction of T cells. Advantages of this method include the efficiency of permanent transduction of T cells that is safe and easier to produce than the previous process[213]. Lentiviral vectors provide another viral-based method of DNA transfection, which can permanently transduce dividing and non-dividing T cells and is potentially safer than retroviral transduction[213]. Both viral methods integrate the DNA sequence into the host genome and induce maintained CAR surface expression, which has been shown to extend CAR T cell survival[213,220].

CAR T cells overcome the impediments of immunotherapies and other adoptive T cell therapies. Anti-PD-L1 mAb immunotherapies are limited in part by 1) off-tumor immune modulation leading to adverse inflammatory effects, 2) attenuation of efficacy in "cold" tumors or tumors lacking infiltrating lymphocytes, and 3) post-translational modifications of PD-L1 that impair mAb binding[221–223]. Restrictions of classical non-CAR T ACTs include the necessity of MHC antigen presentation, tolerance to self-antigens, and the difficulty of culturing and expanding tumor-infiltrating lymphocytes (TILs)[213]. Normal T cell receptors (TCRs) are restricted by the necessity of MHC-dependent antigen presentation, which limits specificity and regulates T cell activation[213]. Perhaps the major feature of CAR T cells is that they do not require antigen processing;

these cells are engineered to engage a target antigen in its native confirmation via antibody-mediated detection, thereby inducing MHC-independent cytotoxic activity.

Although showing therapeutic success, CAR T cell therapies have associated adverse effects including on-target, off-tumor effects, cytokine release syndrome, anaphylaxis, neurologic toxicity and insertional mutagenesis[215,220]. These adverse effects in CAR T cell clinical trials can be life-threatening and sometimes fatal[216]. On-target but off-tumor toxicities in solid tumors has posed a major obstacle. The use of CAR T cells to treat solid tumors are hindered by the requirement for protein targets that are expressed on malignant cells but have limited expression on normal tissue[224]. Another challenge in treating solid tumors is that CAR T cells may not penetrate tissues, either due to the tumor being avascular or lack of homing receptors[220]. Intratumoral injection or local delivery may help overcome this limitation[220].

Overall, CAR T cells stimulate enhanced tumor recognition, overcome self-tolerance and can escape mechanisms exploited by cancer cells. This results in the continued expansion and sustained survival of circulating engineered T cells capable of providing continued antitumor activity. Herein, third generation anti-PD-L1 CAR T cells were developed and tested for the ability to kill PD-L1^{+} human and mouse tumor cells. Targeting PD-L1 using CAR T cells can address clinical gaps in immune checkpoint mAbs and extend the application of anti-PD-L1 immunotherapy

Materials and Methods

Construction of anti-PD-L1 scFv CAR

Cloning of the PD-L1 specific single chain variable fragment antibody into a 3rd generation CAR vector was completed using the published DNA sequence of the clinical anti-PD-L1 mAb atezolizumab. The construct contained a short, flexible linker (RGSTSGSGKSSEGKGGS), connecting the variable light chain region (V_L) to the variable heavy chain region (V_H). Generation of the scFv was performed by PCR overlap extension of the fragments using the linker as overlapping complementary ends. The scFv was subcloned into the CAR vector using XbaI and XhoI restriction enzymes. A FLAG-tag (DYKDDDDK) was incorporated for detection of CAR expression on the cell surface. The scFv was inserted between an iCasp9 safety switch and signaling domains. The 3rd generation CAR vector contained a CD8 α-chain hinge region, co-stimulatory domains CD28 and 4-1BB, and CD3 ζ-chain for T cell activation.

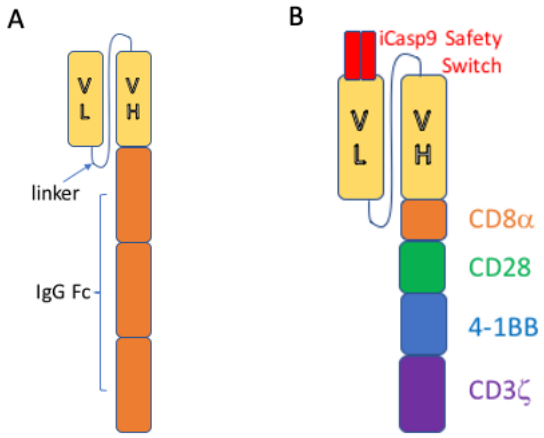

Figure 33. Anti-PD-L1 scFv and CAR T cell constructs. (A) Atezo scFv-Fc construct generated from published atezolizumab sequence. VL and VH fragments were connected by a polypeptide flexible linker and fused to an IgG Fc domain. (B) Atezo scFv CAR T cell construct containing anti-PD-L1 scFv, iCasp9 safety switch and T cell signaling domains.

Cell lines

RCJ-41T2 is a Mayo Clinic patient-derived sarcomatoid renal cell carcinoma (RCC) cell line. Clinically, RCJ-41T2 tumor was resistant to both anti-angiogenic and immune checkpoint therapies. A549 human lung carcinoma (CLL-185), 786-O human renal cell adenocarcinoma (CRL-1932), Jurkat human T cell leukemia (TIB-152), Renca murine renal adenocarcinoma (CRL-2947), and BALB/3T3 murine fibroblast cells (CCL-163) were purchased from ATCC. All cell lines were maintained in DMEM media supplemented with 10% fetal bovine serum (FBS), 1% Glutamax, 1% penicillin/streptomycin. Lenti-X 293T cells (human embryonic kidney (HEK) 293T subclone) were cultured in complete DMEM media and were purchased from Takara Bio. Cells were cultured at 37°C, 5% CO_2.

Isolation, activation and cultivation of T cells

Human T cells were isolated from PBMC (HLA A1/A2$^+$) using EasySep Human T Cell Isolation Kit (17951; Stemcell Technologies). T cells were cultured in RPMI complete medium (10% FBS, 1% penicillin/streptomycin) supplemented with 10 ng/ml recombinant human IL-7 (200-07; PeproTech) and 5 ng/ml recombinant human IL-15 (200-15; PeproTech) at 37°C, 5% CO_2. CD3/CD28 activation was performed using 5 µg/ml plate bound anti-human CD3 mAb (clone OKT3; Invitrogen) and 5 µg/ml final concentration of soluble anti-human CD28 mAb (clone CD28.2; Invitrogen). Cell densities were maintained at 1-2x10^6 cells/ml in 24-well plates. Cells were supplemented with rIL-7/rIL-15 at the concentrations listed for continued expansion of T cells.

Lentivirus production and transduction of T cells

Lentiviral particles were produced from Lenti-X 293T cells using lipid-mediated transient transfection of virion and CAR-encoding plasmids. 293T cells were cultured in DMEM medium without antibiotics and plated at $5x10^4$ cells per well in a collagen-coated 6-well plate, 24 hours pre-transfection. Cells were incubated at 37°C, 5% CO_2 overnight. FuGENE HD Transfection reagent (E2311; Promega) was co-incubated with the following plasmids: anti-PD-L1 CAR-encoding DNA plasmid (transfer vector), pCMV-VSV-G, pRSV-REV, pCgpV at 2:1:1:1 lipid:DNA ratio then added to the cells. The three plasmid VSV-G pseudotyped lentiviral packing system was purchased from Cell Biolabs (ViraSafe Lentiviral Packaging System, Pantropic; VPK-206). It was determined that 48 hours post-transfection yielded the highest viral titer by transduction of 293T cells. Lentiviral supernatant was harvested at 48 hours post-transduction, filtered with 0.45 μm filter, aliquoted and stored at -80°C.

24 hours post CD3/CD28 activation, $CD3^+$ T cells were transduced with lentivirus encoding the anti-PD-L1 CAR. 1 ml lentiviral supernatant (thawed on ice) and 4 μg/ml polybrene were added to cells and incubated for 48 hours at 37°C, 5% CO_2. Successfully transduced cells were determined by CAR expression detected by surface staining for FLAG-tag expression.

Flow cytometry

To assess mAb and scFv-Fc binding to cell surface PD-L1, $2x10^5$ cells were washed twice in PBS the blocked in 5% FBS/PBS for 1 h at room temperature. The cells were then incubated with atezolizumab or Atezo scFv-Fc at 10 μg/ml for 1 h at room

temperature. Antibody binding was detected with Dylight 488-conjugated anti-human IgG secondary antibody (SA5-10110; Thermo Fisher). To detect anti-PD-L1 CAR surface expression, transduced T cells were stained with Alexa Fluor 700-conjugated CD3 monoclonal antibody (clone UCHT1; eBioscience) and Alexa Fluor 488-conjugated anti-DYKDDDDK (FLAG) epitope tag mAb (clone 1042E; R&D Systems). For cytotoxicity assays, target cells were labeled with CFSE (10009853; Cayman Chemical) and cell death was assessed by propidium iodide (00-6990-50; eBioscience) staining. Samples were analyzed using BD FACSCelesta Flow Cytometer and BD FACSDiva software.

Cytotoxicity assay

Cell-mediated cytotoxicity of anti-PD-L1 CAR T cells was analyzed in a previously described CFSE/PI staining flow cytometry assay[225]. Effector CAR T cells were co-cultured with CFSE-labeled target tumor cells at indicated E:T ratios for four hours. Target cells alone were plated to measure intrinsic cell death and target cells co-incubated with non-transduced PBMCs were used to measure allogeneic cell killing. Propidium iodide (PI) was added prior to flow cytometry analysis. CFSE-labeling was used to distinguish target ($CFSE^+$) from effector ($CFSE^-$) cells. PI uptake measured dead or dying $CFSE^+$ target cells. $CFSE^+/PI^+$ indicated dead or dying target cells via CAR T cell mediated cytotoxicity.

Results

Atezolizumab and Atezo scFv-Fc bind to cell surface human and murine PD-L1$^+$ cells

To potentially boost the efficacy of immune checkpoint blockade in "cold" tumors, we constructed scFvs from the published sequence of atezolizumab, expressed and purified the Atezo scFv-Fc protein, and then compared the binding characteristics with the FDA-approved IgG antibody. The scFvs were fused to a human IgG Fc region for purification by Protein A chromatography and detection by cell surface staining. As demonstrated in Figure 34, Atezo mAb and Atezo scFv-Fc bind to PD-L1$^+$ cells by flow, including A549 (treated with IFN-γ), RCJ-41T2, 786-O, Renca and Jurkat cells. Flow cytometry was performed using A549 cells stimulated with IFN-γ for 48 hours to induce PD-L1 expression. Binding of Atezo scFv-Fc is indistinguishable from the intact clinical grade IgG, suggesting that Atezo scFv will recognize PD-L1 on tumor cells.

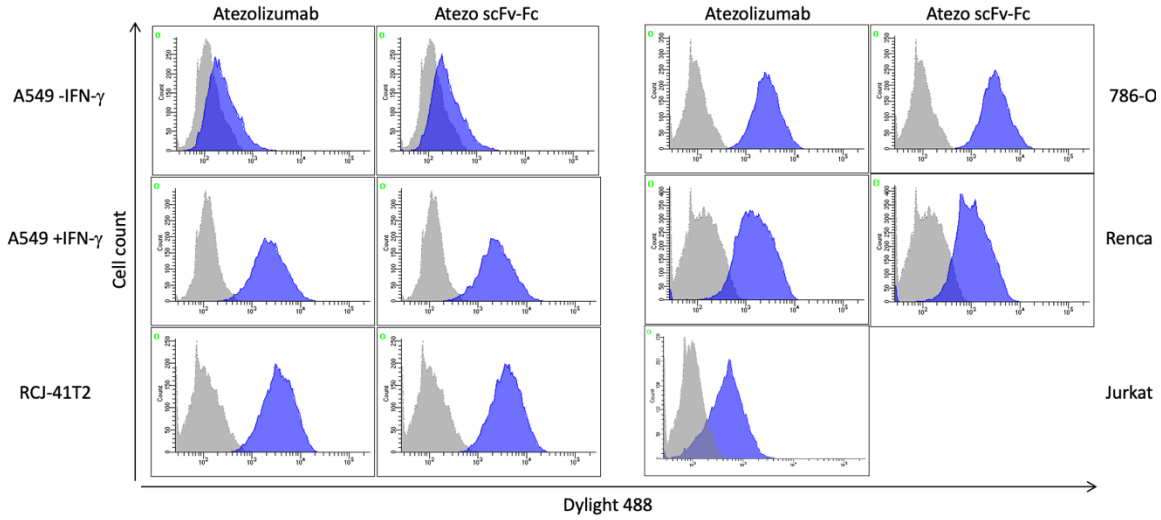

Figure 34. Atezolizumab and Atezo scFv-Fc bind to cell surface PD-L1 on tumor cells. MAb and scFv-Fc binding to RCJ-41T2, 786-O (human renal cell carcinomas), Jurkat (human T cell leukemia), A549 (human lung carcinoma) treated with IFN-γ and not to A549 (- IFN-γ), and Renca cells (mouse renal cell carcinoma). Positive binding is indicated by blue peak shift to the right. Blue peaks are atezolizumab or Atezo scFv-Fc staining. Gray peaks are anti-human IgG secondary antibody alone.

Atezo scFv-Fc dimerizes to form a bivalent antibody

Since Atezo scFv-Fc contains Fc domains with cysteine residues, we speculated that it dimerized, forming a bivalent antibody. To test this, reducing (Figure 35A) and non-reducing (Figure 35B) SDS-PAGE was performed, comparing Atezo mAb and Atezo scFv-Fc. As shown in Figure 35A, Atezo mAb IgG bands were observed at 50 and 25 kDa, indicative of heavy and light chains, while the scFv-Fc ran at the predicted molecular weight, 66 kDa. When both molecules were run under non-reduced conditions, Atezo mAb was observed at the expected ~150 kDa molecular weight, while Atezo scFv-Fc was detected at ~132 kDa (Figure 35B). Compared to the reduced form at 66 kDa, the non-reduced scFv-Fc is roughly double the molecular weight at 132 kDa, demonstrating scFv-Fc dimerization due to disulfide bonding.

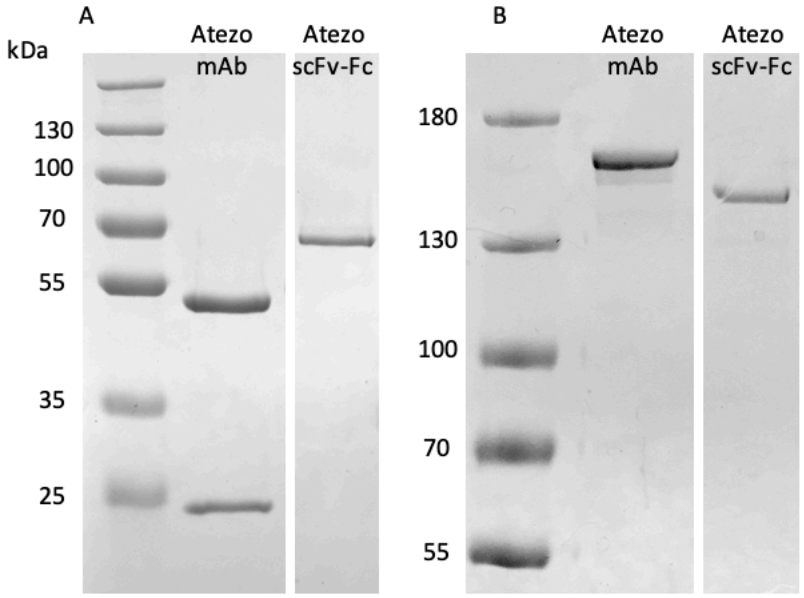

Figure 35. Atezo scFv-Fc dimerizes to form a bivalent antibody. Atezolizumab and Atezo scFv-Fc were run under (A) reducing conditions and (B) non-reducing conditions on SDS-PAGE. Molecular weight marker is labeled on the left for each gel.

Anti-PD-L1 CAR T cells kill human tumor cells in vitro

After testing scFv-Fc binding, the VL-VH sequence was cloned into a 3rd generation CAR vector to produce the anti-PD-L1 scFv CAR construct. Using this vector, lentiviral particles encoding the scFv CAR were produced by transfection of 293T cells. Lentivirus was subsequently used to transduce $CD3^+$ T cells isolated from human PBMC. Transduced T cells were expanded for 14 days with anti-CD3/CD28 and rIL-7/rIL-15. After expansion, cells were stained with CD3 and FLAG-tag antibodies, then analyzed by flow cytometry. Figure 36 shows the percent of $CD3^+$ T cells that express the scFv CAR (70.4%), measured by FLAG-tag expression.

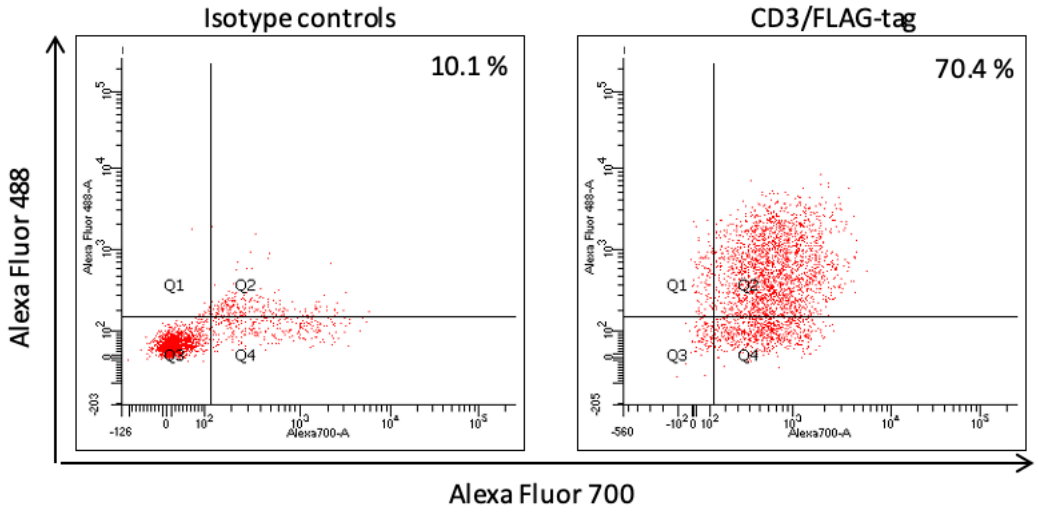

Figure 36. Expansion of anti-PD-L1 CAR T cells. CD3 and FLAG-tag expression were measured after 14-day culture of CAR-transduced PBMC. After expansion, 70.4% of cells were $CD3^+$ and FLAG-tag^+, indicating the majority of $CD3^+$ cells expressed the CAR construct.

Once scFv CAR expression was verified by flow cytometry, the anti-PD-L1 CAR T cells were used to determine their ability to kill cancer cell lines that overexpress PD-L1 (from Figure 34). Tumor cells were labeled with CFSE and co-incubated with anti-PD-L1 scFv CAR-transduced PBMC or non-transduced PBMC as a control. Target cells were also incubated alone to measure intrinsic cell death. After a four hour incubation, propidium iodide (PI) was added and the cells were analyzed by flow cytometry (Figure 37). Cell killing by anti-PD-L1 CAR T cells resulted in cell death measured by percent $CFSE^{+}PI^{+}$ as follows: 50.4% for RCJ-41T2, 54.9% for A549 treated with IFN-γ, 71.3% for 786-O, and 51.2% for Jurkat. Compared to cell death when incubated with non-transduced PBMC or target cells alone, CAR T cell-mediated cell death of target cells increased by > 26%.

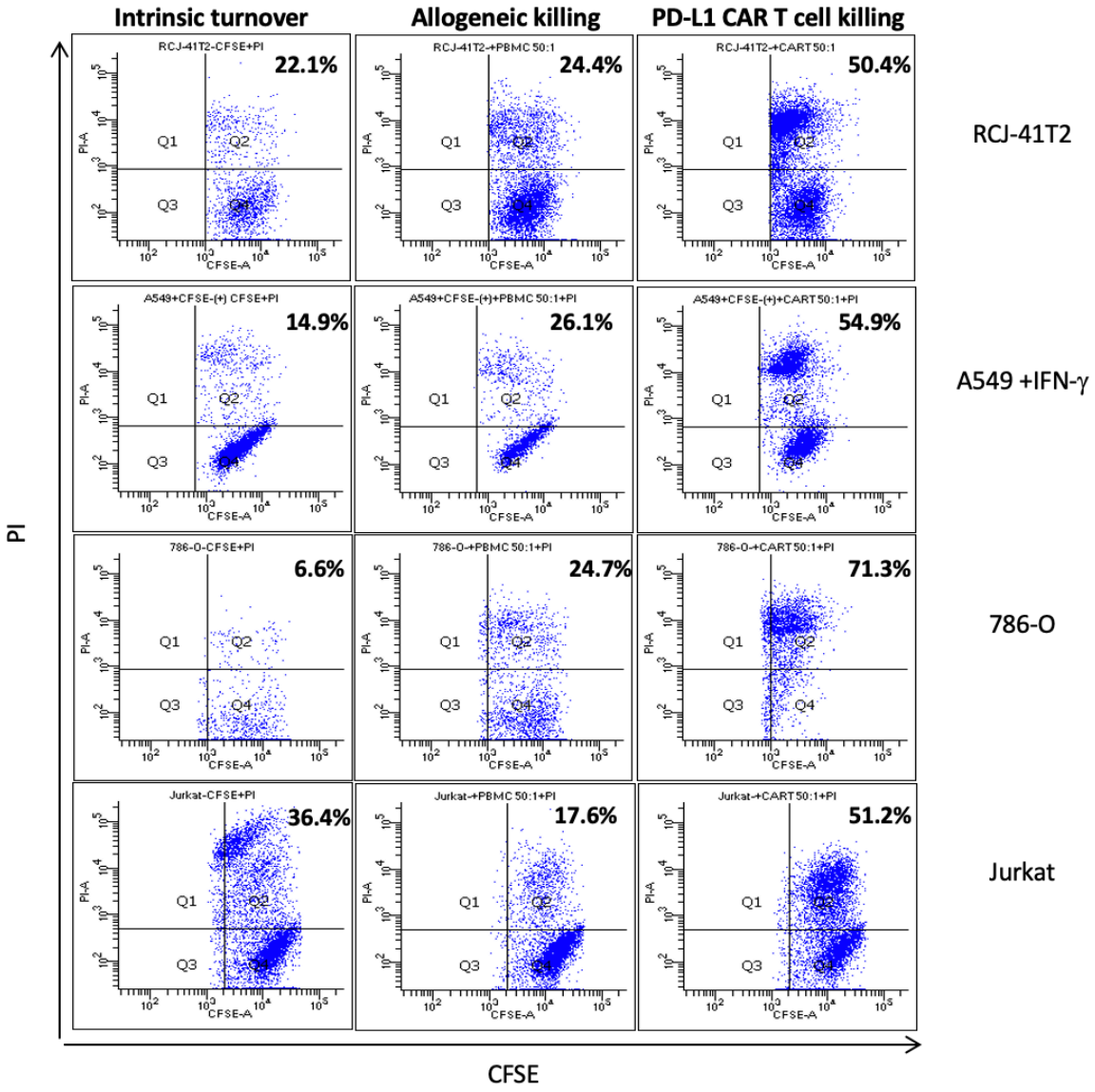

Figure 37. Anti-PD-L1 CAR T cells demonstrate killing of PD-L1^{+} tumor cells. Anti-PD-L1 CAR T cells were co-incubated with CFSE-labeled target cells at 50:1 ratio. Cytotoxicity was measured by CFSE/PI staining and analyzed by flow cytometry. Q2 is labeled with percent CFSE^{+}PI^{+} cells indicating dead or dying target cells. Intrinsic turnover indicates basal level of tumor cell death. Allogeneic killing indicates percent killed by non-transduced PBMC. RCJ-41T2 and 786-O (human renal cell carcinomas), A549 treated with IFN-γ for 48 h (human lung carcinoma), Jurkat (human T cell leukemia).

CAR T cell killing of tumor cells is specific

Anti-PD-L1 CAR T cells were incubated for four hours with RENCA tumor cells at an E:T ratio of 25:1. As shown microscopically in Figure 38A, 97% of RENCA cells were killed, leaving only anti-PD-L1 CAR T cells in the well. To demonstrate the specificity of the anti-PD-L1 CAR T cells, atezolizumab was used to block anti-PD-L1 CAR T cell killing. Atezolizumab (10 µg/ml) was pre-incubated with Renca cells prior to adding anti-PD-L1 CAR T cells. As shown in Figure 38B, atezolizumab blocked the killing (84.6% survival of RENCA cells) of anti-PD-L1 CAR T cells, compared to complete killing (97%) of Renca (Figure 38A) after 6 h incubation. In Figure 38A, only circular CAR T cells remain in the culture post-incubation, compared to circular CAR T cells and elongated Renca cells observed in Figure 38B.

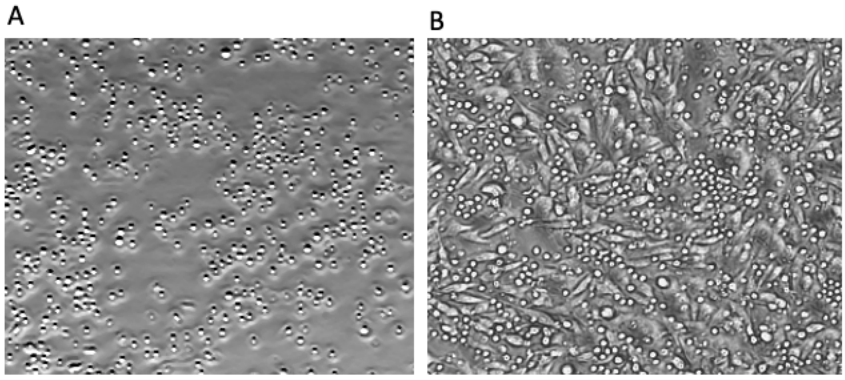

Figure 38. Anti-PD-L1 mAb blocks CAR T cell-mediated killing of Renca cells (murine RCC). (A) Renca cells co-incubated with anti-PD-L1 CAR T cells. (B) Renca cells pre-incubated with 10 µg/ml atezolizumab for 1 hr followed by the addition of anti-PD-L1 CAR T cells (E:T ratio 25:1) for 6 hours. Circular cells are CAR T cells. Elongated cells are Renca cells.

To demonstrate that anti-PD-L1 CAR T cells do kill non-malignant cells, anti-PD-L1 CAR T cells were incubated with CFSE-labeled Balb/c 3T3 cells, a non-tumorigenic murine fibroblast cell line. After incubation, $CFSE^{+}$ Balb/c 3T3 cells were imaged and appeared to maintain their normal elongated, adherent phenotype in the presence of anti-PD-L1 CAR T cells (Figure 39).

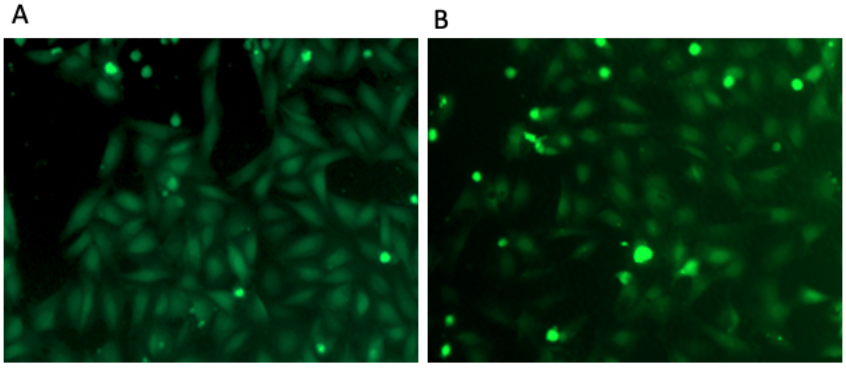

Figure 39. CAR T cells do not kill non-malignant cells. Anti-PD-L1 CAR T cells incubated with non-malignant Balb/c 3T3 cells (murine fibroblast cells). (A) Balb/c 3T3 cells alone, (B) CAR T cells incubated with Balb/c 3T3 cells at effector to target ratio 10:1. Balb/c 3T3 cells were labeled with CFSE and imaged after 6 hour incubation alone or with anti-PD-L1 CAR T cells.

Discussion

There is a significant clinical need for improved therapeutics that target solid tumors, especially tumors that develop resistance to traditional radio- and chemotherapeutics and existing immunotherapies. While immunotherapies can exhibit immune-mediated toxicity, they do not have systemic toxicities associated with traditional non-targeted chemotherapies. However, they are limited by life-threatening autoimmune side effects due to overactivation of pro-inflammatory immune responses[226]. To improve the efficacy of existing therapies, we designed CAR T cells to target PD-L1 expressed on tumor cells. Anti-PD-L1 scFv was constructed based on the sequence of the FDA-approved anti-PD-L1 antibody, atezolizumab. The scFv was produced and its binding characteristics were compared to the full mAb IgG to ensure the VL-VH construct was able to bind PD-L1. Binding of Atezo scFv-Fc to the cell surfaces of human and mouse tumor cells by flow cytometry is indistinguishable from Atezo IgG antibody (Figure 34). This suggests that Atezo scFv recognizes PD-L1 on tumor cells.

Once the scFv demonstrated binding to PD-L1 on tumor cells, CAR T cells were generated to express the scFv targeting PD-L1, thus combining an immune checkpoint antibody-based therapy with a cell-based engineered T cell therapy. A distinct advantage of using an antibody that blocks the PD-L1–PD-1 interaction is that blocking/neutralizing PD-L1 protects CAR T cells from tumors expressing PD-L1. Otherwise, they would meet the same fate via tumor PD-L1-induced anergy, as any other cytotoxic T cell. Another advantage of using CAR T cells over antibody immunotherapies is their potential for expansion and persistence in the recipient[227,228], overcoming the need for repeated mAb infusions. A study by Porter et al. showed that *in vivo* expansion of CD19 CAR T cells

infused into patients with relapsed and/or refractory chronic lymphocytic leukemia (CLL) maintained CAR T cell persistence and function over four years, with some patients achieving complete or partial remissions[229]. Another study by Melenhorst et al. monitored two patients with CLL that received CD19-directed CAR T cells and found detectable CAR T cells more than ten years post-infusion, which resulted in sustained remission in both patients[230]. Thus, CAR T cell therapy may provide long-term immunosurveillance.

Transduction of purified human T cells with anti-PD-L1 CAR T lentiviral construct resulted in the majority of T cells (> 70%) expressing the scFv on the cell surface post-expansion (Figure 36). Successful transduction of T cells can be a difficult and inefficient process, limiting successful gene engineering. Obstacles in this study included low transduction efficiency and generation of adequate high-titer lentivirus to transduce T cells. These difficulties were overcome with optimization of transduction conditions. The anti-PD-L1 CAR T cells were then tested for the ability to kill PD-L1$^+$ tumor cell targets in cytotoxicity assays (Figure 37). Compared to killing by allogeneic non-transduced PBMC, there was a significant increase in anti-PD-L1 CAR T cell-mediated killing, measured by percent increase as follows: 26% for RCJ-41T2, 29% for A549, 47% for 786-O, 33.6% for Jurkat. All cell lines demonstrated > 26% increase in cell death when incubated with anti-PD-L1 CAR T cells compared to non-transduced PBMC or cells alone. A limitation is the lack of cell lines that are negative for PD-L1 or the use of PD-L1 knockout cells as a control. The increase in cell killing suggests that anti-PD-L1 CAR T cells are capable of killing PD-L1-expressing cells. This is a

significant outcome, especially for sarcomatoid RCC, a tumor type for which none or very few effective treatments exist.

CAR T cell killing was demonstrated to be specific for PD-L1-expressing tumor cells. Since the CAR T cells were designed to express scFvs specific for PD-L1, binding to PD-L1 should induce tumor cell recognition and T cell stimulation. Thus, PD-L1 must be present on the cell for effective cell killing. To prove specificity, tumor cells were first incubated with atezolizumab before anti-PD-L1 CAR T cells were added. Since the CAR T cells are based on the sequence of atezolizumab, adding the soluble antibody first would result in blocking of the binding epitope. In Figure 38, it was observed that killing can be blocked by adding atezolizumab, since after incubation with CAR T cells, the target cells maintained their elongated phenotype and exhibited reduced cell death compared to the control without mAb. Additionally, other mAbs that bind PD-L1 at different epitopes should be tested. This suggests that anti-PD-L1 CAR T cells are mediating cell killing through recognition of PD-L1. A limitation of our *in vitro* study was that we did not test our anti-PD-L1 CAR T cells on non-malignant cells that express PD-L1. This would be an example of on-target off-tumor effect.

In order to test the safety and efficacy of the anti-PD-L1 CAR T cells, *in vivo* studies using a mouse model may be conducted. The immunocompetent renal cell carcinoma mouse model using Renca cells is an orthotopic syngeneic model that develops lung metastases. Since we show that Atezo scFv recognizes murine PD-L1 (Figure 34) and anti-PD-L1 CAR T cells kill Renca cells *in vitro* (Figure 38) but not non-malignant murine cells (Figure 39), this model could be employed to test the safety and efficacy of the CAR T cells. We can utilize this model to monitor mouse survival,

measure primary tumor size and metastatic burden post-infusion of CAR T cells. The use of anti-PD-L1 CAR T cells may improve upon the efficacy of existing therapies and advance our understanding of PD-L1 in the tumor microenvironment. Compared to existing CAR T cell therapies that target an antigen specifically expressed on a single cell type (e.g. CD19 on B cells), targeting PD-L1 offers a wider application for treating a range of malignancies, both in hematological and solid tumors. This study was discontinued due lack of funding and competition with large biotech companies.

CHAPTER 6

DISCUSSION

T cells play a critical role in regulating immune responses that can lead to autoimmunity and provide immunosurveillance to prevent tumor formation. These immune cells discriminate self from non-self, inhibiting destruction of self-tissue and protecting the host from foreign pathogens[17]. T cells can become activated in response to a target antigen[25]. Once activated, $CD8^+$ T cells perform direct cell killing of infected cells while $CD4^+$ T cells function by activating or inhibiting other immune cells via production of cytokines. $CD4^+$ T cell function is further classified based on distinct pro- or anti-inflammatory cytokine profiles in response to stimulation[20]. Regulatory T cells, a subset of $CD4^+$ T cells, are crucial for maintaining mechanisms of self-tolerance by suppressing unwanted inflammatory responses that could lead to autoimmunity if left uncontrolled[19]. In cancer, Tregs are recruited to the tumor microenvironment where they suppress anti-tumor immune responses[124]. Targeting Treg suppressive function and other mechanisms of tumor-induced suppression may be crucial for increasing responses to cancer immunotherapies and improving patient prognosis.

In Chapter 2, "Identification of a $CD4^+$ T cell line with Treg-like activity," a Treg-like cell line, MoT cells, was demonstrated to suppress $CD4^+$ PBMC in a cell-to-cell contact manner, similar to $Foxp3^+$ Tregs isolated from human peripheral blood. Since Tregs limit therapeutic effects by suppressing anti-tumor responses, there is a high clinical and scientific need to better understand Treg function and their interactions with other immune cells. However, development of therapeutics targeting Tregs is limited by several factors including high heterogeneity, low abundance in circulation and lack of a

specific cell surface marker. We isolated and expanded human Tregs from multiple donors, characterized as $CD4^+$ $CD25^{high}$ $Foxp3^+$ cells. We evaluated numerous $CD4^+$ T cell lines and identified MoT cells as being phenotypically and functionally comparable to PBMC-derived Tregs. MoT cells express Treg-associated surface markers and intracellular Foxp3. MoT cells, like Tregs, functionally suppress the proliferation of activated $CD4^+$ PBMC in a cell ratio-dependent manner. It was found that suppression requires direct cell contact between the suppressor cells and responder cells. The mechanism of suppression is independent of known Treg mechanisms including IL-2 deprivation, production of IL-10 and immune checkpoint pathways, since mAbs targeting these receptors could not attenuate Treg or MoT-mediated suppression.

These results suggest that human PBMC-derived Tregs and MoT cells mediate cell contact-dependent suppression by an uncharacterized suppressive mechanism. Further studies may be conducted to identify the molecule(s) mediating suppression, using MoT cells as a model for Tregs. Once a suppressive protein is identified, downstream signaling pathways being activated or inhibited in Tregs and responder cells can be evaluated. Additionally, transcriptional profiling of MoT cells should be performed to validate the usefulness of these cells as a Treg model cell line. It is unclear if the mechanism of suppression observed by Tregs and MoT cells is the same but future studies may be conducted to elucidate the suppressive mechanism(s). These findings increase our understanding of Treg function and discovery of a cell line with Treg-like properties may be useful in downstream applications, such as testing small molecules and biologics that target Tregs.

In Chapter 3, "Generation and characterization of a monoclonal antibody that binds to Galectin-1," monoclonal antibodies were generated to Galectin-1 (Gal-1) to investigate this protein as a potential cell surface molecule involved in MoT and Treg-mediated suppression. Gal-1 is a human lectin that has been shown to interact with and influence the function of Foxp3, a transcription factor that regulates Treg function[154]. It has been demonstrated to exert immunosuppressive function by inducing T cell apoptosis and increasing the number of tumor-infiltrating Foxp3$^+$ Tregs, resulting in poor patient outcome[161,162,231]. Proteomic analysis revealed Gal-1 is expressed on the surface of Tregs and MoT cells. Thus, targeting Gal-1 may provide a new prognostic indicator or therapeutic target to modulate Treg function in cancer.

One of the anti-Gal-1 antibodies generated, mAb 6F3, was shown to detect Gal-1 in multiple assays, including western blot, ELISA, and flow cytometry techniques. MAb 6F3 specifically binds to rGal-1 and does not cross-react with other secreted, immunosuppressive galectins. MAb 6F3 detects cell surface and intracellular Gal-1 in human Tregs and MoT cells. Addition of mAb 6F3 in a suppression assay did not block/reverse suppressive activity, suggesting this antibody is non-neutralizing or Gal-1 does not solely facilitate MoT-mediated suppression. Although it did not demonstrate neutralization, development of anti-Gal-1 mAb 6F3 provides a tool in studying the expression and immunosuppressive function of Gal-1, as well as its interactions with other immune-modulating proteins in various tumor cell types.

In Chapter 4, "Characterization of monoclonal antibodies (mAbs) that bind to MoT cells," antibodies were generated to MoT cell surface proteins by whole cell immunization and hybridoma generation techniques. In Chapter 2, it was demonstrated

that MoT cells and PBMC-derived Tregs suppress the proliferation of $CD4^+$ PBMC by direct cell-contact. Since suppression requires cell-cell contact, it was hypothesized that one or more suppressive proteins on Treg/MoT cell surface mediates suppression. Thus, antibodies were generated to MoT cell surface proteins to identify candidate suppressive molecules. Antibody-secreting hybridomas were screened in a two-step process: detection of binding to MoT cells by cell surface staining and then functionally in a suppression assay. Thirty-two candidate hybridomas exhibited a functional effect on MoT-mediated suppression, over half demonstrating a reversal of a suppression. From the candidate functional hybridomas, mAb 12E7 stood out as a potential blocking antibody and was further characterized. MAb 12E7 bound to the cell surface of MoT cells and human Tregs, but not Jurkat.

It was discovered that mAb 12E7 recognizes CD44 antigen, a cell surface receptor involved in T cell activation, proliferation, adhesion and migration[192,194,195]. Further studies beyond the scope of this dissertation may be conducted to elucidate the mechanism of CD44 in Tregs, its potential role in MoT and Treg contact-dependent suppression and the application of mAb 12E7 neutralizing antibody. Moreover, the repertoire of antibodies generated in this study can be further evaluated for a greater reversal of suppression compared to mAb 12E7. In addition to functional mAbs, binding mAbs that were generated to MoT cells may be further utilized to identify a distinct cell surface protein present on MoT cells and Tregs, in which expression may be found to be restricted to the Treg lineage. Identification of a Treg-specific cell surface protein would be immensely valuable for targeting Tregs in cancer and in the treatment of autoimmunity and graft rejection to isolate a more pure population of Tregs.

In Chapter 5, "Construction and characterization of anti-PD-L1 chimeric antigen receptor T cells that selectively kill PD-L1-positive tumor cells," anti-PD-L1 CAR T cells were developed and characterized. Anti-PD-L1 scFv was constructed based on an FDA-approved mAb and shown to recognize PD-L1 expressed on tumor cells. The scFv construct was then incorporated into the CAR T cell design to generate CAR T cells specific for PD-L1. It was observed that anti-PD-L1 CAR T cells kill human and mouse tumor cells that express PD-L1, while sparing non-malignant cells. Targeting an immune checkpoint such as PD-L1 provides a mechanism to overcome tumor-mediated suppression while also re-directing cytotoxic T cells to the tumor.

Future studies beyond the scope of this dissertation may be conducted to test the safety and efficacy of anti-PD-L1 CAR T cells *in vivo*. Long-term control and protection of CAR T cell therapy can be attributed to epitope spreading that occurs due to CAR T cell killing of tumor cells. Since most CAR T cells target a single antigen, tumor escape via antigen loss or downregulation of antigen expression can occur as a mechanism of resistance to CAR T cell therapy[232]. Epitope spreading is the generation of an immune response that is distinct from the initial epitope, and is directed to neo-epitopes or subdominant immunogens[232–234]. Epitope spreading is induced by CAR T cell lysis of tumor cells in the tumor microenvironment[235]. Therefore, epitope spreading may be crucial to avoid or reduce antigen escape, induce durable responses and provide long-term protection. To determine if epitope spreading occurs, endogenous $CD8^+$ CTLs can be harvested from anti-PD-L1 CAR T cell treated mice that have reduced or completely eliminated tumors. CTLs can then be tested *in vitro* for the ability to kill $PD\text{-}L1^{-/-}$ RENCA-luciferase tumor cells post-treatment. If cytotoxic CTLs are identified, these

results would suggest endogenous CTLs were generated to neo-epitopes due to tumor cell lysis. Demonstration of epitope spreading will increase the usefulness of anti-PD-L1 CAR T cell therapy. Overall, development of anti-PD-L1 CAR T cells may improve upon the efficacy of existing immunotherapies and is applicable to a range of hematologic and solid malignancies.

REFERENCES

1. Cunningham AJ. *Self-Tolerance, or Why the Immune System Is So Highly Regulated*. ACADEMIC PRESS, INC.; 1980. doi:10.1016/b978-0-12-637140-6.50008-5

2. Orrù V, Steri M, Sole G, et al. Genetic variants regulating immune cell levels in health and disease. *Cell*. 2013;155(1):242. doi:10.1016/j.cell.2013.08.041

3. De Arras L, Guthrie BS, Alper S. Using RNA-interference to investigate the innate immune response in mouse macrophages. *J Vis Exp*. 2014;(93):1-5. doi:10.3791/51306

4. Netea MG, Schlitzer A, Placek K, Joosten LAB, Schultze JL. Innate and Adaptive Immune Memory: an Evolutionary Continuum in the Host's Response to Pathogens. *Cell Host Microbe*. 2019;25(1):13-26. doi:10.1016/j.chom.2018.12.006

5. Zhang W, Niu Y, Xiong Y, Zhao M, Yu R, Liu J. Computational prediction of conformational B-cell epitopes from antigen primary structures by ensemble learning. *PLoS One*. 2012;7(8):1-9. doi:10.1371/journal.pone.0043575

6. Sakaguchi SH SN. Thymus and autoimmunity. Transplantation of the thymus from cyclosporin A-treated mice causes organ-specific autoimmune disease in athymic nude mice. *J Exp Med*. 1988;167(April):1479-1485.

7. Sakaguchi SH, Fukuma KA, Kuribayashi KA MT. Organ-specific autoimmune diseases induced in mice by elimination of T cell subset. I. Evidence for the active participation of T cells in natural self-tolerance; deficit of a T cell subset as a possible cause of autoimmune disease. *J Exp Med*. 1985;161(January):72-87.

8. Suri-Payer E, Amar AZ, Thornton AM, Shevach EM. CD4+CD25+ T cells inhibit both the induction and effector function of autoreactive T cells and represent a unique lineage of immunoregulatory cells. *J Immunol*. 1998.

9. Nikolić-Žugić J. Phenotypic and functional stages in the intrathymic development of αβ T cells. *Immunol Today*. 1991;12(2):65-70. doi:10.1016/0167-5699(91)90160-U

10. Germain RN. T-cell development and the CD4-CD8 lineage decision. *Nat Rev Immunol*. 2002;2(5):309-322. doi:10.1038/nri798

11. Godfrey DI, Zlotnik A. Control points in early T-cell development. *Immunol Today*. 1993;14(11):547-553. doi:10.1016/0167-5699(93)90186-O

12. Mallick CA, Dudley EC, Viney JL, Owen MJ, Hayday AC. Rearrangement and diversity of T cell receptor β chain genes in thymocytes: A critical role for the β chain in development. *Cell*. 1993;73(3):513-519. doi:10.1016/0092-8674(93)90138-G

13. Gerondakis S, Fulford TS, Messina NL, Grumont RJ. NF-κB control of T cell development. *Nat Immunol*. 2014;15(1):15-25. doi:10.1038/ni.2785

14. Jensen KDC, Su X, Shin S, et al. Thymic Selection Determines γδ T Cell Effector Fate: Antigen-Naive Cells Make Interleukin-17 and Antigen-Experienced Cells Make Interferon γ. *Immunity*. 2008;29(1):90-100. doi:10.1016/j.immuni.2008.04.022

15. Yasutomo K, Doyle C, Miele L, Germain RN. The duration of antigen receptor signalling determines CD4+ versus CD8+ T-cell lineage fate. *Nature*. 2000;404(6777):506-510. doi:10.1038/35006664

16. Kaye J, Hsu ML, Sauron ME, Jameson SC, Gascoigne NRJ, Hedrick SM. Selective development of CD4+ T cells in transgenic mice expressing a class II MHC-restricted antigen receptor. *Nature*. 1989;341(6244):746-749. doi:10.1038/341746a0

17. Guidos BCJ, Danska JS, Fathman CG, Weissman IL. T Cell Receptor-mediated Negative Selection of Autoreactive T Lymphocyte Precursors Occurs after Commitment to the CD4 or CD8 Lineages. 1990;172(September).

18. Sakaguchi S, Miyara M, Costantino CM, Hafler DA. FOXP3 + regulatory T cells in the human immune system. *Nat Rev Immunol*. 2010;10(7):490-500. doi:10.1038/nri2785

19. Bluestone JA, Abbas AK. Natural versus adaptive regulatory T cells. *Nat Rev Immunol*. 2003;3(3):253-257. doi:10.1038/nri1032

20. Wan YY, Flavell RA. How diverse-CD4 effector T cells and their functions. *J Mol Cell Biol*. 2009;1(1):20-36. doi:10.1093/jmcb/mjp001

21. Glimcher LH, Murphy KM. Lineage commitment in the immune system: The T helper lymphocyte grows up. *Genes Dev*. 2000;14(14):1693-1711. doi:10.1101/gad.14.14.1693

22. Luckheeram RV, Zhou R, Verma AD, Xia B. CD4 +T cells: Differentiation and functions. *Clin Dev Immunol*. 2012;2012. doi:10.1155/2012/925135

23. Zhang X, Ge R, Chen H, et al. Follicular Helper CD4+T Cells, Follicular Regulatory CD4+T Cells, and Inducible Costimulator and Their Roles in Multiple Sclerosis and Experimental Autoimmune Encephalomyelitis. *Mediators Inflamm*. 2021;2021. doi:10.1155/2021/2058964

24. Wülfing C, Davis MM. A receptor/cytoskeletal movement triggered by costimulation during T cell activation. *Science (80-)*. 1998;282(5397):2266-2269. doi:10.1126/science.282.5397.2266

25. Janeway CA Jr, Travers P, Walport M et al. General properties of armed effector T cells. In: *Immunobiology: The Immune System in Health and Disease*. 5th editio. Garland Science; 2001.

26. Tubo NJ, Pagán AJ, Taylor JJ, et al. Single naive CD4+ T cells from a diverse repertoire produce different effector cell types during infection. *Cell*. 2013;153(4):785-796. doi:10.1016/j.cell.2013.04.007

27. Janeway CA Jr, Travers P, Walport M et al. Macrophage activation by armed CD4 TH1 cells. In: *Immunobiology: The Immune System in Health and Disease. 5th Edition.* New York: Garland Science; 2001.

28. Pape KA, Kouskoff V, Nemazee D, et al. Visualization of the genesis and fate of isotype-switched B cells during a primary immune response. *J Exp Med*. 2003;197(12):1677-1687. doi:10.1084/jem.20012065

29. Lee SK, Rigby RJ, Zotos D, et al. B cell priming for extrafollicular antibody responses requires Bcl-6 expression by T cells. *J Exp Med*. 2011;208(7):1377-1388. doi:10.1084/jem.20102065

30. Tian T, Olson S, Whitacre JM, Harding A. The origins of cancer robustness and evolvability. *Integr Biol*. 2011;3(1):17-30. doi:10.1039/c0ib00046a

31. National Center for Health Statistics. Health, United States, 2020–2021: Annual Perspective. *Health (Irvine Calif)*. 2023:1-32. https://www.cdc.gov/nchs/data/hus/hus20-21.pdf.

32. Hanahan D, Weinberg RA. Hallmarks of cancer: The next generation. *Cell*. 2011;144(5):646-674. doi:10.1016/j.cell.2011.02.013

33. Choueiri TK, Regan MM, Rosenberg JE, et al. Carbonic anhydrase IX and pathological features as predictors of outcome in patients with metastatic clear-cell renal cell carcinoma receiving vascular endothelial growth factor-targeted therapy. *BJU Int*. 2010;106(6):772-778. doi:10.1111/j.1464-410X.2010.09218.x

34. Adams JM, Cory S. The Bcl-2 apoptotic switch in cancer development and therapy. *Oncogene*. 2007;26(9):1324-1337. doi:10.1038/sj.onc.1210220

35. Burkhart DL, Sage J. Cellular mechanisms of tumour suppression by the retinoblastoma gene. *Nat Rev Cancer*. 2008;8(9):671-682. doi:10.1038/nrc2399

36. Junttila MR, Evan GI. P53 a Jack of all trades but master of none. *Nat Rev Cancer*. 2009;9(11):821-829. doi:10.1038/nrc2728

37. Snyder CM, Chandel NS. Mitochondrial regulation of cell survival and death during low-oxygen conditions. *Antioxidants Redox Signal*. 2009;11(11):2673-2683. doi:10.1089/ars.2009.2730

38. Artandi SE, DePinho RA. Telomeres and telomerase in cancer. *Carcinogenesis*. 2009;31(1):9-18. doi:10.1093/carcin/bgp268

39. Baeriswyl V, Christofori G. The angiogenic switch in carcinogenesis. *Semin Cancer Biol*. 2009;19(5):329-337. doi:10.1016/j.semcancer.2009.05.003

40. Carmeliet P, Jain RK. Angiogenesis in cancer and other diseases. *Nature*. 2000:249-257. doi:https://doi.org/10.1038/35025220

41. Paschall A V., Liu K. An Orthotopic mouse model of spontaneous breast cancer metastasis. *J Vis Exp*. 2016;2016(114):1-7. doi:10.3791/54040

42. Adler AJ. Mechanisms of tumor-associated T-cell tolerance. *Tumor Induc Immune Suppr Mech Ther Reversal*. 2008:7-27. doi:10.1007/978-0-387-69118-3_2

43. Fidler IJ. The pathogenesis of cancer metastasis: the 'seed and soil' hypothesis revisited. *Nat Rev Cancer*. 2003;3(6):453-458. doi:10.1097/00006454-199103000-00027

44. Esposito A, Criscitiello C, Trapani D, Curigliano G. The Emerging Role of "Liquid Biopsies," Circulating Tumor Cells, and Circulating Cell-Free Tumor DNA in Lung Cancer Diagnosis and Identification of Resistance Mutations. *Curr Oncol Rep*. 2017;19(1):1-6. doi:10.1007/s11912-017-0564-y

45. Molparia B, Oliveira G, Wagner JL, Spencer EG, Torkamani A. A feasibility study of colorectal cancer diagnosis via circulating tumor DNA derived CNV detection. *PLoS One*. 2018;13(5):1-10. doi:10.1371/journal.pone.0196826

46. Jones RG, Thompson CB. Tumor suppressors and cell metabolism: A recipe for cancer growth. *Genes Dev*. 2009;23(5):537-548. doi:10.1101/gad.1756509

47. Adeegbe DO, Nishikawa H. Natural and induced T regulatory cells in cancer. *Front Immunol*. 2013;4(JUL):1-14. doi:10.3389/fimmu.2013.00190

48. Chen DS, Mellman I. Oncology meets immunology: The cancer-immunity cycle. *Immunity*. 2013;39(1):1-10. doi:10.1016/j.immuni.2013.07.012

49. Sharma P, Allison JP. The future of immune checkpoint therapy. *Science (80-)*. 2015;348(6230):56-61. doi:10.1126/science.aaa8172

50. Roychoudhuri R, Eil RL, Restifo NP. The interplay of effector and regulatory T cells in cancer. *Curr Opin Immunol*. 2015;33:101-111. doi:10.1016/j.coi.2015.02.003

51. Teng MWL, Swann JB, Koebel CM, Schreiber RD, Smyth MJ. Immune-mediated dormancy: an equilibrium with cancer. *J Leukoc Biol*. 2008;84(4):988-993. doi:10.1189/jlb.1107774

52. Motz GT, Coukos G. Deciphering and Reversing Tumor Immune Suppression. *Immunity*. 2013;39(1):61-73. doi:10.1016/j.immuni.2013.07.005

53. Kandalaft LE, Motz GT, Duraiswamy J, Coukos G. Tumor immune surveillance and ovarian cancer : Lessons on immune mediated tumor rejection or tolerance. *Cancer Metastasis Rev*. 2011;30(1):141-151. doi:10.1007/s10555-011-9289-9

54. Bouzin C, Brouet A, De Vriese J, DeWever J, Feron O. Effects of Vascular Endothelial Growth Factor on the Lymphocyte-Endothelium Interactions: Identification of Caveolin-1 and Nitric Oxide as Control Points of Endothelial Cell Anergy. *J Immunol*. 2007;178(3):1505-1511. doi:10.4049/jimmunol.178.3.1505

55. Buckanovich RJ, Facciabene A, Kim S, et al. Endothelin B receptor mediates the endothelial barrier to T cell homing to tumors and disables immune therapy. *Nat Med*. 2008;14(1):28-36. doi:10.1038/nm1699

56. Sata M, Walsh K. TNFa regulation of Fas ligand expression on the vascular endothelium modulates leukocyte extravasation. *Nat Med*. 1998;4(4):415-420.

57. Secchiero P, Zauli G. The puzzling role of TRAIL in endothelial cell biology. *Arterioscler Thromb Vasc Biol*. 2008;28(2):158451. doi:10.1161/ATVBAHA.107.158451

58. Huang X, Bai X, Cao Y, et al. Lymphoma endothelium preferentially expresses Tim-3 and facilitates the progression of lymphoma by mediating immune evasion. *J Exp Med*. 2010;207(3):505-520. doi:10.1084/jem.20090397

59. Hernández GL, Volpert O V., Íñiguez MA, et al. Selective inhibition of vascular endothelial growth factor-mediated angiogenesis by cyclosporin A: Roles of the nuclear factor of activated T cells and cyclooxygenase 2. *J Exp Med*. 2001;193(5):607-620. doi:10.1084/jem.193.5.607

60. Hurwitz AA, Gabrilovich DI. Immune-suppressive mechanisms and cancer: Understanding the implications, paradoxes, and burning questions. *Tumor Induc Immune Suppr Mech Ther Reversal*. 2008:1-5. doi:10.1007/978-0-387-69118-3_1

61. Guo Z, Zhang R, Yang AG, Zheng G. Diversity of immune checkpoints in cancer immunotherapy. *Front Immunol*. 2023;14(March):1-15. doi:10.3389/fimmu.2023.1121285

62. Rebucci M, Michiels C. Molecular aspects of cancer cell resistance to chemotherapy. *Biochem Pharmacol*. 2013;85(9):1219-1226. doi:10.1016/j.bcp.2013.02.017

63. Raguz S, Yagüe E. Resistance to chemotherapy: New treatments and novel insights into an old problem. *Br J Cancer*. 2008;99(3):387-391. doi:10.1038/sj.bjc.6604510

64. Garattini S. Pharmacokinetics in cancer chemotherapy. *Eur J Cancer*. 2007;43(2):271-282. doi:10.1016/j.ejca.2006.10.015

65. Juengel E, Makarević J, Reiter M, et al. Resistance to the mTOR inhibitor temsirolimus alters adhesion and migration behavior of renal cell carcinoma cells through an integrin α5- and integrin β3-dependent mechanism. *Neoplasia (United States)*. 2014;16(4):291-300. doi:10.1016/j.neo.2014.03.011

66. Du Z, Lovly CM. Mechanisms of receptor tyrosine kinase activation in cancer. *Mol Cancer*. 2018;17(1):1-13. doi:10.1186/s12943-018-0782-4

67. Cavenee K. Tumorigemcity on Human Glioblastoma Cells by Increasing Proliferation and Reducing Apoptosis '. *Control*. 1996;10(2):5079-5086.

68. Zhang Q, Liu JH, Liu JL, et al. Activation and function of receptor tyrosine kinases in human clear cell renal cell carcinomas. *BMC Cancer*. 2019;19(1):1-13. doi:10.1186/s12885-019-6159-2

69. Ansari J, Fatima A, Fernando K, Collins S, James ND, Porfiri E. Sunitinib in patients with metastatic renal cell carcinoma: Birmingham experience. *Oncol Rep*. 2010;24(2):507-510. doi:10.3892/or_00000886

70. Arao T, Matsumoto K, Furuta K, et al. Acquired drug resistance to vascular endothelial growth factor receptor 2 tyrosine kinase inhibitor in human vascular endothelial cells. *Anticancer Res*. 2011;31(9):2787-2796.

71. Poulikakos PI, Persaud Y, Janakiraman M, et al. RAF inhibitor resistance is mediated by dimerization of aberrantly spliced BRAF(V600E). *Nature*. 2011;480(7377):387-390. doi:10.1038/nature10662

72. Sharma P, Goswami S, Raychaudhuri D, et al. Immune checkpoint therapy—current perspectives and future directions. *Cell*. 2023;186(8):1652-1669. doi:10.1016/j.cell.2023.03.006

73. Sondak VK, Smalley KSM, Kudchadkar R, Grippon S, Kirkpatrick P. Ipilimumab. *Nat Rev Drug Discov*. 2011;10(6):411-412. doi:10.1038/nrd3463

74. Pardoll DM. The blockade of immune checkpoints in cancer immunotherapy. *Nat Rev Cancer*. 2012. doi:10.1038/nrc3239

75. Sharpe AH, Pauken KE. The diverse functions of the PD1 inhibitory pathway. *Nat Rev Immunol*. 2018;18(3):153-167. doi:10.1038/nri.2017.108

76. Butte MJ, Keir ME, Phamduy TB, Sharpe AH, Freeman GJ. Programmed Death-1 Ligand 1 Interacts Specifically with the B7-1 Costimulatory Molecule to Inhibit T Cell Responses. *Immunity*. 2007;27(1):111-122. doi:10.1016/j.immuni.2007.05.016

77. Abdin SM, Zaher DM, Arafa ESA, Omar HA. Tackling cancer resistance by immunotherapy: Updated clinical impact and safety of PD-1/PD-L1 inhibitors. *Cancers (Basel)*. 2018;10(2):1-17. doi:10.3390/cancers10020032

78. Brahmer JR, Tykodi SS, Chow LQM, et al. Safety and activity of anti-PD-L1 antibody in patients with advanced cancer. *N Engl J Med*. 2012;366(26):2455-2465. doi:10.1056/NEJMoa1200694

79. Chocarro L, Blanco E, Arasanz H, et al. Clinical landscape of LAG-3-targeted therapy. *Immuno-Oncology Technol*. 2022;14(C):100079. doi:10.1016/j.iotech.2022.100079

80. Huo JL, Wang YT, Fu WJ, Lu N, Liu ZS. The promising immune checkpoint LAG-3 in cancer immunotherapy: from basic research to clinical application. *Front Immunol*. 2022;13(July):1-10. doi:10.3389/fimmu.2022.956090

81. Ruffo E, Wu RC, Bruno TC, Workman CJ, Vignali DAA. Lymphocyte-activation gene 3 (LAG3): The next immune checkpoint receptor. *Semin Immunol*. 2019;42(May):101305. doi:10.1016/j.smim.2019.101305

82. Sugiyama D, Nishikawa H, Maeda Y, et al. Anti-CCR4 mAb selectively depletes effector-Type FoxP3+CD4+ regulatory T cells, evoking antitumor immune responses in humans. *Proc Natl Acad Sci U S A*. 2013;110(44):17945-17950. doi:10.1073/pnas.1316796110

83. Plitas G, Wu K, Carlson J, et al. Phase I/II study of mogamulizumab, an anti-CCR4 antibody targeting regulatory T cells in advanced cancer patients. *J Clin Oncol*. 2016. doi:10.1200/jco.2016.34.15_suppl.tps3098

84. Duvic M, Pinter-Brown LC, Foss FM, et al. Phase 1/2 study of mogamulizumab, a defucosylated anti-CCR4 antibody, in previously treated patients with cutaneous T-cell lymphoma. *Blood*. 2015;125(12):1883-1889. doi:10.1182/blood-2014-09-600924

85. Chen YJ, Abila B, Mostafa Kamel Y. CAR-T: What Is Next? *Cancers (Basel)*. 2023;15(3). doi:10.3390/cancers15030663

86. Kalos M, June CH. Adoptive T Cell Transfer for Cancer Immunotherapy in the Era of Synthetic Biology. *Immunity*. 2013;39(1):49-60. doi:10.1016/j.immuni.2013.07.002

87. Zhu Y, Qian Y, Li Z, Li Y, Li B. Neoantigen-reactive T cell: An emerging role in adoptive cellular immunotherapy. *MedComm*. 2021;2(2):207-220. doi:10.1002/mco2.41

88. Kalos M, Levine BL, Porter DL, et al. T cells with chimeric antigen receptors have potent antitumor effects and can establish memory in patients with advanced leukemia. *Sci Transl Med*. 2011;3(95):1-12. doi:10.1126/scitranslmed.3002842

89. Brentjens RJ, Rivière I, Park JH, et al. Safety and persistence of adoptively transferred autologous CD19-targeted T cells in patients with relapsed or chemotherapy refractory B-cell leukemias. *Blood*. 2011;118(18):4817-4828. doi:10.1182/blood-2011-04-348540

90. Kochenderfer JN, Dudley ME, Feldman SA, et al. B-cell depletion and remissions of malignancy along with cytokine-associated toxicity in a clinical trial of anti-CD19 chimeric-antigen-receptor-transduced T cells. *Blood*. 2012;119(12):2709-2720. doi:10.1182/blood-2011-10-384388

91. Rodríguez-Perea AL, Arcia ED, Rueda CM, Velilla PA. Phenotypical characterization of regulatory T cells in humans and rodents. *Clin Exp Immunol*. 2016;185(3):281-291. doi:10.1111/cei.12804

92. Yu N, Li X, Song W, et al. CD4+CD25+CD127low/- T cells: A more specific treg population in human peripheral blood. *Inflammation*. 2012;35(6):1773-1780. doi:10.1007/s10753-012-9496-8

93. Shevyrev D, Tereshchenko V. Treg Heterogeneity, Function, and Homeostasis. *Front Immunol*. 2020;10(January):1-13. doi:10.3389/fimmu.2019.03100

94. Bensinger SJ, Bandeira A, Jordan MS, Caton AJ, Laufer TM. Major histocompatibility complex class II-positive cortical epithelium mediates the selection of CD4+25+immunoregulatory T cells. *J Exp Med*. 2001;194(4):427-438. doi:10.1084/jem.194.4.427

95. Shevach EM. Foxp3+ T regulatory cells: Still many unanswered Questions-A perspective after 20 years of study. *Front Immunol*. 2018;9(MAY). doi:10.3389/fimmu.2018.01048

96. Thornton AM, Donovan EE, Piccirillo CA, Shevach EM. Cutting Edge: IL-2 Is Critically Required for the In Vitro Activation of CD4+ CD25+ T Cell Suppressor Function. 2004:1-5.

97. Zou T, Caton AJ, Koretzky GA, Kambayashi T. Dendritic Cells Induce Regulatory T Cell Proliferation through Antigen-Dependent and -Independent Interactions. *J Immunol*. 2010;185(5):2790-2799. doi:10.4049/jimmunol.0903740

98. Dario A. A. Vignali LWC and CJW. How regulatory T cells work. *Nat rev immunol*. 2008;8(7):523-532. doi:10.1038/nri2343.How

99. Sakaguchi S, Wing K, Yamaguchi T. Dynamics of peripheral tolerance and immune regulation mediated by Treg. *Eur J Immunol*. 2009;39(9). doi:10.1002/eji.200939688

100. Wang HY, Lee DA, Peng G, et al. Tumor-Specific Human CD4+ Regulatory T Cells and Their Ligands: Implications for Immunotherapy. *Immunity*. 2004;20(1):107-118. doi:10.1016/S1074-7613(03)00359-5

101. Brunkow ME, Jeffery EW, Hjerrild KA, et al. Disruption of a new forkhead / winged-helix protein , scurfin , results in the fatal lymphoproliferative disorder © 2001 Nature Publishing Group http://genetics.nature.com. 2001;27(january):68-73.

102. Ohkura N, Hamaguchi M, Morikawa H, et al. T Cell Receptor Stimulation-Induced Epigenetic Changes and Foxp3 Expression Are Independent and Complementary Events Required for Treg Cell Development. *Immunity*. 2012;37(5):785-799. doi:10.1016/j.immuni.2012.09.010

103. Thornton AM, Korty PE, Tran DQ, et al. Expression of Helios, an Ikaros Transcription Factor Family Member, Differentiates Thymic-Derived from Peripherally Induced Foxp3 + T Regulatory Cells . *J Immunol*. 2010. doi:10.4049/jimmunol.0904028

104. Tai X, Laethem F Van, Pobezinsky L, et al. Basis of CTLA-4 function in regulatory and conventional CD4 T cells. *Blood*. 2012;119(22):5155-5163. doi:10.1182/blood-2011

105. Wing K, Onishi Y, Prieto-Martin P, et al. CTLA-4 control over Foxp3+ regulatory T cell function. *Science (80-)*. 2008. doi:10.1126/science.1160062

106. Liao G, Nayak S, Regueiro JR, et al. GITR engagement preferentially enhances proliferation of functionally competent CD4+CD25+FoxP3+ regulatory T cells. *Int Immunol*. 2010;22(4):259-270. doi:10.1093/intimm/dxq001

107. Ko K, Yamazaki S, Nakamura K, et al. Treatment of advanced tumors with agonistic anti-GITR mAb and its effects on tumor-infiltrating Foxp3+CD25+CD4+ regulatory T cells. *J Exp Med*. 2005;202(7):885-891. doi:10.1084/jem.20050940

108. Anderson AC, Joller N, Kuchroo VK. Lag-3, Tim-3, and TIGIT: Co-inhibitory Receptors with Specialized Functions in Immune Regulation. *Immunity*. 2016;44(5):989-1004. doi:10.1016/j.immuni.2016.05.001

109. Camisaschi C, Casati C, Rini F, et al. LAG-3 Expression Defines a Subset of CD4+CD25highFoxp3+ Regulatory T Cells That Are Expanded at Tumor Sites. *J Immunol*. 2010;184(11):6545-6551. doi:10.4049/jimmunol.0903879

110. Tanaka A, Sakaguchi S. Regulatory T cells in cancer immunotherapy. *Cell Res*. 2017. doi:10.1038/cr.2016.151

111. Baatar D, Olkhanud P, Sumitomo K, Taub D, Gress R, Biragyn A. Human Peripheral Blood T Regulatory Cells (Tregs), Functionally Primed CCR4+ Tregs and Unprimed CCR4− Tregs, Regulate Effector T Cells Using FasL. *J Immunol*. 2007;178(8):4891-4900. doi:10.4049/jimmunol.178.8.4891

112. Sojka DK, Huang YH, Fowell DJ. Mechanisms of regulatory T-cell suppression - A diverse arsenal for a moving target. *Immunology*. 2008;124(1):13-22. doi:10.1111/j.1365-2567.2008.02813.x

113. Ohue Y, Nishikawa H. Regulatory T (Treg) cells in cancer: Can Treg cells be a new therapeutic target? *Cancer Sci*. 2019;110(7):2080-2089. doi:10.1111/cas.14069

114. Arellano B, Graber DJ, Sentman CL. Regulatory T cell-based therapies for autoimmunity. *Discov Med*. 2016.

115. Shevach EM. Mechanisms of Foxp3+ T Regulatory Cell-Mediated Suppression. *Immunity*. 2009. doi:10.1016/j.immuni.2009.04.010

116. Cao X, Cai SF, Fehniger TA, et al. Granzyme B and Perforin Are Important for Regulatory T Cell-Mediated Suppression of Tumor Clearance. *Immunity*. 2007;27(4):635-646. doi:10.1016/j.immuni.2007.08.014

117. Deaglio S, Dwyer KM, Gao W, et al. Adenosine generation catalyzed by CD39 and CD73 expressed on regulatory T cells mediates immune suppression. *J Exp Med*. 2007;204(6):1257-1265. doi:10.1084/jem.20062512

118. Von Boehmer H. Mechanisms of suppression by suppressor T cells. *Nat Immunol*. 2005;6(4):338-344. doi:10.1038/ni1180

119. Costantino CM, Baecher-allan CM, Hafler DA. Human Tregs and autoimmunity. *Eur J Immunol*. 2009;38(4):921-924. doi:10.1002/eji.200738104.Human

120. Koreth J, Matsuoka K, Kim HT, et al. Interleukin-2 and Regulatory T Cells in Graft-versus-Host Disease. *N Engl J Med*. 2011;365(22). doi:10.1056/nejmoa1108188

121. Saadoun D, Rosenzwajg M, Joly F, et al. Regulatory T-Cell Responses to Low-Dose Interleukin-2 in HCV-Induced Vasculitis. *N Engl J Med*. 2011;365(22). doi:10.1056/nejmoa1105143

122. Beers DR, Zhao W, Wang J, et al. ALS patients' regulatory T lymphocytes are dysfunctional, and correlate with disease progression rate and severity. *JCI Insight*. 2017;2(5):1-14. doi:10.1172/jci.insight.89530

123. Thonhoff JR, Beers DR, Zhao W, et al. Expanded autologous regulatory T-lymphocyte infusions in ALS A phase I, first-in-human study. *Neurol Neuroimmunol NeuroInflammation*. 2018;5(4). doi:10.1212/NXI.0000000000000465

124. Wang RF. Immune suppression by tumor-specific CD4+ regulatory T-cells in cancer. *Semin Cancer Biol*. 2006;16(1):73-79. doi:10.1016/j.semcancer.2005.07.009

125. Nishikawa H, Sakaguchi S. Regulatory T cells in tumor immunity. *Int J Cancer*. 2010;127(4):759-767. doi:10.1002/ijc.25429

126. Curiel TJ, Coukos G, Zou L, et al. Specific recruitment of regulatory T cells in ovarian carcinoma fosters immune privilege and predicts reduced survival. *Nat Med*. 2004;10(9):942-949. doi:10.1038/nm1093

127. Antony PA, Piccirillo CA, Akpinarli A, et al. CD8+ T Cell Immunity Against a Tumor/Self-Antigen Is Augmented by CD4+ T Helper Cells and Hindered by Naturally Occurring T Regulatory Cells. *J Immunol*. 2005;174(5):2591-2601. doi:10.4049/jimmunol.174.5.2591

128. Shevach EM. From Vanilla to 28 Flavors: Multiple Varieties of T Regulatory Cells. *Immunity*. 2006. doi:10.1016/j.immuni.2006.08.003

129. Belkaid Y, Blank RB, Suffia I. Natural regulatory T cells and parasites: A common quest for host homeostasis. *Immunol Rev*. 2006. doi:10.1111/j.0105-2896.2006.00409.x

130. Lanteri MC, O'Brien KM, Purtha WE, et al. Tregs control the development of symptomatic West Nile virus infection in humans and mice. *J Clin Invest*. 2009. doi:10.1172/JCI39387

131. Hill JA, Feuerer M, Tash K, et al. Foxp3 Transcription-Factor-Dependent and -Independent Regulation of the Regulatory T Cell Transcriptional Signature. *Immunity*. 2007. doi:10.1016/j.immuni.2007.09.010

132. Asseman C, Mauze S, Leach MW, Coffman RL, Powrie F. An essential role for interleukin 10 in the function of regulatory T cells that inhibit intestinal inflammation. *J Exp Med*. 1999. doi:10.1084/jem.190.7.995

133. Collison LW, Workman CJ, Kuo TT, et al. The inhibitory cytokine IL-35 contributes to regulatory T-cell function. *Nature*. 2007. doi:10.1038/nature06306

134. Campbell DJ, Koch MA. Phenotypical and functional specialization of FOXP3+ regulatory T cells. *Nat Rev Immunol*. 2011. doi:10.1038/nri2916

135. Battaglia M, Stabilini A, Roncarolo MG. Rapamycin selectively expands CD4+CD25+FoxP3 + regulatory T cells. *Blood*. 2005. doi:10.1182/blood-2004-10-3932

136. Sauer S, Bruno L, Hertweck A, et al. T cell receptor signaling controls Foxp3 expression via PI3K, Akt, and mTOR. *Proc Natl Acad Sci U S A*. 2008. doi:10.1073/pnas.0800928105

137. Strainic MG, Shevach EM, An F, Lin F, Medof ME. Absence of signaling into CD4 + cells via C3aR and C5aR enables autoinductive TGF-β1 signaling and induction of Foxp3 + regulatory T cells. *Nat Immunol*. 2013. doi:10.1038/ni.2499

138. Fallarino F, Grohmann U, Hwang KW, et al. Modulation of tryptophan catabolism by regulatory T cells. *Nat Immunol*. 2003. doi:10.1038/ni1003

139. Zeng H, Zhang R, Jin B, Chen L. Type 1 regulatory T cells: A new mechanism of peripheral immune tolerance. *Cell Mol Immunol*. 2015. doi:10.1038/cmi.2015.44

140. Saxon A, Stevens RH, Quan SG, Golde DW. Immunologic characterization of hairy cell leukemias in continuous culture. *J Immunol*. 1978;120(3):777-782. http://www.jimmunol.org/content/120/3/777.

141. Akkaya B, Oya Y, Akkaya M, et al. Regulatory T cells mediate specific suppression by depleting peptide–MHC class II from dendritic cells. *Nat Immunol*. 2019. doi:10.1038/s41590-018-0280-2

142. Hamano R, Wu X, Wang Y, Oppenheim JJ, Chen X. Characterization of MT-2 cells as a human regulatory T cell-like cell line. *Cell Mol Immunol*. 2015;12(6):780-782. doi:10.1038/cmi.2014.123

143. Schneider U, Schwenk H -U, Bornkamm G. Characterization of EBV-genome negative “null” and “T” cell lines derived from children with acute lymphoblastic leukemia and leukemic transformed non-Hodgkin lymphoma. *Int J Cancer*. 1977. doi:10.1002/ijc.2910190505

144. Kleiner G, Marcuzzi A, Zanin V, Monasta L, Zauli G. Cytokine levels in the serum of healthy subjects. *Mediators Inflamm*. 2013;2013. doi:10.1155/2013/434010

145. Bluestone JA, Buckner JH, Fitch M, et al. Type 1 diabetes immunotherapy using polyclonal regulatory T cells. *Sci Transl Med*. 2015. doi:10.1126/scitranslmed.aad4134

146. Ezzelarab MB, Thomson AW. Adoptive Cell Therapy with Tregs to Improve Transplant Outcomes: the Promise and the Stumbling Blocks. *Curr Transplant Reports*. 2016. doi:10.1007/s40472-016-0114-9

147. Fisher SA, Lamikanra A, Dorée C, et al. Increased regulatory T cell graft content is associated with improved outcome in haematopoietic stem cell transplantation: a systematic review. *Br J Haematol*. 2017. doi:10.1111/bjh.14433

148. Wang W, Lau R, Yu D, Zhu W, Korman A, Weber J. PD1 blockade reverses the suppression of melanoma antigen-specific CTL by CD4+CD25Hi regulatory T cells. *Int Immunol*. 2009. doi:10.1093/intimm/dxp072

149. NCT02691247. Safety and Efficacy of CLBS03 in Adolescents With Recent Onset Type 1 Diabetes (The Sanford Project T-Rex Study). *Https://clinicaltrials.gov/show/nct02691247*. 2016.

150. Chellappa S, Kushekhar K, Munthe LA, et al. The PI3K p110δ Isoform Inhibitor Idelalisib Preferentially Inhibits Human Regulatory T Cell Function. *J Immunol*. 2019. doi:10.4049/jimmunol.1701703

151. Camby I, Le Mercier M, Lefranc F, Kiss R. Galectin-1: A small protein with major functions. *Glycobiology*. 2006;16(11). doi:10.1093/glycob/cwl025

152. Hughes RC. Secretion of the galectin family of mammalian carbohydrate-binding proteins. *Biochim Biophys Acta - Gen Subj*. 1999;1473(1):172-185. doi:10.1016/S0304-4165(99)00177-4

153. Raymond E. OTX008, a selective small-molecule inhibitor of galectin-1, downregulates cancer cell proliferation, invasion and tumour angiogenesis. *Eur J Cancer*. 2014;50(14):2463-2477. doi:10.1016/j.ejca.2014.06.015

154. Gao Y, Li X, Shu Z, et al. Nuclear galectin-1-FOXP3 interaction dampens the tumor-suppressive properties of FOXP3 in breast cancer. *Cell Death Dis*. 2018;9(4). doi:10.1038/s41419-018-0448-6

155. Astorgues-Xerri L, Riveiro ME, Tijeras-Raballand A, et al. Unraveling galectin-1 as a novel therapeutic target for cancer. *Cancer Treat Rev*. 2014;40(2):307-319. doi:10.1016/j.ctrv.2013.07.007

156. Cedeno-Laurent F, Dimitroff CJ. Galectin-1 research in T cell immunity: Past, present and future. *Clin Immunol*. 2012;142(2):107-116. doi:10.1016/j.clim.2011.09.011

157. Perillo Nl, Pace Ke, Seilhamer Jj, Baum Lg. Apoptosis of T cells mediated by galectin-1. *Nature*. 1995;378(6558):736-739.

158. Deák M, Hornung Á, Novák J, et al. Novel role for galectin-1 in T-cells under physiological and pathological conditions. *Immunobiology*. 2015;220(4):483-489. doi:10.1016/j.imbio.2014.10.023

159. Croci DO, Salatino M, Rubinstein N, et al. Disrupting galectin-1 interactions with N-glycans suppresses hypoxia-driven angiogenesis and tumorigenesis in Kaposi's sarcoma. *J Exp Med*. 2012;209(11):1985-2000. doi:10.1084/jem.20111665

160. Verschuere T, De Vleeschouwer S, Lefranc F, Kiss R, Van Gool SW. Galectin-1 and immunotherapy for brain cancer. *Expert Rev Neurother*. 2011;11(4):533-543. doi:10.1586/ern.11.40

161. Huang Y, Wang HC, Zhao J, Wu MH, Shih TC. Immunosuppressive roles of galectin-1 in the tumor microenvironment. *Biomolecules*. 2021;11(10). doi:10.3390/biom11101398

162. Lau LS, Mohammed NBB, Dimitroff CJ. Decoding Strategies to Evade Immunoregulators Galectin-1, -3, and -9 and Their Ligands as Novel Therapeutics in Cancer Immunotherapy. *Int J Mol Sci*. 2022;23(24):1-22. doi:10.3390/ijms232415554

163. Ouyang J, Juszczynski P, Rodig SJ, et al. Viral induction and targeted inhibition of galectin-1 in EBV+ posttransplant lymphoproliferative disorders. *Blood*. 2011;117(16):4315-4322. doi:10.1182/blood-2010-11-320481

164. Pérez Sáez JM, Hockl PF, Cagnoni AJ, et al. Characterization of a neutralizing anti-human galectin-1 monoclonal antibody with angioregulatory and immunomodulatory activities. *Angiogenesis*. 2021;24(1):1-5. doi:10.1007/s10456-020-09749-3

165. Garín MI, Chu NC, Golshayan D, Cernuda-Morollón E, Wait R, Lechler RI. Galectin-1: A key effector of regulation mediated by CD4 +CD25+ T cells. *Blood*. 2007;109(5):2058-2065. doi:10.1182/blood-2006-04-016451

166. Ho TH, Pfeffer K, Weiss GJ, Ruiz Y, Lake DF. Identification of a CD4+ T cell line with Treg-like activity. *Hum Immunol*. 2022;83(4):281-294. doi:10.1016/j.humimm.2022.01.008

167. Comşa Ş, Cîmpean AM, Raica M. The story of MCF-7 breast cancer cell line: 40 Years of experience in research. *Anticancer Res*. 2015;35(6):3147-3154.

168. Köhler G, Milstein C. Continuous cultures of fused cells secreting antibody of predefined specificity. *Nature*. 1975;256(5517). doi:10.1038/256495a0

169. Dierks SE, Butler JE, Richerson HB. Altered recognition of surface-adsorbed compared to antigen-bound antibodies in the ELISA. *Mol Immunol*. 1986;23(4):403-411. doi:10.1016/0161-5890(86)90138-0

170. Oomizu S, Arikawa T, Niki T, et al. Cell Surface Galectin-9 Expressing Th Cells Regulate Th17 and Foxp3+ Treg Development by Galectin-9 Secretion. *PLoS One*. 2012;7(11). doi:10.1371/journal.pone.0048574

171. Hsu DK, Chen H. Galectin-3 regulates T-cell functions. 2009;230:114-127.

172. Elola MT, Chiesa ME, Alberti AF, Mordoh J, Fink NE. Galectin-1 receptors in different cell types. *J Biomed Sci*. 2005;12(1):13-29. doi:10.1007/s11373-004-8169-5

173. Blaskó A, Fajka-Boja R, Ion G, Monostori E. How does it act when soluble? Critical evaluation of mechanism of galectin-1 induced T-cell apoptosis. *Acta Biol Hung*. 2011;62(1):106-111. doi:10.1556/ABiol.61.2011.1.11

174. Fernandes Â, Azevedo CM, Silva MC, et al. Glycans as shapers of tumour microenvironment: A sweet driver of T-cell-mediated anti-tumour immune response. *Immunology*. 2023;168(2):217-232. doi:10.1111/imm.13494

175. Collison LW, Pillai MR, Chaturvedi V, Vignali DAA. Regulatory T Cell Suppression Is Potentiated by Target T Cells in a Cell Contact, IL-35- and IL-10-Dependent Manner. *J Immunol*. 2009;182(10):6121-6128. doi:10.4049/jimmunol.0803646

176. Thornton AM, Shevach EM. CD4+CD25+ immunoregulatory T cells suppress polyclonal T cell activation in vitro by inhibiting interleukin 2 production. *J Exp Med*. 1998;188(2):287-296. doi:10.1084/jem.188.2.287

177. Dieckmann D, Bruett CH, Ploettner H, Lutz MB, Schuler G. Human CD4+CD25+ regulatory, contact-dependent T cells induce interleukin 1-producing, contact-independent type 1-like regulatory T cells. *J Exp Med*. 2002;196(2):247-253. doi:10.1084/jem.20020642

178. Ren X, Ye F, Jiang Z, Chu Y, Xiong S, Wang Y. Involvement of cellular death in TRAIL/DR5-dependent suppression induced by CD4+CD25+ regulatory T cells. *Cell Death Differ*. 2007;14(12):2076-2084. doi:10.1038/sj.cdd.4402220

179. Powrie BF, Carlino J, Smita WL, Coffman RL. A Critical Role for Transforming Growth Factor-Beta but Not Interleukin 4 in the Suppression of T Helper Type 1-mediated Colitis by CD45RBlow CD4+ T Cells. *J Exp Med*. 1996;183(June).

180. Brooks PC, Lin JM, French DL, Quigley JP. Subtractive immunization yields monoclonal antibodies that specifically inhibit metastasis. *J Cell Biol*. 1993;122(6):1351-1359. doi:10.1083/jcb.122.6.1351

181. Haynesworth SE, Barer MA, Caplan AI. Cell surface antigens on human marrow-derived mesenchymal cells are detected by monoclonal antibodies. *Bone*. 1992;13(1):69-80. doi:10.1016/8756-3282(92)90363-2

182. Choi HS, Kim WT, Ryu CJ. Antibody approaches to prepare clinically transplantable cells from human embryonic stem cells: Identification of human embryonic stem cell surface markers by monoclonal antibodies. *Biotechnol J*. 2014;9(7):915-920. doi:10.1002/biot.201300495

183. Storz U. Rituximab: How approval history is reflected by a corresponding patent filing strategy. *MAbs*. 2014;6(4):820-837. doi:10.4161/mabs.29105

184. Grillo-Lopez A, White C, Dallaire B, et al. Rituximab The First Monoclonal Antibody Approved for the Treatment of Lymphoma. *Curr Pharm Biotechnol*. 2005;1(1):1-9. doi:10.2174/1389201003379059

185. Long ET, Baker S, Oliveira V, Sawitzkib B, Wood KJ. Alpha-1,2-mannosidase and hence N-glycosylation are required for regulatory t cell migration and allograft tolerance in mice. *PLoS One*. 2010;5(1). doi:10.1371/journal.pone.0008894

186. Cabral J, Hanley SA, Gerlach JQ, et al. Distinctive surface glycosylation patterns associated with mouse and human cD4+ regulatory T cells and their suppressive function. *Front Immunol*. 2017;8(AUG). doi:10.3389/fimmu.2017.00987

187. An HJ, Froehlich JW, Lebrilla CB. Determination of glycosylation sites and site-specific heterogeneity in glycoproteins. *Curr Opin Chem Biol*. 2009;13(4):421-426. doi:10.1016/j.cbpa.2009.07.022

188. Gahmberg CG, Tolvanen M. Why mammalian cell surface proteins are glycoproteins. *Trends Biochem Sci*. 1996;21(8):308-311. doi:10.1016/S0968-0004(96)10034-7

189. Saxon A, Stevens RH, Quan SG, Golde DW. Immunologic characterization of hairy cell leukemias in continuous culture. *J Immunol*. 1978.

190. Xu H, Niu M, Yuan X, Wu K, Liu A. CD44 as a tumor biomarker and therapeutic target. *Exp Hematol Oncol*. 2020;9(1):1-14. doi:10.1186/s40164-020-00192-0

191. Senbanjo LT, Chellaiah MA. CD44: A multifunctional cell surface adhesion receptor is a regulator of progression and metastasis of cancer cells. *Front Cell Dev Biol*. 2017;5(MAR). doi:10.3389/fcell.2017.00018

192. Huet S, Groux H, Valentin H, Prieur M, Bernard A. CD44 contributes to T cell activation. 1989;143(3):798-801.

193. Chen C, Zhao S, Karnad A, Freeman JW. The biology and role of CD44 in cancer progression: Therapeutic implications. *J Hematol Oncol*. 2018;11(1):1-23. doi:10.1186/s13045-018-0605-5

194. DeGrendele HC, Estess P, Siegelman MH. Requirement for CD44 in activated T cell extravasation into an inflammatory site. *Science (80-)*. 1997;278(5338):672-675. doi:10.1126/science.278.5338.672

195. Haynes BF, Telen MJ, Hale LP, Denning SM. CD44 - A molecule involved in leukocyte adherence and T-cell activation. *Immunol Today*. 1989;10(12):423-428. doi:10.1016/0167-5699(89)90040-6

196. Kawai T, Iwata K, Shinotsuka Y, et al. CD44v8-10 and CD44s are age-dependently expressed in primary cultured papillary thyroid carcinoma cells and are associated with cell proliferation. *Kobe J Med Sci*. 2019;65(1):E1-E9.

197. Yamakawa Y, Kusuhara M, Terashima M, et al. Cd44 variant 9 expression as a predictor for gastric cancer recurrence: immunohistochemical and metabolomic analysis of surgically resected tissues. *Biomed Res*. 2017;38(1):41-52. doi:10.2220/biomedres.38.41

198. Zheng Z, Katoh S, He Q, et al. Monoclonal antibodies to CD44 and their influence on hyaluronan recognition. *J Cell Biol*. 1995;130(2):485-495. doi:10.1083/jcb.130.2.485

199. Denning SM, Le PT, Singer KH, Haynes BF. Antibodies against the CD44 p80, lymphocyte homing receptor molecule augment human peripheral blood T cell activation. *J Immunol*. 1990;144(1):7-15. doi:10.4049/jimmunol.144.1.7

200. Wessels D, Lusche DF, Voss E, et al. *Melanoma Cells Undergo Aggressive Coalescence in a 3D Matrigel Model That Is Repressed Byanti-CD44*. Vol 12.; 2017. doi:10.1371/journal.pone.0173400

201. Song JM, Im J, Nho RS, Han YH, Upadhyaya P, Kassie F. Hyaluronan-CD44/RHAMM interaction-dependent cell proliferation and survival in lung cancer cells. *Mol Carcinog*. 2019;58(3):321-333. doi:10.1002/mc.22930

202. Zhang S, Wu CCN, Fecteau JF, et al. Targeting chronic lymphocytic leukemia cells with a humanized monoclonal antibody specific for CD44. *Proc Natl Acad Sci U S A*. 2013;110(15):6127-6132. doi:10.1073/pnas.1221841110

203. Alamgeer M, Neil Watkins D, Banakh I, et al. A phase IIa study of HA-irinotecan, formulation of hyaluronic acid and irinotecan targeting CD44 in extensive-stage small cell lung cancer. *Invest New Drugs*. 2018;36(2):288-298. doi:10.1007/s10637-017-0555-8

204. Li Y, Duy Le TM, Nam Bui Q, Yang HY, Lee DS. Tumor acidity and CD44 dual targeting hyaluronic acid-coated gold nanorods for combined chemo- and photothermal cancer therapy. *Carbohydr Polym*. 2019;226(August). doi:10.1016/j.carbpol.2019.115281

205. Chen L, Azuma T, Yu W, Zheng X, Luo L, Chen L. B7-H1 maintains the polyclonal T cell response by protecting dendritic cells from cytotoxic T lymphocyte destruction. *Proc Natl Acad Sci U S A*. 2018;115(12):3126-3131. doi:10.1073/pnas.1722043115

206. Seetharamu N, Preeshagul IR, Sullivan KM. New PD-L1 inhibitors in non-small cell lung cancer – Impact of atezolizumab. *Lung Cancer Targets Ther*. 2017;8:67-78. doi:10.2147/LCTT.S113177

207. Markham A. Atezolizumab: First Global Approval. *Drugs*. 2016;76(12):1227-1232. doi:10.1007/s40265-016-0618-8

208. Siegler EL, Wang P. Preclinical Models in Chimeric Antigen Receptor-Engineered T-Cell Therapy. *Hum Gene Ther*. 2018;29(5):534-546. doi:10.1089/hum.2017.243

209. Sadelain M, Brentjens R, Rivière I. The promise and potential pitfalls of chimeric antigen receptors. *Curr Opin Immunol*. 2009;21(2):215-223. doi:10.1016/j.coi.2009.02.009

210. Textor A, Listopad JJ, Wührmann L Le, et al. Efficacy of CAR T-cell therapy in large tumors relies upon stromal targeting by IFNγ. *Cancer Res*. 2014;74(23):6796-6805. doi:10.1158/0008-5472.CAN-14-0079

211. Chmielewski M, Hombach AA, Abken H. Antigen-specific T-cell activation independently of the MHC: Chimeric antigen receptor-redirected T cells. *Front Immunol*. 2013;4(NOV):1-7. doi:10.3389/fimmu.2013.00371

212. Shi H, Sun M, Liu L, Wang Z. Chimeric antigen receptor for adoptive immunotherapy of cancer: Latest research and future prospects. *Mol Cancer*. 2014;13(1):1-8. doi:10.1186/1476-4598-13-219

213. Maus M V., Grupp SA, Porter DL, June CH. Antibody-modified T cells: CARs take the front seat for hematologic malignancies. *Blood*. 2014;123(17):2625-2635. doi:10.1182/blood-2013-11-492231

214. Geldres C, Savoldo B, Dotti G. Chimeric antigen receptor-redirected T cells return to the bench. *Semin Immunol*. 2016;28(1):3-9. doi:10.1016/j.smim.2015.12.001

215. Tey SK. Adoptive T-cell therapy: adverse events and safety switches. *Clin Transl Immunol*. 2014;3(6):1-7. doi:10.1038/cti.2014.11

216. Gargett T, Brown MP. The inducible caspase-9 suicide gene system as a "safety switch" to limit on-target, off-tumor toxicities of chimeric antigen receptor T-cells. *Front Pharmacol*. 2014;5(OCT):1-7. doi:10.3389/fphar.2014.00235

217. Shi ZD, Tchao J, Wu L, Carman AJ. Precision installation of a highly efficient suicide gene safety switch in human induced pluripotent stem cells. *Stem Cells Transl Med*. 2020;9(11):1378-1388. doi:10.1002/sctm.20-0007

218. Straathof KC, Pulè MA, Yotnda P, et al. An inducible caspase 9 safety switch for T-cell therapy. *Blood*. 2005;105(11):4247-4254. doi:10.1182/blood-2004-11-4564

219. Li J, Li W, Huang K, Zhang Y, Kupfer G, Zhao Q. Chimeric antigen receptor T cell (CAR-T) immunotherapy for solid tumors: Lessons learned and strategies for moving forward. *J Hematol Oncol*. 2018;11(1). doi:10.1186/s13045-018-0568-6

220. Xu X, Qiu J, Sun Y. The basics of CAR T design and challenges in immunotherapy of solid tumors — Ovarian cancer as a model. *Hum Vaccines Immunother*. 2017;13(7):1548-1555. doi:10.1080/21645515.2017.1291473

221. Feng C, Zhang L, Chang X, Qin D, Zhang T. Regulation of post-translational modification of PD-L1 and advances in tumor immunotherapy. *Front Immunol*. 2023;14(July):1-17. doi:10.3389/fimmu.2023.1230135

222. Dai X, Gao Y, Wei W. Post-translational regulations of PD-L1 and PD-1: Mechanisms and opportunities for combined immunotherapy. *Semin Cancer Biol*. 2022;85(April 2021):246-252. doi:10.1016/j.semcancer.2021.04.002

223. Pitt JM, Vétizou M, Daillère R, et al. Resistance Mechanisms to Immune-Checkpoint Blockade in Cancer: Tumor-Intrinsic and -Extrinsic Factors. *Immunity*. 2016;44(6):1255-1269. doi:10.1016/j.immuni.2016.06.001

224. Haas AR, Tanyi JL, O'Hara MH, et al. Phase I Study of Lentiviral-Transduced Chimeric Antigen Receptor-Modified T Cells Recognizing Mesothelin in Advanced Solid Cancers. *Mol Ther*. 2019;27(11):1919-1929. doi:10.1016/j.ymthe.2019.07.015

225. Zaritskaya L, Shurin MR, Sayers TJ, Malyguin AM. New flow cytometric assays for monitoring cell-mediated cytotoxicity. *Expert Rev Vaccines*. 2010;9(6):601-616. doi:doi:10.1586/erv.10.49

226. Seidel JA, Otsuka A, Kabashima K. Anti-PD-1 and anti-CTLA-4 therapies in cancer: Mechanisms of action, efficacy, and limitations. *Front Oncol*. 2018;8(MAR):1-14. doi:10.3389/fonc.2018.00086

227. McLellan AD, Ali Hosseini Rad SM. Chimeric antigen receptor T cell persistence and memory cell formation. *Immunol Cell Biol*. 2019;97(7):664-674. doi:10.1111/imcb.12254

228. Gupta A, Gill S. CAR-T cell persistence in the treatment of leukemia and lymphoma. *Leuk Lymphoma*. 2021;62(11):2587-2599. doi:10.1080/10428194.2021.1913146

229. Porter DL, Hwang WT, Frey N V., et al. Chimeric antigen receptor T cells persist and induce sustained remissions in relapsed refractory chronic lymphocytic leukemia. *Sci Transl Med*. 2015;7(303):1-13. doi:10.1126/scitranslmed.aac5415

230. Melenhorst JJ, Chen GM, Wang M, et al. Decade-long leukaemia remissions with persistence of CD4+ CAR T cells. *Nature*. 2022;602(7897):503-509. doi:10.1038/s41586-021-04390-6

231. Wu H, Chen P, Liao R, et al. Overexpression of galectin-1 is associated with poor prognosis in human hepatocellular carcinoma following resection. *J Gastroenterol Hepatol*. 2012;27(8):1312-1319. doi:10.1111/j.1440-1746.2012.07130.x

232. Conde E, Vercher E, Soria-Castellano M, et al. Epitope spreading driven by the joint action of CART cells and pharmacological STING stimulation counteracts tumor escape via antigen-loss variants. *J Immunother Cancer*. 2021;9(11):1-16. doi:10.1136/jitc-2021-003351

233. Vanderlugt CL, Miller SD. Epitope spreading in immune-mediated diseases: Implications for immunotherapy. *Nat Rev Immunol*. 2002;2(2):85-95. doi:10.1038/nri724

234. Jackson HJ, Brentjens RJ. Overcoming antigen escape with CAR T-cell therapy. *Cancer Discov*. 2015;5(12):1238-1240. doi:10.1158/2159-8290.CD-15-1275

235. Majzner RG, Mackall CL. Tumor antigen escape from car t-cell therapy. *Cancer Discov*. 2018;8(10):1219-1226. doi:10.1158/2159-8290.CD-18-0442

APPENDIX A

STATEMENT OF PERMISSIONS

All co-authors have granted permission for the use of the articles in this dissertation.

APPENDIX B

SUPPLEMENTAL DATA FOR CHAPTER 2

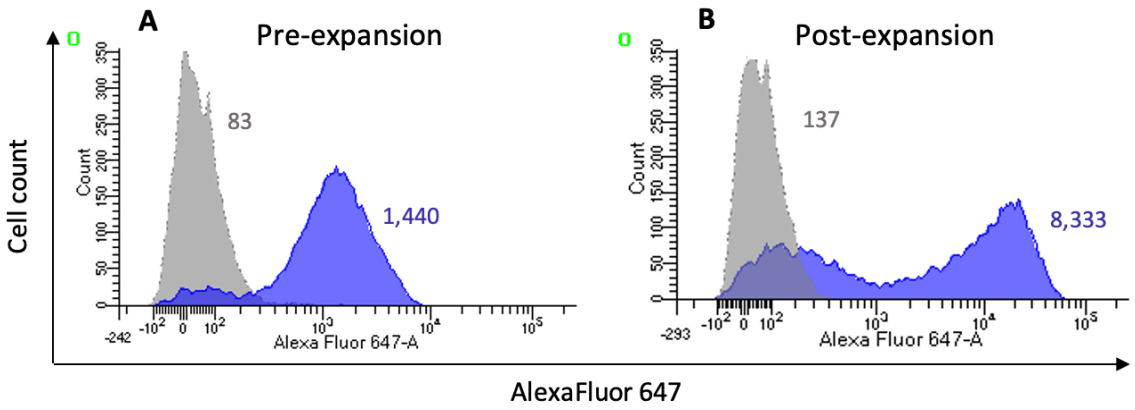

Supplemental Figure 1. Heterogeneity of CD4^{+} CD25^{high} CD127^{low} Treg population from human PBMC pre- and post- rhIL-2 expansion. The majority of this cell population (88.1 and 70.4%, respectively) is Foxp3^{+}. (A) Pre-expansion, (B) Post-expansion. Mean fluorescence intensity of isotype control is in gray on the left and anti-FoxP3 Mab clone 259D staining is shown as blue on the right of each histogram. Results representative of 6 different human PBMC donors. MFI values are indicated on the graph.

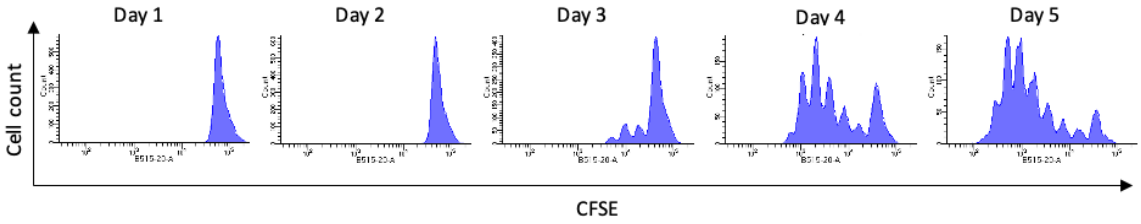

Supplemental Figure 2. Proliferation of CFSE-labeled CD3/CD28 activated CD4$^+$ PBMC over the 5 day time-course. Stimulated CD4$^+$ PBMCs do not proliferate until day 3 or 4. Representative data is shown (N=6).

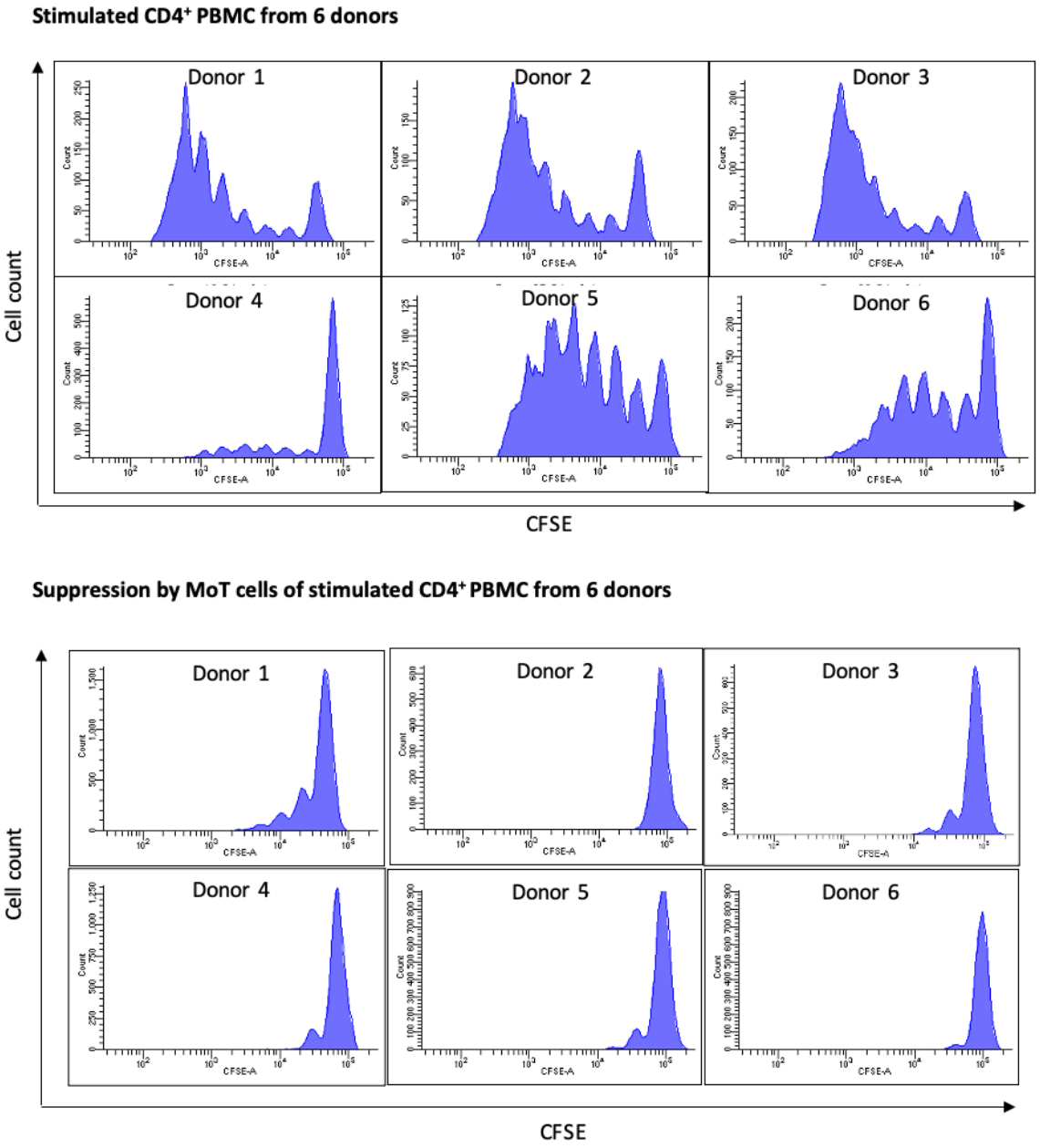

Supplemental Figure 3. CD3/CD28 activation of CD4$^+$ PBMC from 6 different donor PBMC. All biological replicates co-cultured with MoT cells are shown. Each donor is capable of being suppressed, independent of whether there is a small or large population of proliferating cells.

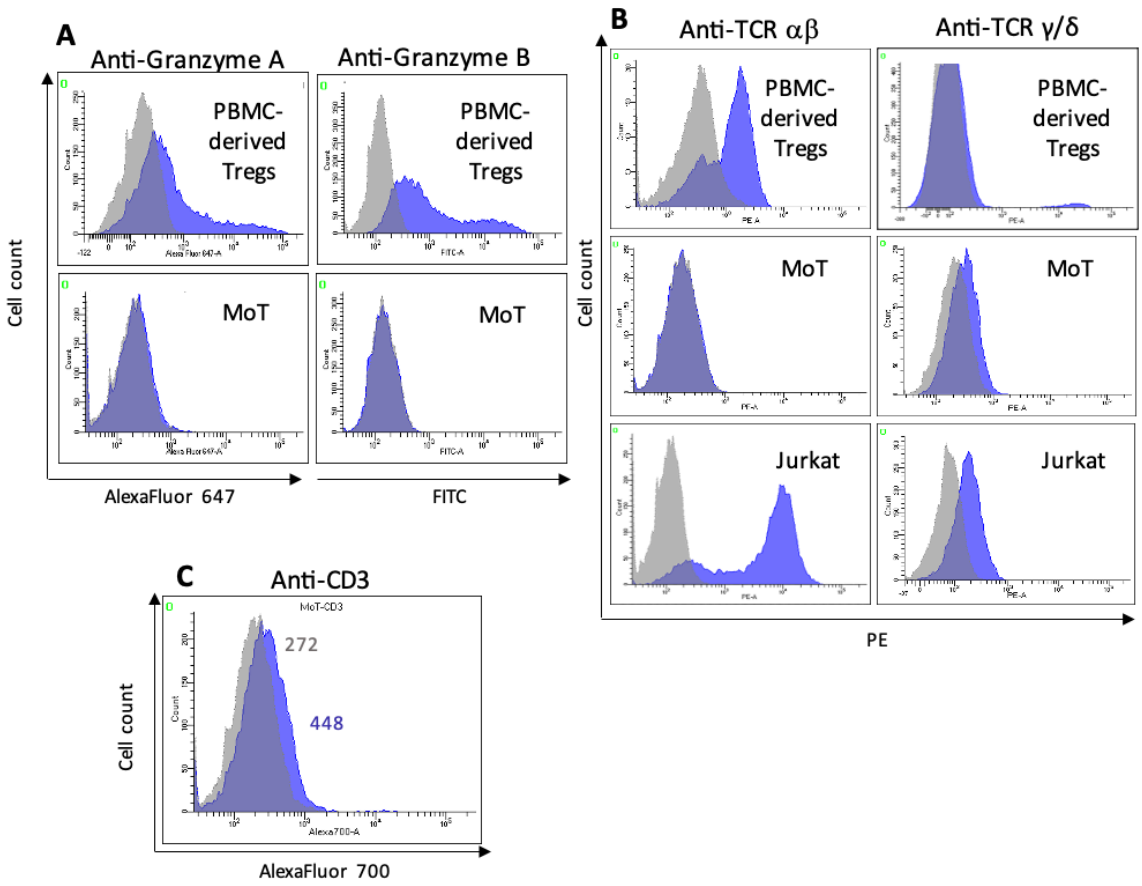

Supplemental Figure 4. (A) Granzyme A and B staining of PBMC-derived Tregs and MoT cells. Anti-Granzyme A and B Mabs (blue); isotype control (gray). (B) MoT cells do not express TCR αβ or γδ. Cell types are as labeled in histograms. Three histograms on the left represent TCR αβ staining while three histograms on the right are γδ. Anti-TCR αβ and γδ Mabs (blue); isotype control (gray). (C) CD3 expression on MoT cells. Anti-CD3 Mab (blue); isotype control (gray).

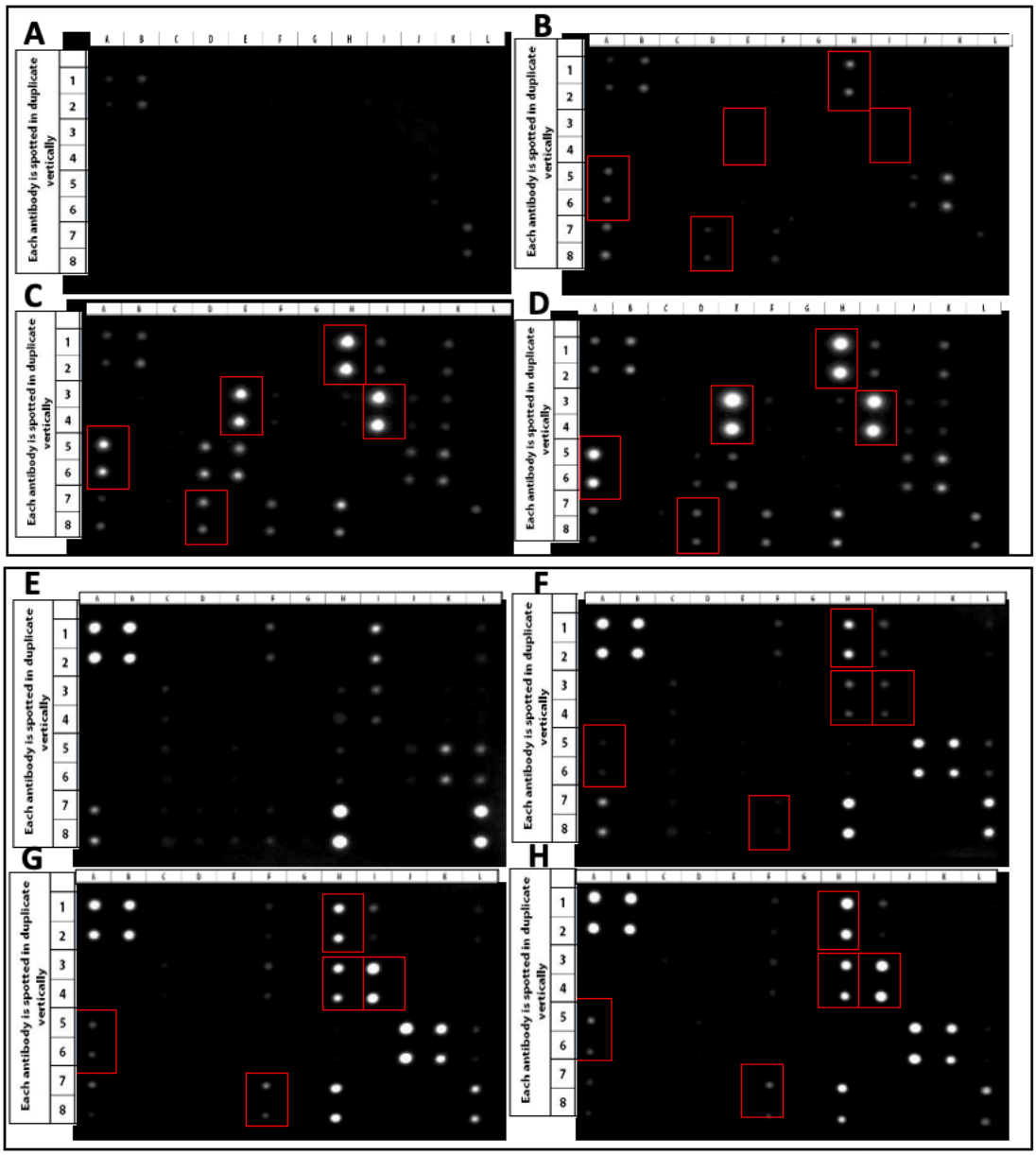

Each antibody is spotted in duplicate vertically	A	B	C	D	E	F	G	H	I	J	K	L
1	POS	POS	NEG	NEG	Eotaxin-1 (CCL11)	Eotaxin-2 (MPIF-2 /CCL24)	GCSF	GM-CSF	ICAM-1 (CD54)	IFN-gamma	I-309 (TCA-3/CCL1)	IL-1 alpha (IL-1 F1)
2												
3	IL-1 beta (IL-1 F2)	IL-2	IL-3	IL-4	IL-6	IL-6 R	IL-7	IL-8 (CXCL8)	IL-10	IL-11	IL-12 p40	IL-12 p70
4												
5	IL-13	IL-15	IL-16	IL-17A	IP-10 (CXCL10)	MCP-1 (CCL2)	MCP-2 (CCL8)	M-CSF	MIG (CXCL9)	MIP-1 alpha (CCL3)	MIP-1 beta (CCL4)	MIP-1 delta (CCL15)
6												
7	RANTES (CCL5)	TGF beta 1	TNF alpha	TNF beta (TNFSF1B)	TNF RI (TNFRSF1A)	TNF RII (TNFRSF1B)	PDGF-BB	TIMP-2	BLANK	BLANK	NEG	POS
8												

Supplemental Figure 5. Cytokine array of cell-free five-day spent supernatants (RayBiotech, AAH-INF-3-4). (A) Media alone. (B) Stimulated $CD4^+$ PBMC alone. (C) MoT cells alone. (D) Stimulated $CD4^+$ PBMC co-cultured with MoT cells (1:1) (E) Media alone. (F) Stimulated $CD4^+$ PBMC alone. (G) PBMC-derived Tregs alone. (H) Stimulated $CD4^+$ PBMC co-cultured with PBMC-derived Tregs (1:2).

	Media alone	Stimulated CD4+ PBMC alone	**MoT cells alone**	Stimulated CD4+ PBMC co-cultured with **MoT cells**
POS	3,120.79	3,120.79	3,120.79	3,120.79
NEG	0.00	0.00	0.00	0.00
Eotaxin	0.00	0.00	0.00	0.00
Eotaxin-2	0.00	0.00	0.00	0.00
G-CSF	0.00	0.00	0.00	0.00
GM-CSF	**0.00**	**8,957.56**	**41,143.95**	**25,988.19**
ICAM-1	0.00	0.00	4,712.17	2,292.42
IFN-gamma	0.00	0.00	0.00	0.00
I-309	0.00	0.00	3,789.73	2,564.39
IL-1a	0.00	0.00	0.00	0.00
IL-1beta	0.00	0.00	0.00	0.00
IL-2	0.00	0.00	0.00	0.00
IL-3	0.00	0.00	0.00	0.00
IL-4	0.00	0.00	0.00	0.00
IL-6	**0.00**	**0.00**	**28,742.45**	**30,953.68**
IL-6 sR	0.00	0.00	582.12	514.15
IL-7	0.00	0.00	0.00	0.00
IL-8	0.00	0.00	1,275.62	603.41
IL-10	**0.00**	**0.00**	**46,538.12**	**26,706.38**
IL-11	0.00	0.00	2,026.08	1,079.89
IL12-p40	0.00	0.00	2,707.07	1,098.70
IL12-p70	0.00	0.00	0.00	0.00
IL-13	**0.00**	**5,189.43**	**17,228.08**	**12,248.23**
IL-15	0.00	0.00	0.00	0.00
IL-16	0.00	0.00	0.00	0.00
IL17	0.00	0.00	10,572.69	802.37
IP-10	0.00	0.00	13,289.09	2,701.93
MCP-1	0.00	0.00	0.00	0.00
MCP-2	0.00	0.00	0.00	0.00
M-CSF	0.00	0.00	0.00	0.00
MIG	0.00	0.00	0.00	0.00
MIP-1-alpha	0.00	2,068.70	4,707.05	3,098.94
MIP-1-beta	1,467.12	14,625.72	7,888.34	6,959.81
MIP-1-delta	0.00	0.00	0.00	0.00
RANTES	0.00	8,710.66	2,603.38	2,105.80
TGF-beta 1	0.00	0.00	0.00	0.00
TNF-alpha	0.00	0.00	0.00	0.00
TNF-beta	**0.00**	**1,937.07**	**7,255.61**	**1,927.78**
sTNF-RI	0.00	0.00	0.00	0.00
sTNF RII	0.00	2,360.54	4,768.97	2,917.49
PDGF-BB	0.00	0.00	0.00	0.00
TIMP-2	0.00	0.00	10,441.85	5,508.75

Supplemental Table 1. Cytokine array spot signal densities. Densitometry analysis performed using ImageJ. Values were normalized to the positive control spots. Highly expressed cytokines are bolded and boxed in the array (Supplemental Figure 5).

	Media alone	Stimulated CD4+ PBMC alone	**PBMC-derived Tregs alone**	Stimulated CD4+ PBMC co-cultured with **PBMC-derived Tregs**
POS	6656.35	6656.35	6656.35	6656.35
NEG	0.00	0.00	0.00	0.00
Eotaxin	0.00	0.00	0.00	0.00
Eotaxin-2	720.69	593.41	284.13	288.28
G-CSF	0.00	0.00	0.00	0.00
GM-CSF	**0.00**	**4319.25**	**6628.67**	**8521.48**
ICAM-1	2704.82	881.69	986.35	639.97
IFN-gamma	0.00	0.00	0.00	0.00
I-309	0.00	0.00	0.00	0.00
IL-1a	416.04	0.00	290.84	0.00
IL-1beta	0.00	0.00	0.00	0.00
IL-2	0.00	0.00	0.00	0.00
IL-3	201.39	239.66	38.59	18.45
IL-4	0.00	0.00	0.00	0.00
IL-6	0.00	0.00	0.00	0.00
IL-6 sR	0.00	0.00	701.74	400.46
IL-7	0.00	0.00	0.00	0.00
IL-8	**455.01**	**1185.29**	**5892.51**	**5464.66**
IL-10	**899.46**	**671.93**	**10270.63**	**8490.66**
IL-11	0.00	0.00	0.00	0.00
IL12-p40	7.93	0.00	0.00	0.00
IL12-p70	0.00	0.00	0.00	0.00
IL-13	**0.00**	**209.78**	**818.47**	**997.60**
IL-15	0.00	0.00	0.00	0.00
IL-16	166.06	69.25	0.00	0.00
IL17	0.00	0.00	0.00	35.44
IP-10	24.40	0.00	0.00	0.00
MCP-1	0.00	0.00	0.00	0.00
MCP-2	0.00	0.00	0.00	0.00
M-CSF	268.39	14.46	0.00	0.00
MIG	0.00	0.00	0.00	0.00
MIP-1-alpha	287.72	5367.38	12028.97	8137.46
MIP-1-beta	2311.77	4550.84	8135.84	5505.99
MIP-1-delta	1649.56	663.33	393.19	43.72
RANTES	1691.23	2579.10	695.28	331.90
TGF-beta 1	0.00	0.00	0.00	0.00
TNF-alpha	284.18	362.60	0.00	0.00
TNF-beta	94.06	0.00	0.00	0.00
sTNF-RI	227.91	0.00	0.00	0.00
sTNF RII	**489.22**	**77.90**	**1100.14**	**723.36**
PDGF-BB	0.00	0.00	0.00	0.00
TIMP-2	9356.11	6911.19	6938.83	4023.50

Supplemental Table 2. Cytokine array spot signal densities. Densitometry analysis performed using ImageJ. Values were normalized to the positive control spots. Highly expressed cytokines are bolded and boxed in the array (Supplemental Figure 5).

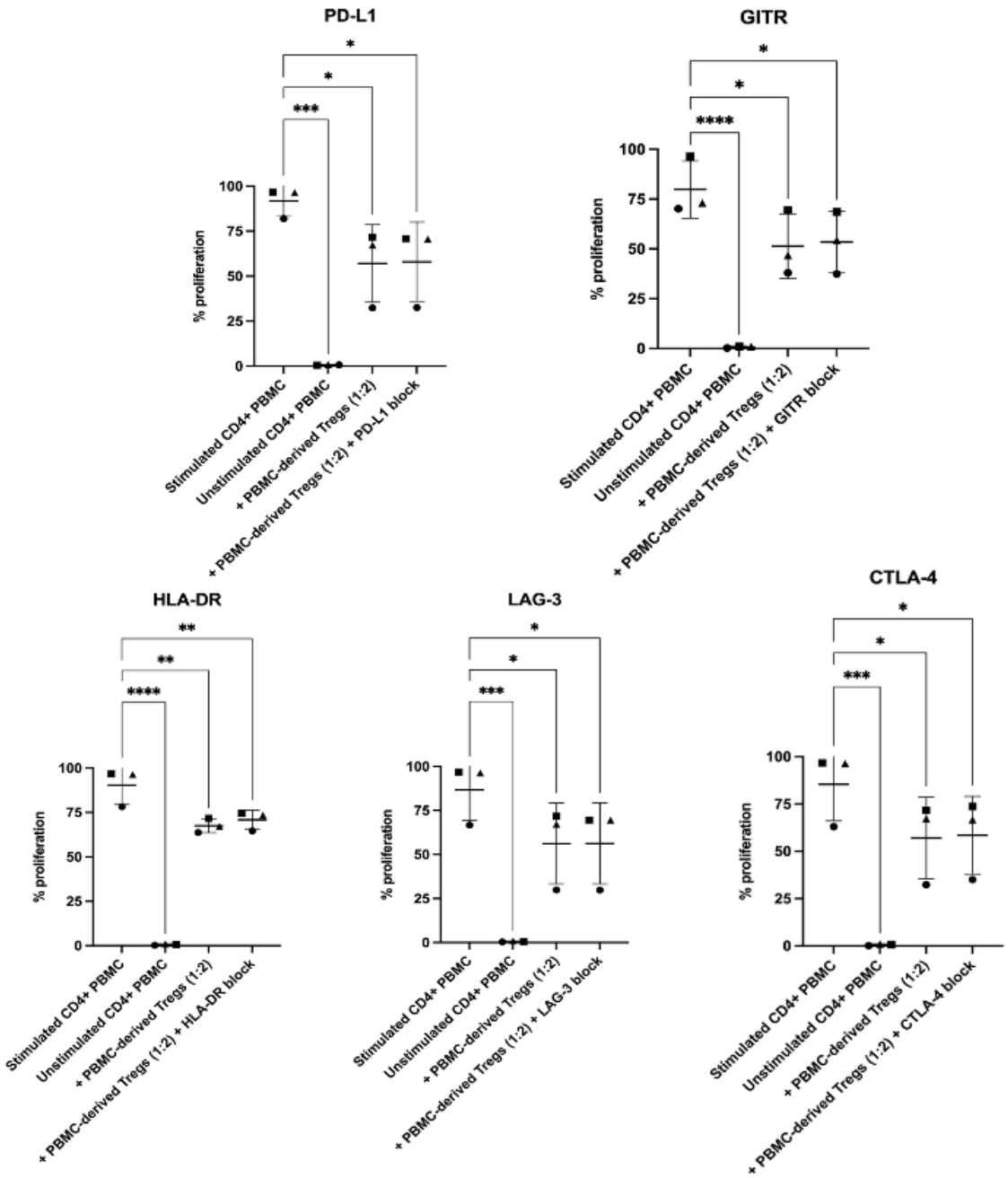

Supplemental Figure 6. Immune checkpoint inhibitors targeting PD-L1, GITR, HLA-DR, LAG-3, and CTLA-4 do not reverse Treg-mediated suppression of CD4$^+$ PBMC. Average percent proliferation for all replicates (N=3) of stimulated, unstimulated CD4$^+$ PBMC, and stimulated CD4$^+$ PBMC co-cultured with PBMC-derived Tregs. Each donor is represented by a shape. Statistical analysis run on the mean percent proliferation, paired by donor. Significance determined by one-way ANOVA; *, $p<0.05$; **, $p<0.005$; ***, $p<0.0005$; ****, $p<0.0001$.

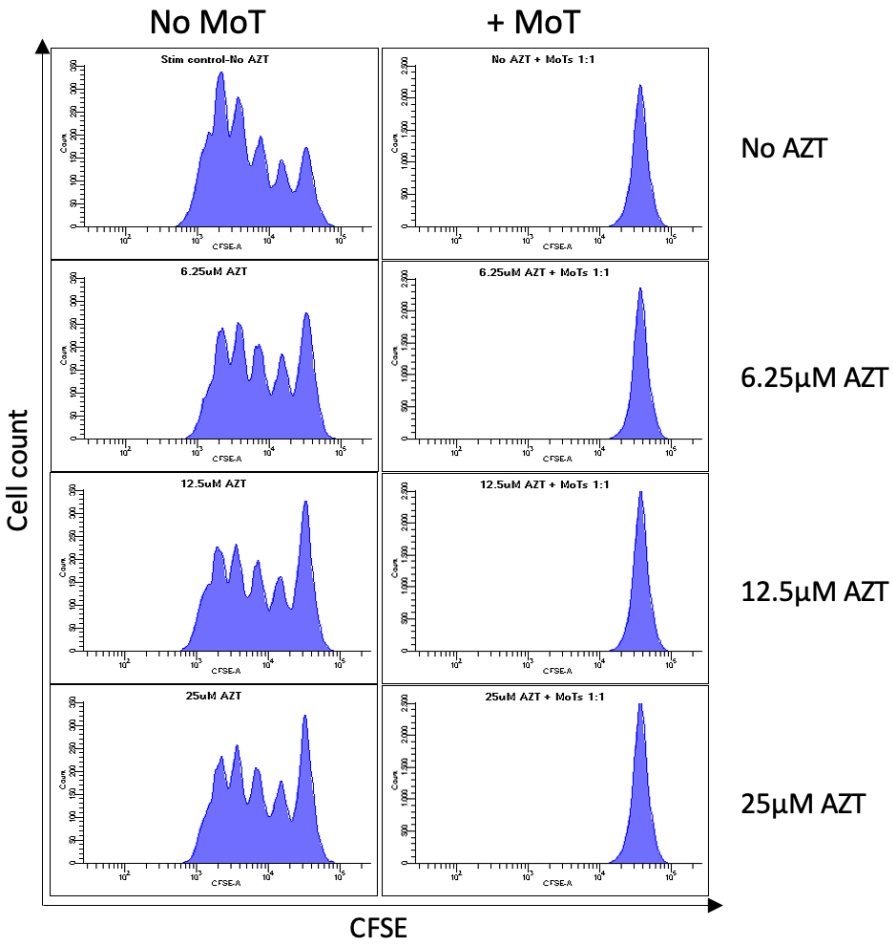

Supplemental Figure 7. Azidothymidine (AZT) does not affect suppression by MoT cells. AZT was incubated at the concentrations listed with MoT and CFSE-labeled CD3/CD28-stimulated $CD4^+$ PBMC throughout the five-day suppression assay

APPENDIX C

SUPPLEMENTAL DATA FOR CHAPTER 3

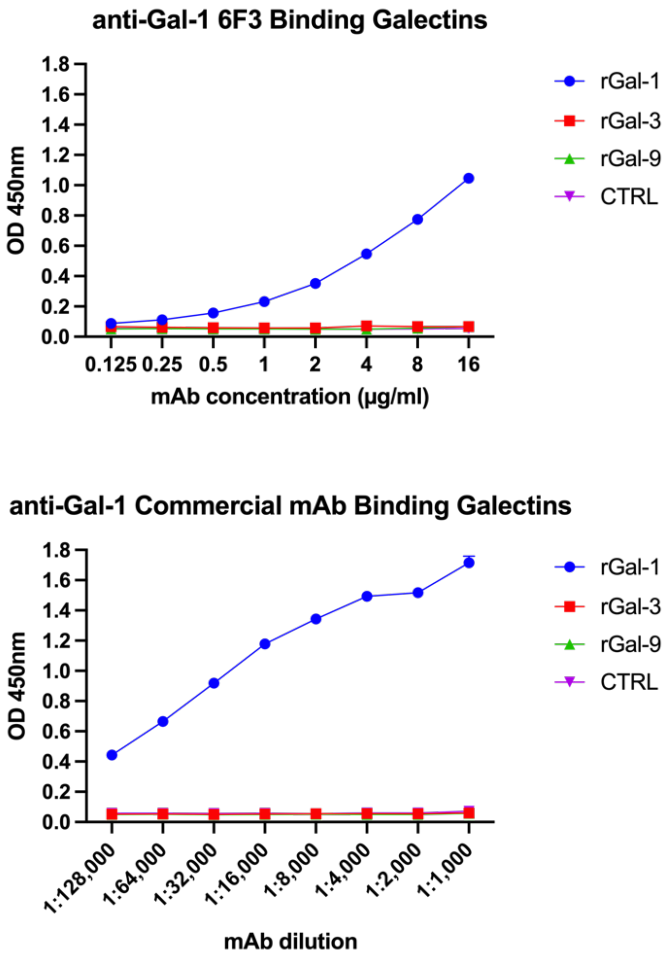

Supplemental Figure 1. MAb 6F3 does not cross-react with other galectins. Cross-reactivity to Galectin-3 and -9 was tested by ELISA. Serial dilutions of mAb 6F3 and commercial mAb were incubated with rGal-1, rGal-3, and rGal-9 coated ELISA plates. Mean and standard deviation are plotted from three independent experiments.

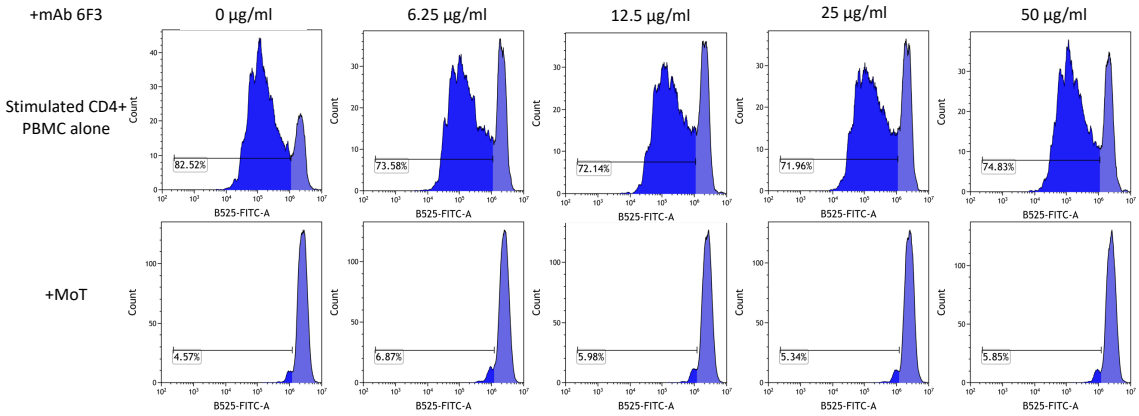

Supplemental Figure 2. Anti-Gal-1 mAb 6F3 does not reverse MoT-mediated suppression of CD4$^+$ PBMC. MAb 6F3 was added to the suppression assay at increasing concentrations, indicated above each graph.

APPENDIX D

SUPPLEMENTAL DATA FOR CHAPTER 4

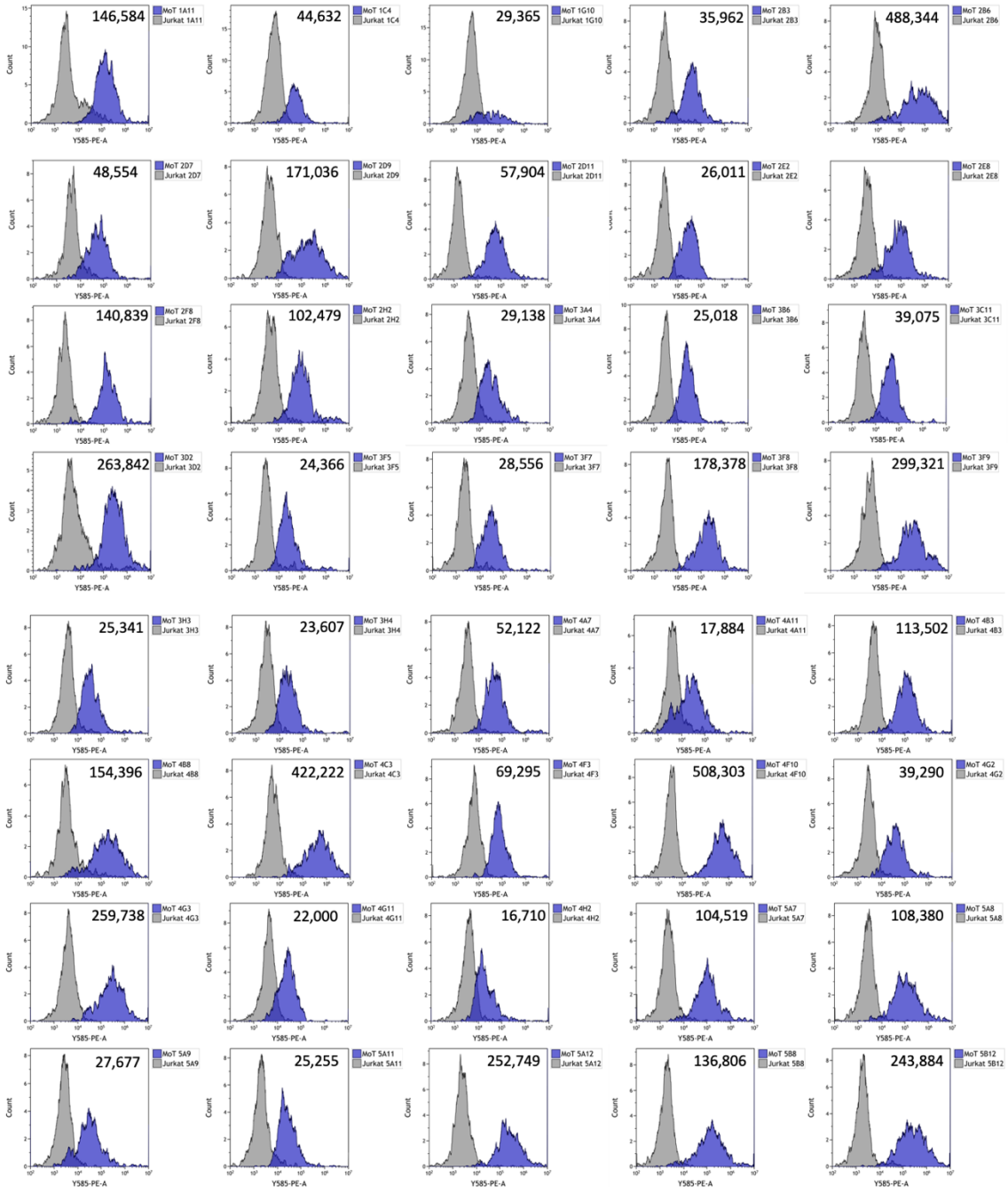
146,584
MoT 1A11
Jurkat 1A11
44,632
MoT 1C4
Jurkat 1C4
29,365
MoT 1G10
Jurkat 1G10
35,962
MoT 2B3
Jurkat 2B3
488,344
MoT 2B6
Jurkat 2B6
48,554
MoT 2D7
Jurkat 2D7
171,036
MoT 2D9
Jurkat 2D9
57,904
MoT 2D11
Jurkat 2D11
26,011
MoT 2E2
Jurkat 2E2
MoT 2E8
Jurkat 2E8
140,839
MoT 2F8
Jurkat 2F8
102,479
MoT 2H2
Jurkat 2H2
29,138
MoT 3A4
Jurkat 3A4
25,018
MoT 3B6
Jurkat 3B6
39,075
MoT 3C11
Jurkat 3C11
263,842
MoT 3D2
Jurkat 3D2
24,366
MoT 3F5
Jurkat 3F5
28,556
MoT 3F7
Jurkat 3F7
178,378
MoT 3F8
Jurkat 3F8
299,321
MoT 3F9
Jurkat 3F9
25,341
MoT 3H3
Jurkat 3H3
23,607
MoT 3H4
Jurkat 3H4
52,122
MoT 4A7
Jurkat 4A7
17,884
MoT 4A11
Jurkat 4A11
113,502
MoT 4B3
Jurkat 4B3
154,396
MoT 4B8
Jurkat 4B8
422,222
MoT 4C3
Jurkat 4C3
69,295
MoT 4F3
Jurkat 4F3
508,303
MoT 4F10
Jurkat 4F10
39,290
MoT 4G2
Jurkat 4G2
259,738
MoT 4G3
Jurkat 4G3
22,000
MoT 4G11
Jurkat 4G11
16,710
MoT 4H2
Jurkat 4H2
104,519
MoT 5A7
Jurkat 5A7
108,380
MoT 5A8
Jurkat 5A8
27,677
MoT 5A9
Jurkat 5A9
25,255
MoT 5A11
Jurkat 5A11
252,749
MoT 5A12
Jurkat 5A12
136,806
MoT 5B8
Jurkat 5B8
243,884
MoT 5B12
Jurkat 5B12
Count
Y585-PE-A

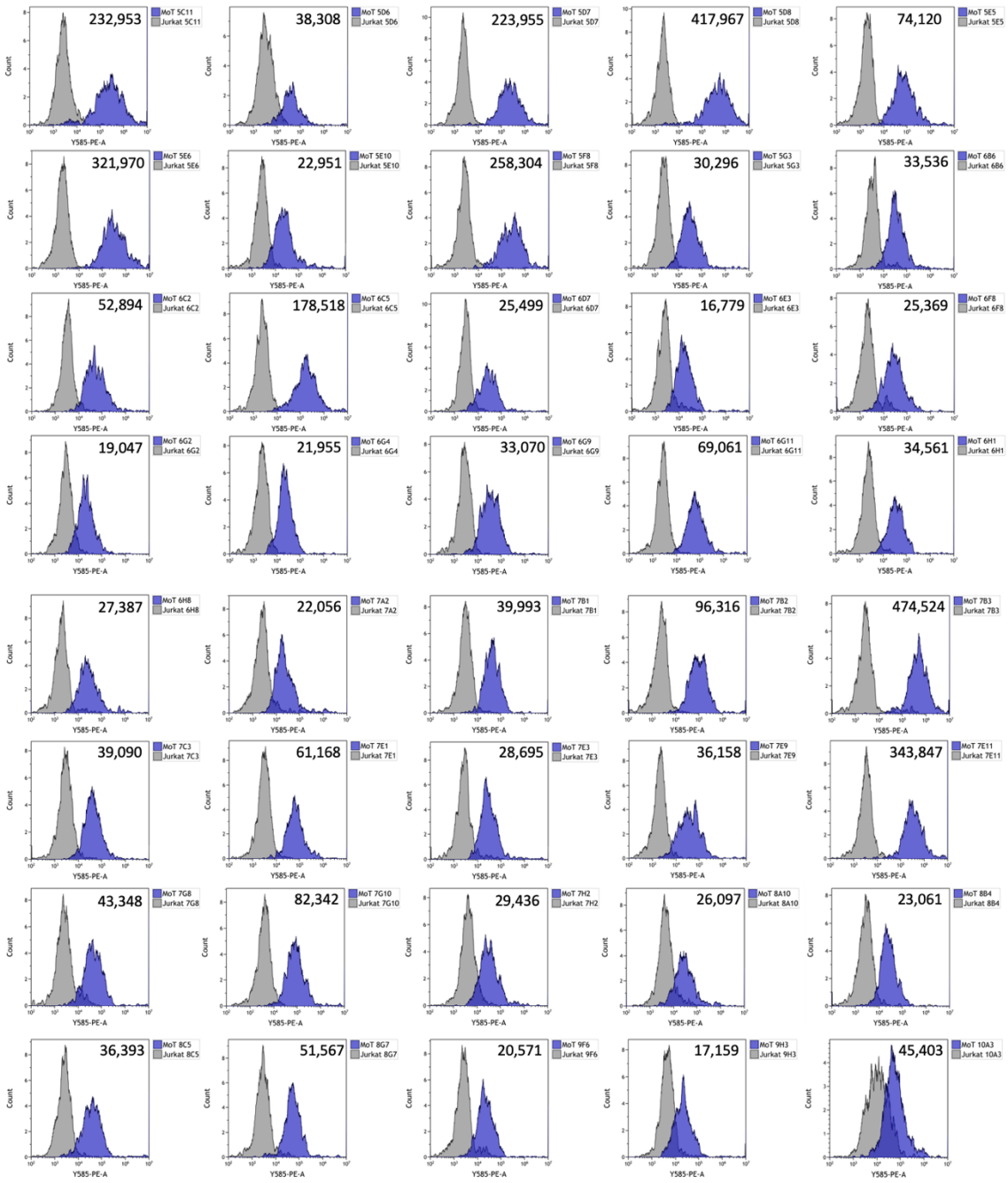
232,953
MoT 5C11
Jurkat 5C11
38,308
MoT 5D6
Jurkat 5D6
223,955
MoT 5D7
Jurkat 5D7
417,967
MoT 5D8
Jurkat 5D8
74,120
MoT 5E5
Jurkat 5E5
321,970
MoT 5E6
Jurkat 5E6
22,951
MoT 5E10
Jurkat 5E10
258,304
MoT 5F8
Jurkat 5F8
30,296
MoT 5G3
Jurkat 5G3
33,536
MoT 6B6
Jurkat 6B6
52,894
MoT 6C2
Jurkat 6C2
178,518
MoT 6C5
Jurkat 6C5
25,499
MoT 6D7
Jurkat 6D7
16,779
MoT 6E3
Jurkat 6E3
25,369
MoT 6F8
Jurkat 6F8
19,047
MoT 6G2
Jurkat 6G2
21,955
MoT 6G4
Jurkat 6G4
33,070
MoT 6G9
Jurkat 6G9
69,061
MoT 6G11
Jurkat 6G11
34,561
MoT 6H1
Jurkat 6H1
27,387
MoT 6H8
Jurkat 6H8
22,056
MoT 7A2
Jurkat 7A2
39,993
MoT 7B1
Jurkat 7B1
96,316
MoT 7B2
Jurkat 7B2
474,524
MoT 7B3
Jurkat 7B3
39,090
MoT 7C3
Jurkat 7C3
61,168
MoT 7E1
Jurkat 7E1
28,695
MoT 7E3
Jurkat 7E3
36,158
MoT 7E9
Jurkat 7E9
343,847
MoT 7E11
Jurkat 7E11
43,348
MoT 7G8
Jurkat 7G8
82,342
MoT 7G10
Jurkat 7G10
29,436
MoT 7H2
Jurkat 7H2
26,097
MoT 8A10
Jurkat 8A10
23,061
MoT 8B4
Jurkat 8B4
36,393
MoT 8C5
Jurkat 8C5
51,567
MoT 8G7
Jurkat 8G7
20,571
MoT 9F6
Jurkat 9F6
17,159
MoT 9H3
Jurkat 9H3
45,403
MoT 10A3
Jurkat 10A3
Count
Y585-PE-A

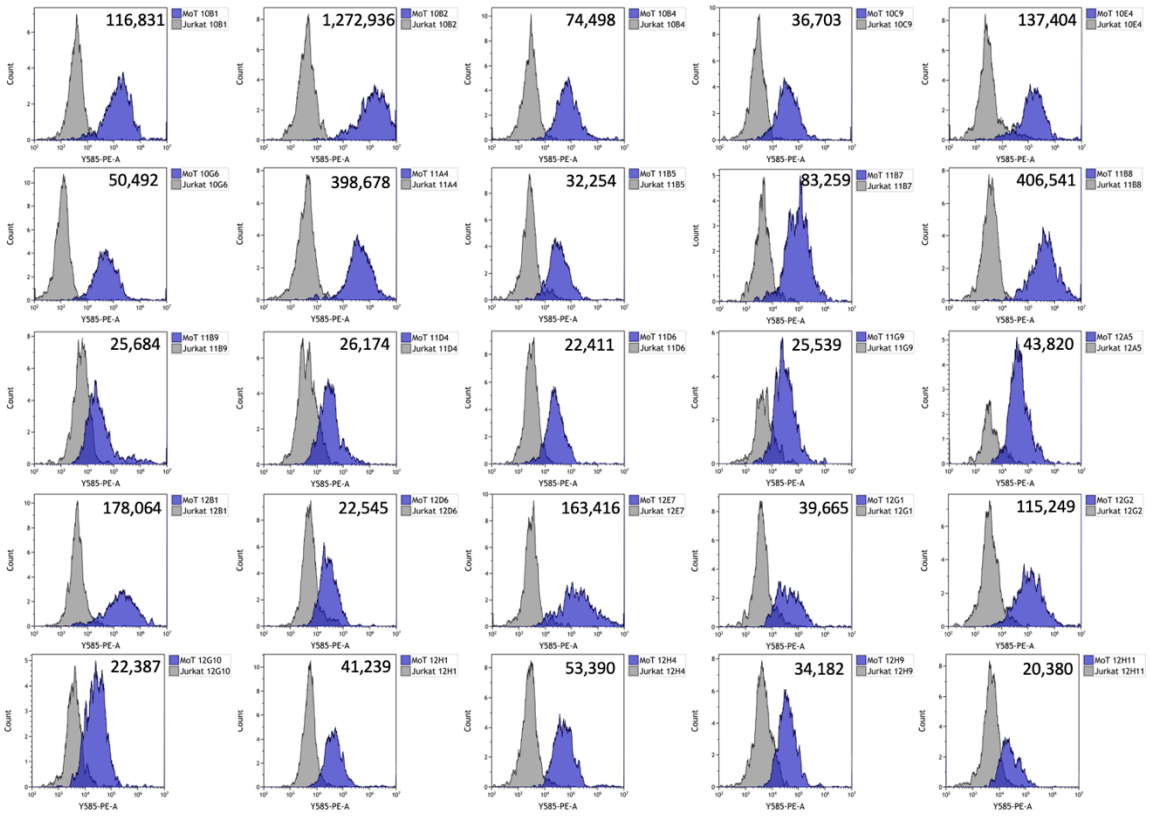

Supplemental Figure 1. Anti-MoT hybridoma parent well screening resulted in 105 positive hybridomas. Histograms show positive shifts to the right (blue), indicating binding to MoT cell surface, and not to Jurkat cells (gray peaks) by flow cytometry. ΔMFI is indicated on each histogram.

Monoclonal Antibody Clone	ΔMean Fluorescence Intensity	Cell Surface Binding Strength (based on ΔMFI)
1A11.D1	245,422	Moderate
2B6.G10	363,869	Moderate
2D7.F1	2,792	Weak
2H2.H10	1,004	Weak
3A4.B9	2,076	Weak
3H4.A3	3,991	Weak
4A7.F9	3,673	Weak
4G3.G4	564,027	Strong
4H2.E6	3,417	Weak
6C5.D12	2,853	Weak
8C5.F8	4,162	Weak
11B5.G4	2,400	Weak
12E7.A4	3,065,272	Strong
12H4.B5	2,160	Weak

Supplemental Table 1. Anti-MoT mAbs that bind to MoT cell surface by flow cytometry.

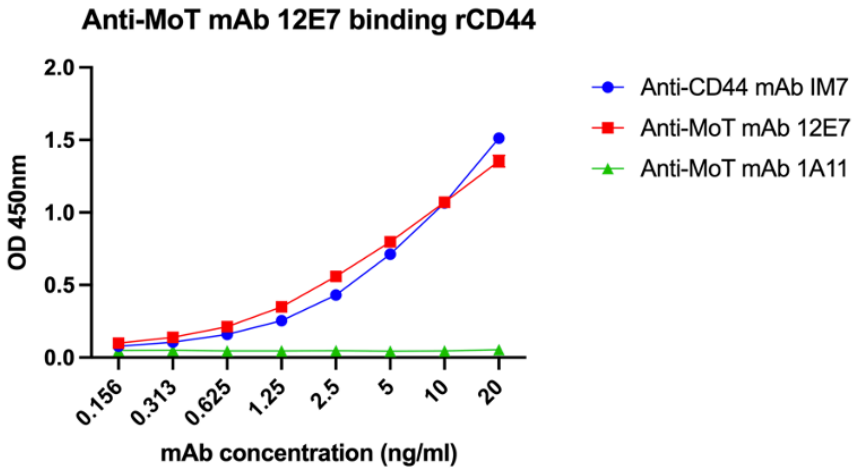

Supplemental Figure 2. Anti-MoT mAb 12E7 binds to rCD44. Indirect ELISA was performed using serial dilutions of anti-MoT mAbs 12E7, 1A11 and commercial anti-CD44 mAb, incubated with rCD44 coated ELISA plates. Secondary antibody HRP-conjugated anti-mouse IgG or SA-HRP were used to detect the interactions. Mean and standard deviation are plotted from three independent experiments.